UNIVERSIDAD NACIONAL AUTONOMA DE MEXICO

FACULTAD DE CIENCIAS

DIVISION DE ESTUDIOS DE POSGRADO

NADO DE DOS CUERPOS ESFERICOS CON MOVIMIENTOS DE PEQUEÑA AMPLITUD.

T E S I S

QUE PARA OBTENER EL GRADO ACADEMICO DE

DOCTOR EN CIENCIAS (FISICA)

P R E S E N T A :

AURORA MANDUJANO GARCIA

DIRECTOR DE TESIS:

PROFR. DR. UBBO FELDERHOF.

MEXICO, D. F. 1998.

Resumen en inglés de la tesis docotral.
Aurora Mandujano García

During the doctoral tesis I studied small amplitud swimming of two sphere at a finite distance from each other. This requieres the calculation of both swimming velocities and the total rate of energy dissipation. I limit the calculation to ptential flow.
I have found expressions for the velocity of each sphere and the total rate of dissipation. We are interested in the case in which both sphere swim with the same velocity, and we want to find the maximum efficiency of swwiming. I have found that there are modes for which the swwiming of two spheres is more effciente than the swimming of a single sphere. If we consider two or less multipoles the spheres swim better if they do it onw behind the other. if we consider more than two, the maximum swimming efficiency is achieved if the spheres swim one aside the other. And the efficiency increase if the distance between the spheres decrease.

Titulo de la tesis:

NADO DE DOS CUERPOS ESFERICOS CON MOVIMIENTOS DE PEQUEÑA AMPLITUD

Grado y nombre del tutor o director de tesis:

PROFR. DR. B. UBBO FELDERHOF

Institución de adscripción del tutor o director de tesis:

RW

Resumen de la tesis: (Favor de escribir el resumen de su tesis a máquina, como máximo en 25 renglones a un espacio, sin salir de la extensión de este cuadro.)

En la tesis doctoral se estudia el nado de pequeña amplitud de dos esferas que están separadas una distancia finita. Esto requiere el cálculo de las velocidades de nado de ambas esferas y la tasa de disipación de energía media. Los cálculos se límitan a flujo potencial. Se estudia el caso en que ambas esféras nadan con la misma velocidad. Se determina la máxima eficiencia de nado. Se encuentran modos para los que las esféras nadan en forma mas eficiente si lo hacen juntas. La máxima eficiencia de nado para más de dos multipolos se encuentra para el caso en que las eféras nadan una al lado de la otra y para dos multiplos o menos nadan mejor una detrás de la otra. La eficiencia de nado aumenta conforme la distancia de separación entre ambas esféras disminuye.

LOS DATOS ASENTADOS EN ESTE DOCUMENTO CONCUERDAN FIELMENTE CON LOS REALES Y QUEDO ENTERADO QUE, EN CASO DE CUALQUIER DISCREPANCIA, QUEDARÁ SUSPENDIDO EL TRÁMITE DEL EXAMEN

Fecha de solicitud: _____

Firma del alumno

Acompaño los siguientes documentos:

- Nombramiento del jurado del examen de grado
- Aprobación del trabajo escrito por cada miembro del jurado
- Copia de la última revisión de estudios
- Comprobante de pago de derechos por registro del grado

Biblioteca del Plantel	Biblioteca Central
Entrega ejemplares de tesis	

Agradecimientos

Antes que nadie quiero agradecerle al doctor B.Ubbo Felderhof por haber dirigido mi trabajo doctoral, el que gracias a sus excelentes comentarios y sugerencias pudo salir adelante. Además de haberme dado la oportunidad de poder realizar la tesis en Alemania.

También le agradezco a los doctores: Leopoldo García Colín, Rosalío Fernando Rodriguez Zepeda, José Julio Emilio Herrera Velazquez, Gerardo Ruiz Chavarría y Steven Peter Reed Czitrom Baus, por los comentarios y correcciones hechas a este trabajo. Muy en especial le agradezco al Dr. Ramóm Peralta-Fabi, quien además de haberme hecho valioso comentarios y correcciones en el presente trabajo, ha sido una persona muy importante durante todos mis estudios desde el inicio de la licenciatura, ya que con su gran alegría y amor por la física contagia a quien lo rodea, en especial a sus alumnos. El hecho de haber llegado hasta este punto de mi carrera en parte se lo debo a él. Cuán productiva sería la física si existieran muchos profesores así.

También quiero agradecerle al Dr. Bernhard Ersfeld, mi esposo, quien corrigió la primera versión de mi tesis, además de haber discutido conmigo parte del trabajo durante la realización de la investigación. El haber conocido a mi esposo fué una de las dos cosas más maravillosas que me sucedió durante la realización de mi tesis doctoral, la otra fué el nacimiento de nuestro bebé Bernhard Nicolas. Ambos me dieron todos los ánimos y entusiasmo necesarios para poder concluir la realización de este trabajo.

Le agradezco también a mis mamás, María Esther García Cruz y Therese Ersfeld por haber aguantado los maratones al ir conmigo en la Ciudad de México del centro a la universidad, para ayudarme a cuidar a Nico y transportar sus cosas durante la etapa de trámites y correcturas de la tesis para la presentación del examen. A la última de ellas por haberme también aguantado durante el comienzo de la escritura de la tesis, en la que además me encontraba al inicio de mi embarazo, y vaya que yo daba lata. En este punto también le quiero agradecer a mi hermano Daniel Mandujano García por también irnos a buscar a la facultad para ayudarnos

a cargar la carreola y cuidar del bebé.

Le agradezco a Eduardo Morales Gamboa por haberme ayudado en la impresión de mi tesis en México, y algunos otros detalles computacionales, además de ser un gran amigo mío.

También quiero agradecerles a mis compañeros Armin Kauerauf, Carsten Lohn, Markus Palenberg y Kenichi Ishikawa por la muy agradable atmósfera de trabajo. Muy en especial a Carsten Lohn, quien me iba a buscar y a dejar a la casa durante la etapa inicial de la escritura de mi tesis, en la que por cierto me encontraba yo esperando a mi bebé.

También quiero agradecerle a mi papá Daniel Mandujano Vera, a mis hermanos y cuñados, Angela, Amalio, María Esther, Juan Arturo, Gabriel Enrique y Daniel, y mis sobrinitos Hendrik, José Carlos, Mayra Carolina, Juan Arturo y Jonathan, porque gracias a todo el amor que siempre me han brindado el estar fuera del país no se me hizo tan difícil. A mis abuelitos, Daniel y Conchita, así como a toda mi familia, quienes siempre nos han apoyado y han estado juntos en los momentos más importantes y difíciles de nuestras vidas. Con una familia como ésta es muy fácil salir adelante.

A Sra. Gabrielle Conin por haber sido tan amable conmigo desde el primer día de mi llegada a Alemania.

A la Sra. Celia Guadalupe García Cruz, secretaria del cuarto piso de la facultad de Ciencias, por haberme ayudado en mis trámites de doctorado.

Le agradezco a la DGAPA, UNAM, por haberme otorgado la beca que hizo posible que pudiera realizar la investigación de la tesis en Alemania y al Institut für Theoretische Physik de la RWTH, Aachen, Alemania por haberme permitido hacer uso de sus instalaciones para poder realizar mi trabajo.

Contenido

Lista de Figuras

Capítulo 1

Introducción

Es fascinante observar el movimiento que los peces realizan al nadar, o el de los pájaros al volar, pero es aún mas interesante el tratar de entender cómo pueden lograrlo. Distintos científicos han trabajado en el problema de encontrar la explicación para el mecanismo de nado. ¿Qué hace un cuerpo para impulsarse por sí mismo a través de un fluido? Para algunos casos, esta pregunta parece ya estar contestada. Existe otra observación muy interesante, algunos nadadores alcanzan velocidades que no corresponden a su potencia muscular. ¿Porqué? ¿Qué es lo que hacen para moverse con tanta eficiencia? También puede observarse el nado o vuelo en grupo, por ejemplo, una parvada de patos, puede verse que éstos vuelan en formaciones peculiares. Se puede pensar que el propósito de dichas formaciones es el volar mas eficientemente.

También existen organismos muy pequeños (espermatozoides, por ejemplo) que nadan muy lentamente, y la dinámica de nado es distinta a la de un pez. Para este tipo de cuerpos vivientes se observa que cuando nadan en grupo, y dos o mas de ellos lo hacen muy cercanos uno al lado del otro y así sucesivamente, entonces el movimiento ondulante de sus colas, que es usada para la propulsión, tiende a estar en fase. De nuevo nos preguntamos, ¿porqué?. Distintos modelos de este tipo de movimientos fueron desarrollados por G. I. Taylor [1], quien además consideró interacción. Posteriormente otros autores se interesaron en el problema, pero solo consideraron un cuerpo. Cuando un cuerpo sólido se mueve con velocidad constante a través de un fluido viscoso e incompresible, el fluido se adhiere a su superficie, lo que queda expresado en la condición de frontera de no deslizamiento que debe satisfacerse en la superficie del cuerpo. El movimiento del fluido puede ser dividido en dos regímenes que son caracterizados por el grosor de la capa límite viscosa. La

capa límite es una capa delgada adyacente al cuerpo dentro de la cual la vorticidad varía rapidamente debido a un efecto combinado de difusión y convección [2]. En esta capa los efectos de viscosidad son muy importantes, y fuera de ella tienden a cero o varían muy lentamente. Para caracterizar la capa límite se define el número de Reynolds: es un número adimensional que da el cociente entre el tamaño del cuerpo y el grosor de la capa límite viscosa $R = L\rho U/\eta$, donde L y U son una dimensión característica y la velocidad del cuerpo, respectivamente, mientras ρ es la densidad de masa y η la viscosidad dinámica del fluido. En casos en los que se trata de un cuerpo que está vibrando, el número adimensional correspondiente es el número de Stokes, que está dado por $S = \omega L^2\rho/\eta$, donde ω es la frecuencia de vibración. En el régimen de Stokes, donde $S << 1$, la inercia puede ser completamente despreciada, y el fluido es descrito por las ecuaciones linealizadas [3]. En la ausencia de inercia la trayectoria seguida por un nadador es determinada completamente por la geometría de la secuencia de formas que asume, y es independiente de la rapidez del movimiento [4, 5].

Taylor fué el primero en mostrar [1] que en el límite de número de Stokes cero, una placa infinita puede nadar realizando movimientos ondulatorios. El extendió su trabajo para explorar las reacciones entre las colas de dos organismos pequeños vecinos con colas propulsantes. El encontró que si las ondas que se propagan por las dos colas están en fase, se disipa mucho menos energía que en el caso en que se encuentren en antifase. Taylor introdujo este modelo con el fin de explicar las observaciones echas por J. Gray et. al., que cuerpos vivientes muy pequeños (por ejemplo, espermatozoides) nadan enviando ondas de desplazamiento lateral hacia el extremo de las colas (el no pegado al cuerpo). Gray también mencionó que muchos autores han observado que cuando dos cabezas de espermatozoides están en contacto, sus colas tienden a vibrar en forma sincronizada [1]. El trabajo de Taylor para el caso de una placa plana, fué extendido por A.J. Reynolds [6], quien incluyó inercia en el fluido y consideró esfuerzos de la superficie ondulatoria, y una superficie cercana al cuerpo. E.O. Tuck [7] corrigió el trabajo de Reynolds, incluyendo efectos de convección, los que Reynolds había despreciado en las ecuaciones de Navier-Stokes. J.E. Drummond [8] extendió el trabajo de Taylor a grandes amplitudes de movimiento de la lámina. En el mismo límite, los movimientos de una esfera fueron estudiados por M. J. Lighthill [9], J. R. Blake [10] y A.Shapere y F.Wilczek [4]. Blake agregó una corrección al artículo de Lighthill sobre movimientos de un cuerpo casi esférico que se deforma. En su artículo Blake intentó modelar la dinámica de la propulsión ciliar. El escribió lo siguiente: "En 1675, el microscopista Leeuwenhoek

fué quizás la primera persona en ver y anotar los movimientos de un cilio. En una carta a la Royal Society, describió la increíble infinidad de pies o patas pequeñas que hacen que pequeños organismos puedan impulsarse por sí mismos a través del agua. En 1876, Muller parece ser la primera persona en haber usado el nombre cilio" [10]. Con el fin de describir el movimiento de estos animales, Blake usó un modelo matemático que involucra una envoltura. El supuso que una superficie instantánea cubre los extremos ondulantes del cilio. En su artículo escribió que un organismo que ha sido estudiado en detalle, de forma oval-plana , llamado Opalina, genera ondas que viajan en la misma dirección como una vibración efectiva. El aproximó su forma con una esfera, ya que éste es el cuerpo mas simple de extensión finita.

Shapere and Wilczek generalizaron el trabajo de Blake. Ellos formularon el problema en términos de campos de normas en el espacio de formas, y aplicaron sus resultados a una esfera y a un cilindro de sección transversal arbitraria y definieron una noción de eficiencia para determinar los modos de nado óptimos. Ahora, en el régimen de Euler, afuera de la capa límite, las fuerzas viscosas pueden despreciarse, y el fluido puede ser considerado como un fluido ideal, es decir un fluido de viscosidad cero, lo que corresponde al límite de número de Reynolds grande. P. G. Saffman [11] mostró que un cuerpo puede nadar en un fluido ideal.

El mecanismo de nado con número de Reynolds grande y con separación de la capa límite fué descrito por Taylor [12] y Lighthill [13]. Taylor estudió el nado de animales tales como culebras, anguilas y lombrices marinas, las idealizó considerando el equilibrio de un cilindro flexible immerso en agua a través del cual viajan ondas de amplitud constante (las ondas viajan del extremo pegado al cuerpo hacia el extremo libre) a velocidad constante. El supuso que la fuerza sobre cada elemento de cilindro es la misma que la que actuaría en el correspondiente elemento de un cilindro recto largo moviéndose a la misma velocidad e inclinación con respecto a la dirección del movimiento. Lighthill trató de explicar porqué la velocidad alcanzada por peces o mamíferos nadadores es muy alta en comparación con la correspondiente a su fuerza muscular. Con el fin de entender ésto, es necesario calcular el flujo exterior a la capa límite. El lo hizo considerando lo que el llamó "pez delgado". Este es un pez o mamífero nadador, cuyas dimensiones y movimientos perpendiculares a su dirección de movimiento son pequeños en comparación a su longitud, mientras su sección transversal varía gradualmente a lo largo de ésta. En su trabajo consideró un pez delgado realizando movimientos de nado solamente en la dirección perpendicular a su dirección de movimiento. El determinó movimientos que producen empuje con una pequeña cuota de un vórtice de arrastre e hizo algunas consideraciones sobre el

desarrollo de la capa límite que podría ser inducida.

T. Yao Tsu Wu [14] estudió la propulsión de un pez considerando números de Reynolds grandes con la imposición de la condición de Kutta en una orilla cortante.

B.U. Felderhof and R.B. Jones [15], consideraron el mecanismo de nado para número de Stokes S arbitrario, pero amplitud de deformación pequeña. Consideraron un cuerpo simplemente conexo de forma arbitraria inmerso en un fluido viscoso e incompresible e incluyeron la posibilidad de movimiento rotacional medio. Se obtiene una velocidad de nado no nula es a segundo orden en teoría de perturbaciones. Para variación temporal armónica dieron una definición natural de la eficiencia de nado, que esencialmente es el cociente entre la velocidad promedio y la rapidez de energía de disipación media. Presentaron en detalle dos ejemplos explícitos en los que el flujo a primer orden es irrotacional. En un artículo posterior [16] aplicaron la teoría a un cuerpo esférico con desplazamiento superficial variando armónicamente en el tiempo. Expresaron la velocidad translacional y la rapidez de disipación de energía, promediada sobre un periodo, como una forma cuadrática en el desplazamiento superficial. La eficiencia de nado es entonces dada como el cociente de estas dos formas cuadráticas. Su óptimo puede ser obtenido del valor propio máximo de un problema de valores propios generalizado que involucra matrices hermitianas.

En el presente trabajo se van a usar los resultados encontrados por Felderhof y Jones para describir el nado de dos cuerpos esféricos. El objetivo del presente trabajo es investigar el nado conjunto de dos cuerpos esféricos deformables inmersos en un fluido viscoso e incompresible. Es de interés particular encontrar las condiciones bajo las cuales los cuerpos nadan más eficientemente juntos, a que si lo hicieran solos, y se va a tratar de encontrar el modo óptimo para nado translacional.

Como el nado conjunto en una situación estacionaria implica que la posicion relativa de los cuerpos no cambia, se han encontrado modos de nado que llevan a velocidades iguales de ambas esferas, tomando en cuenta interacción hidrodinámica. Se va a mostrar que una posibilidad simple para satisfacer este requirimiento, es suponer el mismo tipo de deformaciones en ambas esferas, pero con un retardamiento o una diferencia de fase. Se va a resolver el problema para número de Stokes arbitrario, pero amplitud de deformación pequeña, y se va a suponer que el campo de velocidades a primer orden puede ser descrito como un flujo potencial. Como el problema hidrodinámico de dos esferas no está resuelto en forma exacta, se va a usar un método aproximado para determinar la velocidad de nado. En el primer capítulo, se dará una breve introducción a la hidrodinámica con el fin de proveer las ideas básicas y las ecuaciones necesarias para el entendimiento del presente trabajo.

En el segundo capítulo, se resume el análisis del correspondiente problema de un cuerpo, resuelto por Felderhof y Jones, de forma tal que se puedan usar las expresiones encontradas por ellos para el cálculo de la velocidad media de cada esfera y la disipación de energía. También se intentan adaptar sus métodos para la determinación de la máxima eficiencia de nado al caso de dos cuerpos, y por último se usan sus resultados para comparar el nado conjunto con el separado.

En el tercer capítulo, se resuelve el problema de dos cuerpos en forma analítica y aproximada. Se calcula la velocidad del flujo y la presión a primer orden y con éstas la velocidad de nado de cada esfera promediadas sobre un periodo, y la rapidez de disipación de energía del sistema. Se extiende la definición de eficiencia de nado al problema de dos cuerpos.

En el cuarto capítulo, se dan los métodos numericos usados para determinar la eficiencia de nado máxima y los correspondientes modos de nado, y se presentan los resultados.

Finalmente, se dan las conclusiones y perspectivas del trabajo.

Capítulo 2

Breve introducción a la hidrodinámica

Para entender mejor el presente trabajo, se va a dar una breve introducción a la hidrodinámica. No se van a dar detalles ya que éstos pueden ser encontrados en distintos libros de texto, pero se van a mencionar aspectos básicos y resultados conocidos que están relacionados con el problema de nado dos cuerpos esféricos.

2.1 Ecuaciones de Navier-Stokes

Desde el punto de vista de la dinámica de fluidos, un fluido es considerado como un medio continuo. Lo que quiere decir que si consideramos cualquier volumen de fluido, aún uno pequeño, se va a suponer que siempre es lo suficientemente grande para contener un número grande de moléculas. Tomando ésto en cuenta, en dinámica de fluidos los términos partícula de fluido o punto de un fluido significan pequeños volúmenes de fluidos que matemáticamente son tratados como infinitesimales, pero que en la realidad son grandes en comparación con la distancia entre las moléculas [17].

La descripción matemática del estado de un fluido en movimiento es efectuada al conocer las funciones que dan la distribución de la velocidad del fluido $\boldsymbol{v}(\boldsymbol{r},t)$ y cualesquiera dos cantidades termodinámicas, por ejemplo la densidad del fluido $\rho(\boldsymbol{r},t)$ y su presión $p(\boldsymbol{r},t)$. Todas las cantidades termodinámicas pueden ser determinadas si se conocen cualesquiera dos de ellas y la ecuación de estado [17]. Por lo que si se dan tres componentes de la velocidad, la presión y la densidad, el estado del movimiento del fluido queda completamente determinado. En el presente trabajo se

tiene interés en la descripción de cuerpos sólidos moviéndose a través de un fluido viscoso e incompresible. Un fluido es considerado incompresible, si la densidad de masa en cada elemento de volumen es constante durante su movimiento.

Existen dos diferentes especificaciones para describir el movimiento de un fluido. Son llamadas descripcicones euleriana y lagrangiana.

La desripción euleriana es como la del campo electromagnético, en la que las cantidades de flujo son definidas como funciones de la posición $\boldsymbol{r}$ en el espacio y del tiempo t. La cantidad primaria del flujo es la velocidad del fluido $\boldsymbol{v}(\boldsymbol{r}, t)$. Esta especificación puede ser pensada como que da una imagen de las cantidades del flujo en cada instante del movimiento.

En la descripción lagrangiana, se selecciona un elemento de fluido y se describe su historia dinámica. Las cantidades del flujo son descritas como funciones del tiempo y del elemento de fluido seleccionado. La cantidad primaria del fluido, de acuerdo a la especificación Lagrangiana es la velocidad $\boldsymbol{v}(\boldsymbol{a}, t)$, donde $\boldsymbol{a}$ es la posición del centro de masa del elemento de fluido especificado a algún tiempo inicial t_0. Aquí se entiende que las dimensiones lineales iniciales del elemento son tan pequeñas que garantizan pequeñez en todos los instantes consecutivos para poder despreciar distorsión o extensión del elemento.

Las ecuaciones que describen el movimiento del fluido viscoso en el sistema de Euler son las ecuaciones de Navier-Stokes y la ecuación de continuidad, que para un flujo incompresible toman la forma

$$\rho\left[\frac{\partial \boldsymbol{v}}{\partial t} + (\boldsymbol{v}\cdot\nabla)\boldsymbol{v}\right] = \eta\nabla^2\boldsymbol{v} - \nabla p, \qquad \nabla\cdot\boldsymbol{v} = 0. \tag{2.1}$$

Las cantidades del campo que describen el movimiento del fluido, son su velocidad $\boldsymbol{v}$ y presión p, éstas dependen de la posición y del tiempo. La viscosidad dinámica η, y en el caso incompresible la densidad de masa ρ, son parámetros que caracterizan al fluido. Las ecuaciones de arriba pueden ser obtenidas considerando algún volumen V_0, y aplicándole a éste los principios de conservación del momento y la masa para obtener las ecuaciones de Navier-Stokes y de continuidad, respectivamente.

El flujo de momento está representado por el tensor de esfuerzos, que para un fluido viscoso está dado por

$$\sigma_{ij} = -p\delta_{ij} + \eta\left(\frac{\partial v_i}{\partial x_j} + \frac{\partial v_j}{\partial x_i}\right). \tag{2.2}$$

Si se considera un cuerpo sólido moviéndose en un fluido viscoso, se deben dar las condiciones de frontera a satisfacerse junto con las ecuaciones de movimiento. En

el caso de interacciones entre un fluido viscoso y un cuerpo sólido siempre aparecen fuerzas de atracción molecular entre el fluido y la superficie del cuerpo sólido, y como consecuencia de dichas fuerzas, la capa del fluido inmediatamente adyacente a la superficie del cuerpo, se adhiere a éste. Por lo que la velocidad de un fluido viscoso se anula en la frontera de un cuerpo sólido que está en reposo

$$v|_s = 0. \tag{2.3}$$

Esta es llamada la condición de frontera de adherencia. En el caso general de una superficie en movimiento, la velocidad del fluido debe ser igual a la velocidad de la superficie [17].

2.2 Disipación de energía

En un fluido viscoso la presencia de viscosidad resulta en la disipación de energía, que finalmente es transformada en calor. Con el fin de calcular la disipación de energía en un fluido incompresible, se fija uno en la energía cinética total, que está dada por

$$E_{kin} = \frac{\rho}{2} \int v^2 d\boldsymbol{r}. \tag{2.4}$$

La energía cinética del fluido decrece debido a sus viscosidad. La rapidez de pérdida es llamada tasa de disipación de energía y es denotada por

$$D(t) = -\dot{E}_{kin}, \tag{2.5}$$

donde el punto denota la derivada temporal $\frac{\partial}{\partial t}$. Con el fin de determinar la tasa de disipación de energía se escribe $\partial \rho v^2/2\partial t = \rho v_i \partial v_i/\partial t$ en la derivada temporal de la energía cinética, y se sustituye por $\partial v_i/\partial t$ en la ecuaciones de Navier-Stokes (para detalles ver [17]).

Esta expresión se usa en la integral, que se evalúa sobre todo el volumen ocupado por el fluido. Se encuentra que la tasa de disipación de energía está dada por

$$D(t) = \frac{\eta}{2} \int \left(\frac{\partial v_i}{\partial x_k} + \frac{\partial v_k}{\partial x_i} \right)^2 d\boldsymbol{r} = 2\eta \int (\nabla \boldsymbol{v}(\boldsymbol{r}, t))^s : (\nabla \boldsymbol{v}(\boldsymbol{r}, t))^s d\boldsymbol{r}, \tag{2.6}$$

donde en la primera expresión se usa la convención de suma, así el cuadrado implica la doble suma sobre los subíndices, y en la segunda el superíndice indica la simetrización del tensor. Como la tasa de disipación de energía nos lleva al decremento en la energía cinética, la viscosidad η debe ser positiva.

Alternativamente el integrando anterior se expresa como

$$\frac{\eta}{2}\left(\frac{\partial v_i}{\partial x_k}+\frac{\partial v_k}{\partial x_i}\right)^2=\frac{\partial}{\partial x_i}(\sigma_{ik}v_k)-\left(\frac{\partial}{\partial x_i}\sigma_{ik}\right)v_k=\nabla\cdot(\boldsymbol{\sigma}\cdot\boldsymbol{v})-(\nabla\cdot\boldsymbol{\sigma})\cdot\boldsymbol{v}. \quad (2.7)$$

Ahora, si se considera el caso lineal y estacionario, donde no hay fuerzas ni torcas externas, la divergencia del tensor de esfuerzos se anula, $\nabla\cdot\boldsymbol{\sigma}=0$, y la integral de volumen anterior se puede transformar en una integral de superficie:

$$D=\int_S \boldsymbol{v}\cdot\boldsymbol{\sigma}\cdot\hat{\boldsymbol{n}}\,dS. \quad (2.8)$$

con $\hat{\boldsymbol{n}}$ la normal a S dirigida hacia afuera. Una relación análoga se satisface para la rapidez de disipación media cuando se tienen campos periódicos en el tiempo. En el caso de un fluido de extensión infinita en contacto con cuerpos sólidos, que se encuentren en estado de movimiento constante, la superficie corresponde a la de los cuerpos. La interpretación de la integral de superficie puede ser entonces que la energía disipada en el fluido debe ser compensada por la energía que pasa de los cuerpos al fluido para que éstos puedan mantener su movimiento.

2.3 Ecuaciones de Navier-Stokes en un sistema de referencia en rotación

Para problemas en los que la frontera externa del fluido se encuentra en movimiento, es conveniente escoger un sistema coordenado en el cual ésta se mantenga en reposo. Esto implica transformar las ecuaciones de Navier-Stokes a un sistema nuevo. En lo que sigue se transformarán las ecuaciones de movimiento a un sistema que esté rotando alrededor de un punto fijo O en el sistema inercial de laboratorio con velocidad angular constante $\boldsymbol{\Omega}$. En este punto se debe encontrar la relación entre la aceleración $\boldsymbol{a}_O$ con respecto al sistema inercial y la aceleración con respecto al sistema en rotación.

La posición del elemento de fluido con respecto al sistema inercial se denota por $\boldsymbol{r}_O$, ésta es la misma en ambos sistemas y puede ser expresada en términos de los vectores unitarios $\hat{\boldsymbol{e}}_i$ $(i=1,2,3)$, fijos en el sistema en rotación a través de la relación

$$\boldsymbol{r}_O=\boldsymbol{r}=x_i\hat{\boldsymbol{e}}_i. \quad (2.9)$$

La velocidad $\boldsymbol{v}_O$ y la aceleración $\boldsymbol{a}_O$ con respecto al sistema inercial se definen a través de la primera y segunda derivadas temporales de la posición, respectivamente.

En el sistema en rotación, se debe tomar en cuenta el cambio de los vectores unitarios debido a que el sistema rota, lo cual se expresa por

$$\frac{d\hat{\boldsymbol{e}}_i}{dt} = \boldsymbol{\Omega} \times \hat{\boldsymbol{e}}_i. \tag{2.10}$$

Se encuentra(usando la fórmula de Leibniz para la segunda derivada):

$$\boldsymbol{v}_O = \frac{d\boldsymbol{r}_O}{dt} = v_i\hat{\boldsymbol{e}}_i + x_i\boldsymbol{\Omega} \times \hat{\boldsymbol{e}}_i. \tag{2.11}$$

$$\boldsymbol{a}_O = \frac{d^2\boldsymbol{r}_O}{dt^2} = a_i\hat{\boldsymbol{e}}_i + 2v_i\boldsymbol{\Omega} \times \hat{\boldsymbol{e}}_i + x_i\boldsymbol{\Omega} \times (\boldsymbol{\Omega} \times \hat{\boldsymbol{e}}_i). \tag{2.12}$$

donde

$$v_i = \frac{dx_i}{dt}, \tag{2.13}$$

$$a_i = \frac{d^2x_i}{dt^2}, \tag{2.14}$$

son las componentes de la velocidad $\boldsymbol{v}$ y la aceleración $\boldsymbol{a}$ con respecto al sistema en rotación. Así las relaciones deseadas son

$$\boldsymbol{v}_O = \boldsymbol{v} + \boldsymbol{\Omega} \times \boldsymbol{r}. \tag{2.15}$$

$$\boldsymbol{a}_O = \boldsymbol{a} + 2\boldsymbol{\Omega} \times \boldsymbol{v} + \boldsymbol{\Omega} \times (\boldsymbol{\Omega} \times \boldsymbol{r}), \tag{2.16}$$

En términos de la velocidad $\boldsymbol{v}(\boldsymbol{r}, t)$ relativa al sistema en rotación, se tiene en la descripción euleriana la siguiente relación

$$\boldsymbol{a} = \frac{\partial \boldsymbol{v}}{\partial t} + \boldsymbol{v} \cdot \nabla \boldsymbol{v}. \tag{2.17}$$

Por lo que si se incluye una densidad de fuerza ficticia que actúe sobre el fluido en adición a las fuerzas reales, las ecuaciones de Navier-Stokes en el sistema en rotación son idénticas en forma a las del sistema inercial

$$\boldsymbol{f} = -2\rho\boldsymbol{\Omega} \times \boldsymbol{v} - \rho\boldsymbol{\Omega} \times (\boldsymbol{\Omega} \times \boldsymbol{r}). \tag{2.18}$$

El primer término, $-2\rho\boldsymbol{\Omega} \times \boldsymbol{v}$ corresponde a la fuerza de Coriolis, que es perpendicular tanto a la velocidad $\boldsymbol{v}$ como a la velocidad angular $\boldsymbol{\Omega}$, y el segundo término $-\rho\boldsymbol{\Omega} \times (\boldsymbol{\Omega} \times \boldsymbol{r})$ es la fuerza centrífuga. Como la velocidad angular $\boldsymbol{\Omega}$ no depende de la posición, la fuerza centrífuga puede escribirse como el gradiente de un potencial.

$$-\boldsymbol{\Omega} \times (\boldsymbol{\Omega} \times \boldsymbol{r}) = \frac{1}{2}\nabla(\boldsymbol{\Omega} \times \boldsymbol{r})^2 \tag{2.19}$$

y ser incluida en el término de la presión. De esta forma se obtienen finalmente las ecuaciones de Navier-Stokes en un sistema en rotación:

$$\rho\left[\frac{\partial \boldsymbol{v}}{\partial t}+(\boldsymbol{v}\cdot\nabla)\boldsymbol{v}+2\boldsymbol{\Omega}\times\boldsymbol{v}\right]=\eta\nabla^2\boldsymbol{v}-\nabla p'. \qquad \nabla\cdot\boldsymbol{v}=0. \tag{2.20}$$

donde

$$p'=p-\frac{\rho}{2}(\boldsymbol{\Omega}\times\boldsymbol{r})^2. \tag{2.21}$$

es la presión modificada que contiene la fuerza centrífuga.

Capítulo 3

Solución del problema de un cuerpo

En el presente capítulo se reportan los resultados obtenidos por Felderhof y Jones en su trabajo sobre nado de pequeña amplitud de una esfera deformable en un fluido incompresible e infinito descrito por las ecuaciones de Navier-Stokes (para más detalles ver el apéndice C). Se supone que las deformaciones superficiales de la esfera son armónicas en el tiempo. La teoría está basada en una expansión en peturbaciones en potencias de la amplitud de las deformaciones superficiales. Felderhof y Jones encontraron que a segundo orden el cuerpo adquiere una velocidad de nado no nula. En este análisis se obtiene una definición natural para la eficiencia de nado. En el presente trabajo es de interés primordial calcular dicha cantidad. para poder posteriormente comparar el nado de dos cuerpos con el de uno solo.

3.1 Ecuaciones básicas

A continuación se darán los principales resultados en la formulación de las ecuaciones que describen el movimiento de nado de un solo cuerpo. Se considera un cuerpo esférico de radio a inmerso en un fluido incompresible de extensión infinita. con viscosidad cortante η y densidad de masa ρ. El cuerpo realiza variaciones de forma armónicas en el tiempo. El fluido se adhiere a la esfera, produciéndose de esta forma un patrón de flujo. Como consecuencia, dicho patrón de flujo actúa sobre el cuerpo obligándolo a moverse. El cuerpo adquiere velocidades de nado translacional y rotacional. , Dichas velocidades promediadas en el tiempo sobre un período de deformaciones T, son denotadas por $\boldsymbol{U}$ y $\boldsymbol{\Omega}$, respectivamente. Como la esfera se

translada y rota mientras su superficie se deforma, es conveniente escoger un sistema de referencia que se mueva con movimiento de cuerpo rígido, en el cual, en promedio el cuerpo se mantenga en reposo. A este sistema se le llama K_0. El origen de este sistema se escoge en el centro de la esfera no deformada. Con esta elección, las ecuaciones de movimiento deben incluir los términos centrífugo y de Coriolis. Como se explicó en el capítulo anterior, la fuerza centrífuga puede ser incluida en el término de la presión, y el término de Coriolis debe ser agregado a la ecuación. Se supone que los campos de velocidad $\boldsymbol{v}(\boldsymbol{r},t)$ y presión $p(\boldsymbol{r},t)$ del flujo satisfacen las ecuaciones de Navier-Stokes, que válidas en el sistema de referencia K_0, están dadas por (ecuación (C.1))

$$\rho\left(\frac{\partial \boldsymbol{v}}{\partial t}+(\boldsymbol{v}\cdot\nabla)\boldsymbol{v}+2\boldsymbol{\Omega}\times\boldsymbol{v}\right)=\eta\nabla^2\boldsymbol{v}-\nabla p,\qquad \nabla\cdot\boldsymbol{v}=0. \tag{3.1}$$

Aquí p es la presión modificada que contiene el potencial centrífugo. Un punto sobre la superficie de la esfera deformada tiene las siguientes coordenadas (ecuación (C.2))

$$\boldsymbol{r}_S(\theta,\varphi,t)=a\hat{\boldsymbol{r}}+\boldsymbol{\xi}(\theta,\varphi,t), \tag{3.2}$$

donde $\hat{\boldsymbol{r}}$ es el vector unitario radial y $\boldsymbol{\xi}$ es el vector de desplazamiento. La condición de adherencia implica (ecuación (C.4))

$$\boldsymbol{v}(\boldsymbol{r}_S,t)=\frac{\partial \boldsymbol{\xi}}{\partial t}. \tag{3.3}$$

Para resolver el problema es necesario considerar la condición a satisfacerse en infinito. El campo de velocidades tiende a (ecuación (C.5))

$$\boldsymbol{v}(\boldsymbol{r},t)\approx -\boldsymbol{U}-\boldsymbol{\Omega}\times\boldsymbol{r}\qquad \text{cuando}\quad r\to\infty, \tag{3.4}$$

y el campo de presión a

$$p(\boldsymbol{r},t)\approx p_0+\rho(\boldsymbol{\Omega}\times\boldsymbol{U})\cdot\boldsymbol{r}-\frac{\rho}{2}(\boldsymbol{\Omega}\times\boldsymbol{r})^2\qquad \text{cuando}\qquad r\to\infty, \tag{3.5}$$

donde p_0 es la presión en ausencia de movimiento. Como se muestra en el apéndice C, el problema puede ser resuelto haciendo un desarrollo formal en perturbaciones, tomando como parámetro de perturbación el cociente $\boldsymbol{\xi}/a$. Se encuentra que a primer orden, las velocidades de nado se anulan, es decir, a este orden la esfera no nada. A segundo orden la esfera adquiere velocidades de nado $\boldsymbol{U}_2$ y $\boldsymbol{\Omega}_2$ que, respectivamente, pueden ser escritas como la suma de dos contribuciones

$$\langle \boldsymbol{U}_2\rangle=\langle \boldsymbol{U}_{2B}\rangle+\langle \boldsymbol{U}_{2S}\rangle,\qquad \langle \boldsymbol{\Omega}_2\rangle=\langle \boldsymbol{\Omega}_{2B}\rangle+\langle \boldsymbol{\Omega}_{2S}\rangle, \tag{3.6}$$

donde los subíndices $2S$ y $2B$ corresponden a contribuciones superficiales y volumétricas, respectivamente, para mayores detalles ver el apéndice C.

Se define la velocidad superficial (ecuación (C.20))

$$\boldsymbol{u}_S(\hat{\boldsymbol{r}},t) = -\boldsymbol{\xi}(\hat{\boldsymbol{r}},t)\cdot\nabla\boldsymbol{v}_1(\boldsymbol{r},t)\Big|_{r=a}. \tag{3.7}$$

y se encuentra que la contribucion superficial a la velocidad de nado translacional pueden ser expresada como el promedio esférico (ecuación (C.61))

$$\boldsymbol{U}_{2S} = -\frac{1}{4\pi}\int d\Omega\,\langle\boldsymbol{u}_S\rangle(\hat{\boldsymbol{r}}). \tag{3.8}$$

y la contribución superficial a la velocidad de nado rotacional está dada por C.62.

$$\boldsymbol{\Omega}_{2S} = -\frac{3}{8\pi a}\int d\Omega\,\hat{\boldsymbol{r}}\times\langle\boldsymbol{u}_S\rangle(\hat{\boldsymbol{r}}). \tag{3.9}$$

En el presente trabajo se considera flujo potencial a primer orden en las deformaciones superficiales, y en dicho caso las contribuciones volumétricas se anulan. Existe otra situación en la cual dichas contribuciones se anulan, ésta corresponde al caso en que el flujo se mueve muy lentamente. En dicha situación son bilineales en la velocidad a primer orden y pueden en el caso de flujo lineal, ser despeciadas en comparación con las superficiales. El problema de dos cuerpos estará restringido a flujo potencial, por lo que a partir de este momento se desprecian las contribuciones volumétricas. A continuación se consideran en particular funciones de desplazamiento que varían armónicamente en el tiempo con frecuencia $\omega = 2\pi/T$. Se introduce notación compleja. El desplazamiento superficial se escribe como

$$\boldsymbol{\xi}(\theta,\varphi,t) = \mathrm{Re}\left\{\boldsymbol{\xi}_\omega(\theta,\varphi)e^{-i\omega t}\right\}, \tag{3.10}$$

con amplitud compleja $\boldsymbol{\xi}_\omega(\theta,\varphi)$. Los campos de velocidad y presión correspondientes están dados por

$$\boldsymbol{v}_1(\boldsymbol{r},t) = \mathrm{Re}\left\{\boldsymbol{v}_\omega(\boldsymbol{r})e^{-i\omega t}\right\}, \qquad p_1(\boldsymbol{r},t) = \mathrm{Re}\left\{p_\omega(\boldsymbol{r})e^{-i\omega t}\right\}. \tag{3.11}$$

de la ecuación (C.20), se encuentra que la velocidad superficial $\langle\boldsymbol{u}_S(\hat{\boldsymbol{r}})\rangle$ promediada en el tiempo, está dada por

$$\langle\boldsymbol{u}_S(\hat{\boldsymbol{r}})\rangle = -\frac{1}{2}\left\{\mathrm{Re}\,\boldsymbol{\xi}_\omega^*\cdot\nabla\boldsymbol{v}_\omega\right\}\Big|_{r=a}. \tag{3.12}$$

El promedio de la tasa de disipación de energía, a segundo orden, está dada por (ecuación (C.65))

$$\langle D\rangle = -\frac{1}{2}\mathrm{Re}\left\{\int_{S_0}\boldsymbol{v}_\omega^*\cdot\boldsymbol{\sigma}_\omega\cdot\hat{\boldsymbol{r}}dS\right\}. \tag{3.13}$$

S_0 denota la superficie esférica no desplazada, y $\sigma_{\omega ij}$ es el tensor de esfuerzos viscoso a primer orden, cuyas componentes cartesianas son

$$\sigma_{\omega ij} = \eta \left(\frac{\partial v_{\omega i}}{\partial x_j} + \frac{\partial v_{\omega j}}{\partial x_i} \right) - p_\omega \delta_{ij}. \tag{3.14}$$

El problema de optimizar la eficiencia de nado puede relacionarse con la solución de un problema de valores propios. Es conveniente introducir una notación corta para entender mejor el problema. Por lo que para cualesquiera dos funciones vectoriales complejas $\boldsymbol{f}(s)$ y $\boldsymbol{g}(s)$, definidas sobre la superficie S_0, se introduce el producto escalar

$$\langle \boldsymbol{f} | \boldsymbol{g} \rangle = \int_{S_0} \boldsymbol{f}^* \cdot \boldsymbol{g} dS. \tag{3.15}$$

Con esta notación la velocidad de nado se puede expresar como un valor de expectación de operadores lineales hermitianos con respecto al campo de desplazamiento complejo. En componentes cartesianas

$$\boldsymbol{U}_{2S}^{\alpha z} = \omega L \langle \boldsymbol{x} i_\omega | \underset{\approx}{S}^\alpha | \boldsymbol{\xi}_\omega \rangle, \qquad \alpha = x, y, z. \tag{3.16}$$

En forma similar, la tasa de disipación de energía media se escribe a través de la relación

$$\langle D \rangle = \eta \omega^2 L^3 \langle \boldsymbol{\xi}_\omega | \underset{\approx}{D} | \boldsymbol{\xi}_\omega \rangle. \tag{3.17}$$

Con el operador hermitiano lineal $\underset{\approx}{D}$. El problema de encontrar el modo de nado óptimo consiste en determinar la función de desplazamiento $\boldsymbol{\xi}_\omega$ que maximiza $\boldsymbol{U}_{2S}^{\alpha z}$ para una tasa de disipación de energía media dada. Como a es el radio de la esfera, entonces la medida natural de la velocidad está dada en unidades de $2\omega a$, y la disipación en unidades de $8\eta\omega^2 a^3$. Se define la eficiencia de nado translacional como el cociente

$$\eta_t = \pi \frac{U_{2S}^z}{2\omega a^2} \frac{8\eta\omega^2 a^3}{\langle D_2 \rangle} \tag{3.18}$$

de donde

$$\eta_t = 4\pi\eta\omega a^2 U_2^z / \langle D_2 \rangle. \tag{3.19}$$

Por simetría se ha restringido la atención a modos que producen movimiento de nado en la dirección z.

3.2 Análisis de los modos lineales

Como se puede notar, la velocidad y la disipación de energía media de la esfera a segundo orden, tan solo dependen de los campos de flujo a primer orden. Por lo que conociendo éstos, se puede determinar la eficiencia de nado. A continuación se van a encontrar los campos de flujo a primer orden. De las ecuaciones de Navier-Stokes (C.10), usando notación compleja y eliminando el factor de dependencia temporal, se obtiene

$$\eta[\nabla^2 \boldsymbol{v}_\omega - \alpha'^2 \boldsymbol{v}_\omega] - \nabla p_\omega = 0, \qquad \nabla \cdot \boldsymbol{v}_\omega = 0. \tag{3.20}$$

con el parámetro

$$\alpha' = (-i\omega\rho/\eta)^{1/2}. \tag{3.21}$$

La solución de esta ecuación, considerando solamente flujo irrotacional, (ver apéndice C) está dada por

$$\boldsymbol{v}^-_{lm}(\boldsymbol{r}) = \frac{-1}{\alpha^2(2l+1)} r^{-l-1} \boldsymbol{B}_{lm}(\hat{\boldsymbol{r}}). \tag{3.22}$$

$$p^-_{lm}(\boldsymbol{r}) = \eta \frac{1}{2l+1} r^{-l-1} Y_{lm}(\hat{\boldsymbol{r}}). \tag{3.23}$$

con armónicos esféricos escalares y vectoriales Y_{lm} and $\boldsymbol{B}_{lm}$, dados en el apéndice C. Se ha considerado que el campo de velocidades puede escribirse como el gradiente de un potencial, es decir

$$\boldsymbol{v}_\omega(\boldsymbol{r}) = \nabla \phi_\omega(\boldsymbol{r}), \tag{3.24}$$

además sólo se tomó en cuenta la solución para flujo dispersado, ya que no existe flujo incidente sobre la esfera. El campo de flujo a primer orden puede ser expandido en términos de estos modos.

$$\boldsymbol{v}_\omega = \sum_{lm} v_{lm} \boldsymbol{v}^-_{lm}, \tag{3.25}$$

con amplitudes complejas v_{lm}.

El vector de desplazamiento superficial $\boldsymbol{\xi}(\theta, \varphi)$ puede, en general, ser expandido en términos de vectores armónicos esféricos. De la condición de frontera, con el fin de que se obtenga flujo irrotacional, sólo deben haber contribuciones del tipo $\boldsymbol{B}_{lm}$

en esta expansión, que por conveniencia se se expresa en términos de los modos de la velocidad

$$\boldsymbol{\xi}_\omega = \sum_{lm} \xi_{lm} \boldsymbol{v}_{lm}^-(a\hat{\boldsymbol{r}}). \tag{3.26}$$

Si se aplica la condición de frontera, se encuentra

$$v_{lm} = -i\omega\xi_{lm}. \tag{3.27}$$

La presión puede escribirse como

$$p_\omega(\boldsymbol{r}) = -i\omega \sum_{lm} \xi_{lm} p_{lm}^-. \tag{3.28}$$

El potencial satisface (C.29). En notación compleja está dado por C.76

$$\phi_\omega(\boldsymbol{r}) = -\frac{i}{\omega\rho} p_\omega(\boldsymbol{r}). \tag{3.29}$$

Las expresiones anteriores llevan a escribir las velocidades de nado y la disipación de energía media como formas cuadráticas en el espacio vectorial de dimensión infinita de los desplazamientos superficiales. Las componentes de dichos vectores son las amplitudes de deformación compleja ξ_{lm}. Cada forma está relacionada a una matriz hermitiana. El eje z puede ser siempre escogido de forma tal que coincida con la dirección del movimiento. La eficiencia de nado queda expresada como(ver apéndice C),

$$\eta_t = \frac{1}{\pi} \frac{|\langle \boldsymbol{\xi} | \underset{\approx}{B}^z | \boldsymbol{\xi} \rangle|}{\langle \boldsymbol{\xi} | \underset{\approx}{A} | \boldsymbol{\xi} \rangle}, \tag{3.30}$$

donde

$$\langle \boldsymbol{\xi} | \underset{\approx}{B}^z | \boldsymbol{\xi} \rangle = \sum \xi_{lm}^* B_{lm,l'm'} \xi_{l'm'}, \tag{3.31}$$

y

$$\langle \boldsymbol{\xi} | \underset{\approx}{A} | \boldsymbol{\xi} \rangle = \sum \xi_{lm}^* A_{lm,l'm'} \xi_{l'm'}. \tag{3.32}$$

Con el fin de obtener el modo de nado más eficiente, es necesario maximizar η_t sobre el espacio de desplazamientos superficiales. Esto corresponde a encontrar el valor propio máximo λ_{max} del problema de valores propios generalizado

$$\underset{\approx}{B}^z | \boldsymbol{\xi} \rangle = \lambda \underset{\approx}{A} | \boldsymbol{\xi} \rangle. \tag{3.33}$$

En este caso, $\underset{\approx}{A}$ y $\underset{\approx}{B}^{\dagger}$ son matrices hermitianas y $\underset{\approx}{A}$ es positiva definida. La velocidad máxima para una disipación de energía dada, se encuentra a través de la relación

$$\eta_l = \frac{|\lambda_{max}|}{\pi}. \tag{3.34}$$

El problema puede ser estudiado para cada valor de m, pero si se escoge la dirección z la eficiencia de nado máxima se encuentra para $m = 0$. Por lo que en lo posterior se restringirán los cálculos para este caso. Los campos son independientes del ángulo azimutal φ. Por simplicidad tomaremos coeficientes ξ_l adimensionales. Esto se logra usando la relación

$$\xi_{l0} = -\frac{i\omega a^2 \rho}{\eta}\sqrt{4\pi(2l+1)}\,\xi_l a^{l+1} \tag{3.35}$$

El correspondiente vector de desplazamiento superficial es

$$\boldsymbol{\xi}_s(\hat{\boldsymbol{r}}) = -\sqrt{4\pi}a\sum_{l=0}^{\infty}\frac{1}{\sqrt{2l+1}}\xi_l \boldsymbol{B}_{l0}(\hat{\boldsymbol{r}}). \tag{3.36}$$

y el potencial escalar complejo a primer orden está dado explícitamente por

$$\phi_s = i\omega a^2 \sum_{l=0}^{\infty}\xi_l\left(\frac{a}{r}\right)^{l+1} P_{l+1}(\cos\theta), \tag{3.37}$$

con polinomios de Legendre $P_l(\cos\theta)$.

Capítulo 4

Nado de dos cuerpos

4.1 Solución del problema de dos cuerpos

A continuación se describirá el método seguido para determinar a primer orden el campo de velocidades $\boldsymbol{v}_\omega(1,2)$ y presión $p_\omega(1,2)$, para el problema de dos cuerpos, a partir de los cuales se pueden determinar la tasa de disipación de energía media y sus correspondientes velocidades, cantidades primordiales para la determinación de la eficiencia de nado.

Se hacen las mismas suposiciones sobre los cuerpos y la forma en que se desplazan que para el caso de un solo cuerpo, es decir, se consideran dos cuerpos esféricos iguales de radio a, cuyas superficies sufren pequeñas deformaciones (comparadas con su radio) armónicas en el tiempo $\mathrm{Re}\,\boldsymbol{\xi}_\omega^{(k)} e^{-i\omega t}$. Se busca la solución estacionaria en la que ambas esferas naden juntas, por lo que se toma la distancia de separación $\boldsymbol{R}$ entre los centros de éstas como constante. Además se pide la condición que las esferas no se traslapen: $R > 2a$. Se escoge el sistema de referencia en forma tal que cada esfera en ausencia de la otra nade en la dirección z (ver apéndice D). El vector de separación $\boldsymbol{R}$ forma un ángulo θ_R con su eje, por lo que este ángulo se anula si las esfera 1 nada detrás de la esfera 2, y $\theta_R = \pi/2$, si las esferas nadan una al lado de la otra. El campo de velocidades en presencia de ambas esferas $\boldsymbol{v}_\omega(1,2)$ está dado por la ecuación

$$\boldsymbol{v}_\omega(1,2;\boldsymbol{r}) = \nabla\phi_\omega(1,2;\boldsymbol{r}). \tag{4.1}$$

donde $\phi_\omega(1,2;\boldsymbol{r})$ es el potencial hidrodinámico en presencia de ambas esferas. Los campos pueden ser alternativamente expandidos en términos de coordenadas $\boldsymbol{r}_1$, $\boldsymbol{r}_2$ respecto a los centros de cada esfera (expansión biesférica). El potencial afuera de

cada esfera puede ser escrito como la suma de tres contribuciones. Las primeras dos son debidas a las deformaciones de cada esfera, una en ausencia de la otra: éstas se conocen de la solución del problema de un solo cuerpo. La tercera es debido a las interacciones hidrodinámicas entre ambas esferas. Esto queda expresado en la expansión "gemela" dada por la ecuación (D.3). Los coeficientes A^1_{lm} and A^2_{lm} en la expansión gemela son determinados a partir de la condición de frontera, justo afuera de cada cuerpo. Estos coeficientes son los únicos desconocidos en el potencial hidrodinámico. A continuación se describirá el método seguido para calcularlos.

Para un cuerpo centrado en el origen, el potencial hidrodinámico en la región exterior a los cuerpos, pero dentro de una esfera que excluya las fuentes del campo multipolar aplicado, puede ser analizado en términos de contribuciones multipolares (ecuación (D.4))

$$\varphi(\boldsymbol{r}) = \sum_{l=0}^{\infty} \sum_{m=-l}^{l} \varphi_{lm}(r) P_l^m(\cos\theta) e^{im\varphi}, \tag{4.2}$$

donde θ y φ son los ángulos azimutales y polares de $\boldsymbol{r}$, respectivamente. Las funciones radiales pueden escribirse como (ecuación (D.5))

$$\varphi_{lm}(r) = i\omega a^2 \xi_l \left(\frac{a}{r}\right)^{l+1} \delta_{m0} + \phi_{0,lm}(r) + \varphi_{ind,lm}(r). \tag{4.3}$$

El primer término corresponde al potencial debido a las deformaciones de la esfera en ausencia de campo incidente, este término por sí mismo satisface la condición de que el flujo sigue las deformaciones de la esfera. En el caso de que haya un flujo incidiente aparecen los dos términos restantes; el primero corresponde al flujo incidente sobre la esfera y el segundo al flujo inducido. Ambos términos deben cumplir la condición de que la derivada radial de la suma de ambos se anula en la superficie de la esfera no deformada (D.6). Para obtener los coeficientes anteriormente mencionados, se requiere que justo afuera de la esfera uno, el potencial sea una superposición de potenciales de la forma (D.4) con (D.5) y (D.6), y las coordenadas deben ser las del centro de la esfera 1 y, en forma análoga, justo afuera de la esfera 2. Esto se logra expandiendo los potenciales multipolares centrados en una esfera en términos de los centrados en la otra esfera, lo que se hace usando las ecuaciones (D.9) y (D.10). A continuación se usa la condición de frontera justo afuera de cada esfera y se obtiene un par de ecuaciones para los coeficientes A^1_{lm} y A^2_{lm}. Para resolver estas ecuaciones es necesario hacer el cambio de variable dado en la ecuación (D.13). Después de hacer algunos cambios de variables y definir algunas matrices se encuentran las

siguientes soluciones (ver (D.36)y (D.37))

$$\underset{\sim}{d}^{(1)} = i\omega a^3[\underset{\approx}{D}^1_1\underset{\sim}{\xi}^1 + \underset{\approx}{D}^1_2\underset{\sim}{\xi}^2], \tag{4.4}$$

$$\underset{\sim}{d}^{(2)} = i\omega a^3[\underset{\approx}{D}^2_1\underset{\sim}{\xi}^1 + \underset{\approx}{D}^2_2\underset{\sim}{\xi}^2], \tag{4.5}$$

donde los vectores $\underset{\sim}{d}^{(1)}$ y $\underset{\sim}{d}^{(2)}$ tienen como componentes, respectivamente, los coeficientes ($d^{(1)}_{lm}$ y $d^{(2)}_{lm}$), definidos por la ecuación (D.13). Las componentes de los vectores $\underset{\sim}{\xi}^1$ y $\underset{\sim}{\xi}^2$ son las amplitudes de las deformaciones superficiales ξ^1_l y ξ^2_l respectivamente. Las matrices involucradas son conocidas y dependen implícitamente de la distancia de separación entre los centros de las esferas no deformadas. Usando la relación (D.13), se escribirá el potencial en términos de las componentes de estos vectores.

4.2 Campos de velocidad y presión

En esta sección se calcularán los campos de velocidad y presión del flujo. Como se mencionó anteriormente, las velocidades medias $\boldsymbol{U}_1$, $\boldsymbol{U}_2$ y las tasas de disipación de energía media D_1, D_2 sobre la superficie de cada cuerpo a segundo orden en perturbaciones dependen tan sólo de los campos del flujo a primer orden. La velocidad del campo a primer orden se obtiene de la ecuación (D.38)

$$\boldsymbol{v}_\omega(1,2;\boldsymbol{r}) = \nabla\phi_\omega(\boldsymbol{r}). \tag{4.6}$$

Con el fin de calcular las velocidades medias y las tasas de energía disipada para las esferas 1 y 2, se deben escribir los campos de velocidad y presión en términos de un sistema coordenado centrado en $\boldsymbol{R}_1$ y otro centrado en $\boldsymbol{R}_2$, respectivamente. De esta forma pueden usarse las ecuaciones obtenidas para el problema de un solo cuerpo. Tomando en cuenta un sistema coordenado centrado en $\boldsymbol{R}_1$, y usando las ecuaciones (D.3), (D.9) y (D.13) se obtiene

$$\phi_\omega(1,2;\boldsymbol{r}) = \sum_{l=0}^{\infty}\sum_{m=-l}^{l}\left[\frac{a^l}{r_1^{l+1}}d^{(1)}_{lm} + (-1)^m\frac{r_1^l}{a^{l+1}}e^{(2)}_{lm}\right]P_l^m(\cos\theta_1)e^{im\varphi_1}. \tag{4.7}$$

En forma similar, para un sistema coordenado centrado en $\boldsymbol{R}_2$, las ecuaciones (D.3), (D.10), y (D.13) llevan a:

$$\phi_\omega(1,2;\boldsymbol{r}) = \sum_{l=0}^{\infty}\sum_{m=-l}^{l}\left[\frac{a^l}{r_2^{l+1}}d^{(2)}_{lm} + (-1)^{l+m}\frac{r_2^l}{a^{l+1}}e^{(1)}_{lm}\right]P_l^m(\cos\theta_2)e^{im\varphi_2}. \tag{4.8}$$

donde se han usado las siguientes abreviaciones

$$e_{lm}^{(1)} = \sum_{l'=0}^{\infty} \sum_{m'=-l'}^{l'} \frac{(l+l'+m-m')!}{(l+m)!(l'-m')!} x^{l+l'+1} P_{l+l'}^{m-m'}(\cos\theta_R) d_{l'm'}^{(1)}, \tag{4.9}$$

$$e_{lm}^{(2)} = \sum_{l'=0}^{\infty} \sum_{m'=-l'}^{l'} (-1)^{l'} \frac{(l+l'+m-m')!}{(l+m)!(l'-m')!} x^{l+l'+1} P_{l+l'}^{m-m'}(\cos\theta_R) d_{l'm'}^{(2)}. \tag{4.10}$$

De la ecuación (D.38) se obtiene que la velocidad del flujo para un sistema coordenado centrado en $\boldsymbol{R}_k$, donde $k = 1, 2$, está dado por la ecuación (D.52), que a continuación se escribe

$$\boldsymbol{v}_\omega^{(k)} = \sum_{l=0}^{\infty} \sum_{m=-l}^{l} (-1)^m [a_{lm}^{(k)} r_k^{-l-2} \boldsymbol{Y}_{l\,l+1\,m} + b_{lm}^{(k)} r_k^{l-1} \boldsymbol{Y}_{l\,l-1\,m}]. \tag{4.11}$$

El campo de presión es encontrado a partir de la ecuación (C.76). Escrita en términos de un sistema coordenado centrado en $\boldsymbol{R}_k$, se obtiene la ecuación (D.61), que a continuación se escribe

$$p_{\omega k}(1,2;\boldsymbol{r}_k) = \sum_{l=0}^{\infty} \sum_{m=-l}^{l} \left[a_{p,lm}^{(k)} r_k^{-l-1} + b_{p,lm}^{(k)} r_k^{l} \right] Y_{lm}(\theta_k, \varphi_k). \tag{4.12}$$

Se han encontrado los promedios temporales de los campos de velocidad y presión para el problema de dos cuerpos en términos de un sistema coordenado centrado en $\boldsymbol{R}_k$. Por lo que ya pueden ser calculadas las velocidades medias y la tasa de disipación de energía para las esferas, y a partir de éstas obtener la eficiencia de nado. Se desea calcular la mejor forma de nado para el sistema de dos cuerpos. Con el fin de poder comparar con el nado de un sólo cuerpo, se define la eficiencia de nado en forma tal que ésta coincida con la de un sólo cuerpo si las esferas están separadas una distancia infinita. La definición apropiada es (ver ecuación (D.62))

$$\eta_T = 4\pi\eta\omega a^2 \frac{2|U_{cm}|}{\langle D \rangle}, \tag{4.13}$$

donde $\boldsymbol{U}_{cm}$ es la velocidad del centro de masa y $\langle D \rangle$ es la tasa de disipación de energía media del sistema.

4.3 Velocidad de las esferas y tasa de disipación de energía media

A continuación se calculará la velocidad de las esferas; y se definirá la velocidad del sistema. ésta última será obtenida para el caso en que ambas esferas nadan con la misma velocidad.

Con el fin de obtener la velocidad de la esfera k, con $k = 1, 2$, se usa la ecuación (D.64)

$$\boldsymbol{U}_k = -\frac{1}{4\pi}\int \langle \boldsymbol{u}_S^{(k)} \rangle (\hat{\boldsymbol{r}}_k) d\Omega_k. \tag{4.14}$$

Se calculan las componentes x y z de la velocidad de cada esfera; la componente y es nula, esto puede verse por simetría. Las esferas se deforman en forma tal que si sólo hubiera una esfera se moverían en la dirección $\hat{\boldsymbol{z}}$, ahora. Se supone que las esferas están separadas una distancia R, y el vector de separación se encuentra en el plano $z - x$, entonces las esferas no tienen porqué moverse en la dirección $\hat{\boldsymbol{y}}$. La velocidad de la esfera k se escribe en la forma

$$\boldsymbol{U}_k = U_{k,x}\hat{\boldsymbol{e}}_x + U_{k,z}\hat{\boldsymbol{e}}_z, \tag{4.15}$$

donde $U_{k,z}$ and $U_{k,x}$ son respectivamente las componentes z y x de la esfera k. En el apéndice D se dan explícitamente. Se quiere obtener la velocidad del centro de masa del sistema, que en forma adimensional es definida por la relación

$$\boldsymbol{U} = \frac{2\boldsymbol{U}_{cm}}{\omega a} = \frac{\boldsymbol{U}_1 + \boldsymbol{U}_2}{\omega a}. \tag{4.16}$$

Como se mencionó anteriormente, se quiere encontrar la maxima eficiencia de nado, bajo la condición de que las esferas nadan con la misma velocidad, es decir debe satisfacerse la ecuación

$$\boldsymbol{U}_1 - \boldsymbol{U}_2 = 0. \tag{4.17}$$

Esto se cumple si las amplitudes complejas de los desplazamientos superficiales de la segunda esfera están relacionados con los de la primera a través de la relación (D.92).

$$\underset{\sim}{\xi}^{(2)} = e^{i\varphi}\underset{\sim}{\xi}^{(1)}, \tag{4.18}$$

es decir, solo difieren por una diferencia de fase. Además las amplitudes $\underset{\sim}{\xi}^{(1)}$ deben ser de la forma

$$\xi_l^{(1)} = i^l c_l, \tag{4.19}$$

donde c_l es un número real. Se encuentra que la velocidad puede ser escrita en la forma

$$\boldsymbol{U} = \langle \underset{\sim}{\xi}^{(1)} | \underset{\approx}{B}^z | \underset{\sim}{\xi}^{(1)} \rangle \hat{\boldsymbol{e}}_z + \langle \underset{\sim}{\xi}^{(1)} | \underset{\approx}{B}^x | \underset{\sim}{\xi}^{(1)} \rangle \hat{\boldsymbol{e}}_x, \tag{4.20}$$

donde las matrices $\underset{\approx}{B}^z$ y $\underset{\approx}{B}^x$ pueden descomponerse en sus partes pares e impares:

$$\underset{\approx}{B}^k = \underset{\approx}{B}^k_e + \underset{\approx}{B}^k_o. \tag{4.21}$$

con $k = x, z$. Las matrices $\underset{\approx}{B}^k$ son matrices hermitianas, con la propiedad que sus partes impares son puramente reales, y sus partes pares puramente imaginarias (ver apéndice D). Como puede apreciarse, la velocidad depende en forma cuadrática de los desplazamientos superficiales.

En la determinación de la eficiencia de nado máxima, el problema nos lleva a que no conocemos precisamente la dirección de la velocidad $\boldsymbol{U}$. Por lo que se introduce un grado de libertad adicional y se considera la componente U_γ en una dirección dada de la velocidad que forma un ángulo γ con el eje z (ecuación (D.103)):

$$U_\gamma = U_x \sin\gamma + U_z \cos\gamma = \langle \underset{\sim}{\xi}^1 | (\underset{\approx}{B}^z \cos\gamma + \underset{\approx}{B}^x \sin\gamma) | \underset{\sim}{\xi}^1 \rangle. \tag{4.22}$$

que es de nuevo una forma cuadrática en los desplazamientos superficiales. Esto es importante ya que de ésta manera el problema de maximizar la eficiencia de nado se reducirá a encontrar el valor propio máximo de un problema de valores propios generalizado. Se puede obtener el módulo de la velocidad (numéricamente) maximizando esta componente con respecto a γ

$$U = \max_{\gamma} U_\gamma = U_{\gamma_0}. \tag{4.23}$$

De esta forma también se obtiene la desviación γ_0 del vector velocidad con respecto al eje z.

Ahora se dará el método seguido para calcular la disipación de energía media. Cabe mencionar que en un fluido incompresible, en una situación estacionaria en la que se desprecian fuerzas y torcas externas, la disipación de energía puede ser expresada como una integral sobre la superficie del fluido. Como en el presente trabajo se considera un fluido infinito, con dos cuerpos esféricos inmersos en él, la tasa de disipación de energía se escribe como la suma de dos contribuciones $\langle D_1 \rangle$ y $\langle D_2 \rangle$; cada una corresponde a la integral sobre la superficie de la esfera respectiva. La tasa de disipación de energía total en un periodo de tiempo está dada por la ecuación (D.105), que a continuación se escribe

$$\langle D \rangle = \langle D_1 \rangle + \langle D_2 \rangle. \tag{4.24}$$

Cada contribución se calcula a través de

$$\langle D_k \rangle = -\frac{1}{2} \mathrm{Re} \int_{S_0(k)} \boldsymbol{v}^{k*}_\omega \cdot \boldsymbol{\sigma}^{(k)}_\omega \cdot \boldsymbol{dS}, \tag{4.25}$$

para $k = 1, 2$. La integral se calcula sobre la superficie de la esfera k no deformada. Al calcular las integrales se encuentra que la disipación de energía puede obtenerse de la siguiente relación (ver apéndice D)

$$\langle D \rangle = \langle \xi^{(1)} | \underset{\approx}{A} | \xi^{(1)} \rangle, \tag{4.26}$$

donde la matriz $\underset{\approx}{A}$ es una matriz hermitiana, y positiva definida. Cómo se puede apreciar, la tasa de disipación de energía al igual que la velocidad depende en forma cuadrática del vector de desplazamiento superficial.

4.4 Eficiencia de nado

Se ha mostrado que la rapidez de disipación de energía y la velocidad de nado del sistema pueden expresarse como formas cuadráticas en el espacio de los coeficientes adimensionales ξ_l^1, relacionados a las amplitudes de deformación de las esferas. Por simplicidad, en lo que sigue se quitará el superíndice 1. De las ecuaciones (D.62), (D.103) y (D.118) se encuentra que la eficiencia de nado está dada por

$$\eta_T = \frac{1}{\pi} \frac{\langle \xi | (\underset{\approx}{B}^z \cos\gamma + \underset{\approx}{B}^x \sin\gamma) | \xi \rangle}{\langle \xi | \underset{\approx}{A} | \xi \rangle}. \tag{4.27}$$

donde las matrices $\underset{\approx}{B}^z$, $\underset{\approx}{B}^x$ y $\underset{\approx}{A}$ son matrices hermitianas y $\underset{\approx}{A}$ es positiva definida. De estas expresiones puede apreciarse que el problema de determinar la eficiencia de nado máxima para el problema de dos cuerpos, se reduce a calcular el valor propio máximo del problema de valores propios generalizado

$$(\underset{\approx}{B}^z \cos\gamma + \underset{\approx}{B}^x \sin\gamma) | \xi \rangle = \lambda \underset{\approx}{A} | \xi \rangle. \tag{4.28}$$

Para una disipación de energía dada, la velocidad máxima está dada por

$$\eta_T = \frac{|\lambda_{max}|}{\pi}. \tag{4.29}$$

Se ha reducido el problema de dos cuerpos, en analogía al de un solo cuerpo, a un problema de eigenvalores generalizados. Con la diferencia de que ahora las matrices son mas complicadas. En el siguiente capítulo se darán los resultados encontrados al resolver numéricamente el problema de nado. Detalles de los métodos numéricos se dan en el apéndice E.

Capítulo 5

Resultados numéricos

A continuación se darán los resultados numéricos para distintos modos de nado. Los detalles de cómo se llevan a cabo los cálculos numéricos, pueden verse en el apéndice E.

Los resultados se darán comenzando con el caso mas simple, una esfera nadando detrás de la otra, y posteriormente se darán los resultados mas generales.

Como se mencionó anteriormente el flujo es generado por las deformaciones superficiales de cada esfera y las interacciones hidrodinámicas entre ambas. En el capítulo anterior se supuso que ambas esferas tienen el mismo tipo de deformaciones, con una diferencia de fases entre ellas. Los desplazamientos superficiales correspondientes a la esfera 1 están dados por el vector

$$\boldsymbol{\xi}_\omega^1(\theta) = -\sqrt{4\pi}a \sum_{l=0}^{\infty} \xi_l \left[(l+1) P_l(\cos\theta)\hat{\boldsymbol{r}} + P_l^1(\cos\theta)\hat{\boldsymbol{\theta}} \right], \tag{5.1}$$

y para la esfera 2 por

$$\boldsymbol{\xi}_\omega^2(\theta) = e^{i\varphi}\boldsymbol{\xi}_\omega^1(\theta). \tag{5.2}$$

5.1 Una esfera detrás de la otra

Se comienza con el caso en que una esfera nada detrás de la otra.

5.1.1 Un multipolo

Aquí se va a considerar que sólo contribuye un multipolo a las deformaciones superficiales de cada esfera.

Para el problema de un solo cuerpo Felderhof y Jones demostraron que si sólo se considera un multipolo, el cuerpo no nada. Para el caso de dos cuerpos se encuentra que si se consideran los multipolos $l = 0$ o $l = 1$ la velocidad translacional de las esferas se anula. Mientras que para deformaciones con $l \geq 2$ las esferas adquieren una velocidad de nado distinta de cero. Para multipolos muy altos (del orden de $l = 30$ para $x = 0.45$, $x = a/R$) la velocidad tiende a cero. Esto puede apreciarse en la figura E.1, allí se grafica el eigenvalor máximo (que es proporcional a la eficiencia de nado) contra la fase φ entre las deformaciones de las esferas. Se puede ver que si φ toma los valores 0 o π, las esferas no se desplazan. En la figura 5.1(es igual a l figura E.1), se grafica la eficiencia de nado contra la distancia de separación de los cuerpos. Allí puede apreciarse que conforme los cuerpos se acercan uno al otro la eficiencia de nado se incrementa. Para distancias muy largas ($x \to 0$), que corresponde al caso de nado de un solo cuerpo, la eficiencia tiende a cero, es decir, las esferas no nadan. Para multipolos muy altos ($l \approx 30$) la eficiencia de nado se mantiene muy pequeña.

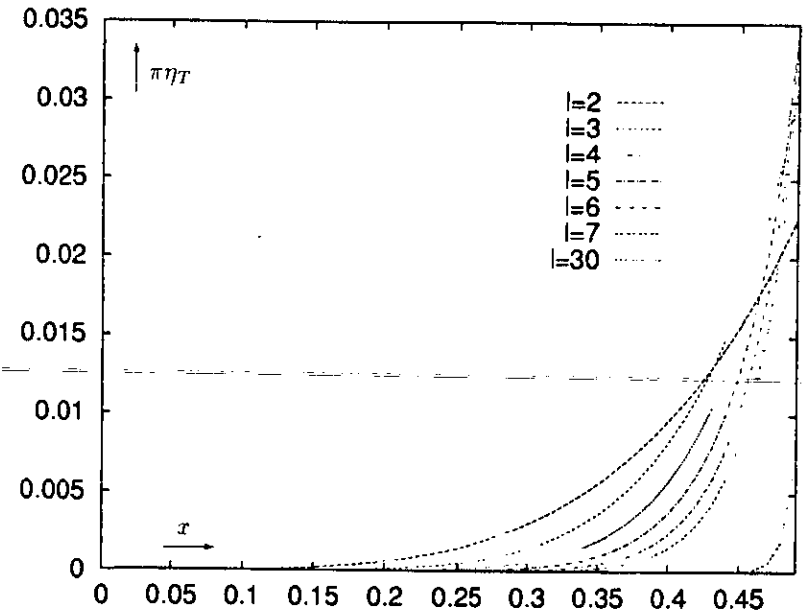

Figure 5.1: eficiencia de nado η_T para dos esferas con deformaciones descritas por dos multipolos de orden l, contra el inverso adimensional de la distancia x.

Se concluye que, siempre y cuando las deformaciones puedan ser descritas tomando en cuenta una contribución multipolar de orden l, los dos cuerpos, en contraste con uno solo, adquieren una velocidad de nado finita para $l \geq 2$. La eficiencia de nado se incrementa conforme las esferas se acercan una a la otra y su máximo se alcanza para multipolos de pequeño orden $l = 2, 3, 4, \ldots$, dependiendo de la distancia.

En las figuras 5.2 (ésta es igual a la figura E.3) y E.4, se visualizan dos modos de nado distinto, descritos cada uno por un solo multipolo $l = 2$, $l = 3$, respectivamente. Se ha seleccionado la distancia entre las esferas, para la cual, la eficiencia de nado máxima pasa de ser alcanzada en el multipolo $l = 2$ al multipolo $l = 3$, $x = 0.43$ (ver figura E.1). En otras palabras, en dicha distancia las curvas correspondientes a la máxima eficiencia de nado para los multipolos $l = 3$ y $l = 4$ se intersectan. Las gráficas muestran 24 figuras, cada una consiste de la forma de ambos cuerpos tomadas a instantes temporales igualmente espaciados en un periodo. La secuencia debe sèr leída como el texto de un libro, de izquierda a derecha, y de arriba a abajo. La dirección de nado es hacia la parte superior de la página, y la esfera 1 nada detrás de la esfera 2.

5.1.2 Dos multipolos

A continuación se consideran contribuciones de dos multipolos de orden consecutivo en las deformaciones superficiales. Por lo que se tiene

$$\xi^1_\omega(\theta) = -\sqrt{4\pi}a\left\{\xi_l\left[(l+1)P_l(\cos\theta)\hat{\boldsymbol{r}} + P^1_l(\cos\theta)\hat{\boldsymbol{\theta}}\right] + \xi_{l+1}\left[(l+2)P_{l+1}(\cos\theta)\hat{\boldsymbol{r}} + P^1_{l+1}(\cos\theta)\hat{\boldsymbol{\theta}}\right]\right\}, \tag{5.3}$$

$$\xi^2_\omega(\theta) = e^{i\varphi}\xi^1_\omega(\theta). \tag{5.4}$$

El problema de encontrar la eficiencia de nado máxima se reduce a encontrar el valor propio máximo de un problema de valores propios (ver apéndice E). En las figuras 5.3 (ésta es igual a la figura E.5) y E.6 se ha graficado la eficiencia de nado η_T contra la diferencia de fase φ entre las deformaciones de ambas esferas. Sólo se ha tomado en cuenta movimiento en la dirección z. La dependencia de la eficiencia de nado con la diferencia de fase φ es débil para multipolos muy altos: en el límite de multipolos de orden infinito la eficiencia tiende a una constante y coincide con la encontrada para el problema de un solo cuerpo. Las esferas pueden nadar en forma mas eficiente juntas para el caso de multipolos de pequeño orden, ya que c'omo se mencionó anteriormente para multipolos de orden grande el efecto

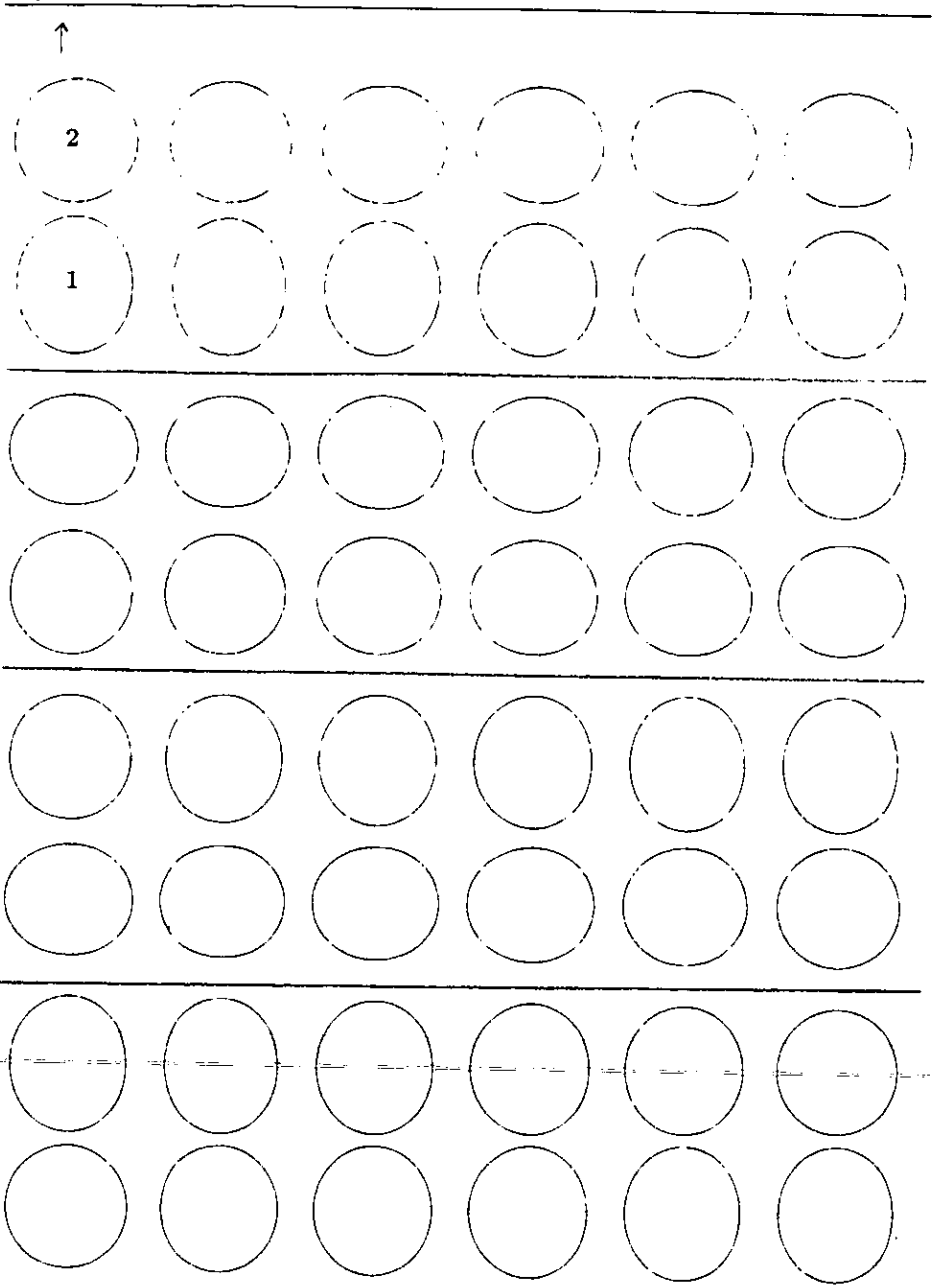

Figure 5.2: Se grafican las formas de las esferas nadando una detrás de otra correspondientes al inverso adimensional de la distancia $x = 0.43$, con deformaciones decritas por el multipolo $l = 2$, a instantes de tiempos espaciados $1/24$ en un periodo.

se puede despreciar. El que tan grande sea el orden del multipolo depende de la distancia de separación entre las esferas.

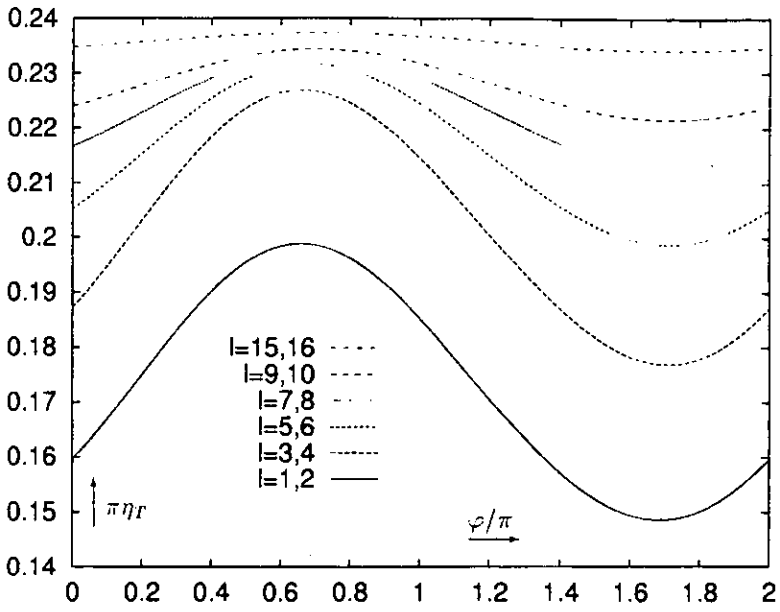

Figure 5.3: Eficiencia de nado η_T para dos esferas correspondientes al inverso de la distancia $x = 0.45$, con deformaciones descritas por dos multipolos de orden consecutivo l (impar), $l + 1$, contra la diferencia de fase φ.

La figura E.7 muestra gráficas de la eficiencia maximizada con respecto a la diferencia de fase φ, contra el inverso de la distancia de separación entre los centros de las esferas no deformadas, x. De esta figura se concluye que existen modos para los cuales los cuerpos nadan mejor en par que solos. Se puede observar que cuando las esferas se aproximan una a la otra, la eficiencia de nado se incrementa. Para los multipolos de órdenes mas bajos el incremento comienza a grandes distancias, en cambio para altos multipolos el efecto puede ser apreciado a distancia cortas. Por lo que dos esferas con multipolos de orden moderado, pueden alcanzar eficiencias para las que un sola necesitaría multipolos de órdenes muchos mas altos. Para multipolos muy altos, la eficiencia crece sólo a distancias muy cortas, donde la validez de la presente descripción se vuelve cuestionable.

Se resume que el nado de dos cuerpos esféricos, que sufren pequeñas deformaciones

superficiales como las descritas por dos multipolos de orden consecutivo, nadando uno detrás del otro a una distancia finita, con la apropiada diferencia de fase entre sus deformaciones, es más eficiente que el del nado de un sólo cuerpo, siempre y cuando el orden de los multipolos no sea muy alto, el que tan alto pueda tomarse, depende de la distancia de separación de las esferas, como se mencionó anteriormente.

5.2 Número arbitrario de multipolos y ángulo arbitrario θ_R

En la presente sección se quitan las restricciones de considerar sólo dos multipolos y que $\theta_R = 0$.

Para encontrar la forma más eficiente de nado para estas condiciones mas generales se usa un método numérico consistente encontrado por Felderhof y Jones [16]. Este valor propio máximo del problema de valores propios generalizado

$$\underset{\approx}{B}|\xi_i\rangle = \lambda_i \underset{\approx}{A}|\xi_i\rangle. \tag{5.5}$$

Este valor propio es el único que interesa, ya que lleva a la máxima eficiencia de nado de los cuerpos. Los autores mencionados utilizaron el método para el caso de un solo cuerpo. En la generalización al caso de dos cuerpos, el problema se complica, ya que la matriz $\underset{\approx}{A}$ no es diagonal y la matriz $\underset{\approx}{B}$ no es positiva definida. Sin embargo usando dos veces el método mencionado puede resolverse (ver apéndice E).

En el capítulo anterior se mencionó que para θ_R distinto de cero, es necesario primero calcular la componente U_γ de la velocidad y entonces determinar su máximo, lo que lleva a la dirección de la velocidad de las esferas con eficencia óptima. Al resolver el problema se encuentra que la máxima eficiencia de nado se alcanza para un ángulo γ_{max} muy pequeño. Debido a la inexactitud de los cálculos numéricos no es posible determinar el ángulo precisamente, pero si se puede asegurar que $\gamma_{max} < 1/500$. Por lo que la componente de la velocidad perpendicular al eje z puede ser despreciada, tomándose $\gamma = 0$. De esta manera se considera que las esferas nadan en la dirección z.

En la figura 5.4 (es igual a la figura E.8), se ha graficado la eficiencia contra el ángulo θ_R, para $x = 0.4$. Las contribuciones a las deformaciones son todos los multipolos con valores menor o igual a L, $0 \leq l \leq L$. Se observa que para un valor arbitrario del ángulo θ_R la eficiencia aumenta conforme crece el número de multipolos que contribuyen a las deformaciones superficiales. En lo que respecta a

la dependencia con θ_R, se observa que para los multipolos mas bajos $L = 1, 2$, las esferas nadan más eficientemente si lo hacen una detrás de la otra, $\theta_R = 0$, y la eficiencia decrece conforme se van aproximando a la posición de nado paralelo $\theta_R = \pi/2$. Conforme se alcanzan los multipolos de orden mayores a 2, el comportamiento cambia y la eficiencia de nado se incrementa conforme θ_R se va acercando al valor $\pi/2$.

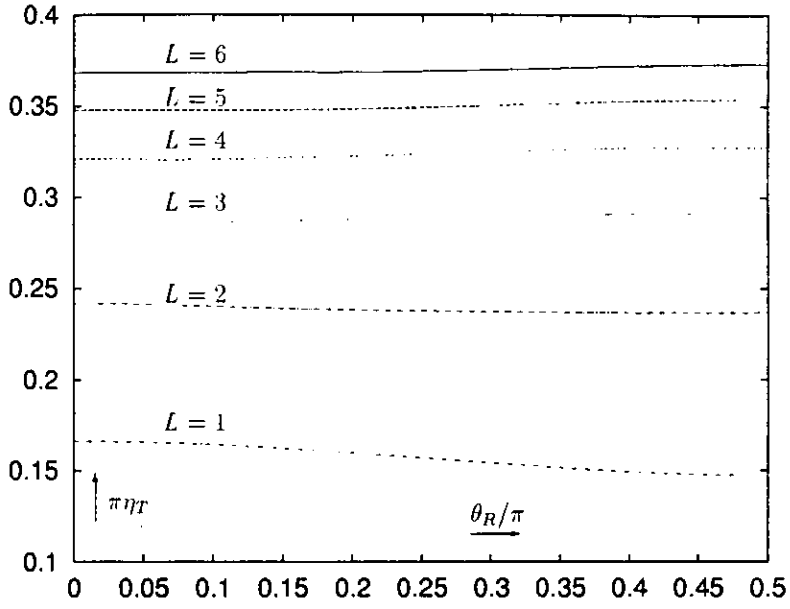

Figure 5.4: Eficiencia de nado η_T para dos esferas correspondientes al inverso adimensional de la distancia $x = 0.40$, con deformaciones descritas por multipolos de orden $l = 0, \ldots, L$, contra el ángulo θ_R.

En la figura E.9 se muestran gráficas de la eficiencia de nado contra el inverso de la distancia x entre los centros de las esferas no deformadas. Se puede ver que para todos los multipolos la eficiencia de nado se incrementa conforme los nadadores se aproximan uno al otro, aunque el efecto se debilita para multipolos muy altos, en forma semejante a los casos mencionados en las secciones anteriores.

En el apéndice E se muestran gráficas tridimensionales donde se muestra la dependencia de la eficiencia de nado con respecto a la distancia de separación de las esferas, y el ángulo θ_R, y gráficas de la eficiencia de nado con respecto al ángulo

θ_R y la diferencia de fase φ. De dichas gráficas puede concluirse que los efectos de interacción hidrodinámica entre los nadadores, conforme se van tomando en cuenta multipolos más altos, se concentra en el nado paralelo, pero desaparece para multipolos muy altos.

Este efecto puede ser explicado usando los resultados dados por Felderhof y Jones en relación al nado de un solo cuerpo. Ellos encontraron que la eficiencia de nado tiende al óptimo cuando se toma un cierto límite. Para dicha solución los desplazamientos superficiales se concentran cerca de $\theta = \pi/2$, donde θ es la medida del ángulo con respecto a la dirección de nado.

En el presente caso, se sabe que conforme se toman más multipolos, la solución se va aproximando a la de un solo cuerpo, por lo que conforme se toman más, las deformaciones superficiales se comienzan a concentrar en el ecuador de las esferas, si ellas nadan en la direción z. De este tipo de deformaciones es de esperarse que las interacciones hidrodinámicas sean más importantes cuando las esferas nadan una al lado de la otra.

Capítulo 6

Discusión y conclusiones

Se ha estudiado el nado de pequeña amplitud de dos cuerpos esféricos en un fluido viscoso e incompresible, tomando en cuenta interacción hidrodinámica entre ellos. Por nado se entiende el hecho de que los cuerpos puedan alcanzar velocidades translacionales o rotacionales debido a que sufren deformaciones superficiales.

Las cantidades básicas que se determinaron son las velocidades medias y la energía disipada por los cuerpos en un periodo de deformaciones. Lo que nos lleva a comparar la eficiencia de distintos modos de nado, cantidad definida como el cociente entre la velocidad y la disipación de energía media.

Con el fin de expresar dichas velocidades en términos de las deformaciones superficiales fué posible adoptar el método desarrollado por Felderhof y Jones para el caso de un solo cuerpo. Este método está basado en un desarrollo en términos de las amplitudes de deformación, hasta segundo orden en dichas deformaciones; a este orden, las velocidades y disipación de energía quedan completamente determinadas por las soluciones a primer orden dependientes del tiempo de las ecuaciones hidrodinámicas. Para deformaciones armónicas en el tiempo, las cantidades se expresan como formas cuadráticas en los desplazamientos superficiales, que se analizan en términos de multipolos.

En el caso de dos cuerpos se ha tomado en cuenta la interacción hidrodinámica entre ellos. Se determinan los campos de velocidad y presión, a primer orden. El problema de dos cuerpos se transforma en dos problemas acoplados de un cuerpo. Nuevamente las velocidades de cada esfera y la disipación de energía medias se expresan como formas cuadráticas, pero ahora las matrices dependen del vector de separación $\boldsymbol{R}$ entre los centros de los cuerpos no deformados, y existen más acoplamientos entre los distintos multipolos.

Con el fin de simplificar el análisis se considera flujo irrotacional a primer orden. Se considera sólo movimiento translacional.

Se define la eficiencia de nado para las dos esferas como una cantidad adimensional proporcional al doble del cociente entre la velocidad del centro de masa y la disipación de energía media total, de tal forma que coincida con la definida para un sólo cuerpo cuando las interacciones hidrodinámicas se anulen.

El optimizar la eficiencia nos lleva a un problema de eigenvalores generalizado para los desplazamientos superficiales. El eigenvalor máximo y el correspondiente eigenvector pueden ser determinados iterativamente en un subespacio finito en el espacio vectorial de las amplitudes superficiales.

Se enfoca la atención al caso en que las esferas nadan con la misma velocidad, de tal forma que la distancia de separación entre sus centros no cambie. Con el fin de satisfacer la condición que la distancia se mantenga constante, se escogen desplazamientos superficiales que tengan la misma forma en ambos cuerpos, pero con una diferencia de fase φ.

Las deformaciones se escogen en foma tal que una sola esfera (o dos separadas una distancia infinita) naden en la dirección z. Se consideró el problema para un ángulo θ_R entre esta dirección y la del vector de separación $\boldsymbol{R}$.

La maximización iterativa de la eficiencia fue llevada a cabo para valores fijos de la distancia, el ángulo θ_R y la diferencia de fase. Posteriormente la dependencia del valor máximo con respecto a dichas cantidades puede ser investigado, por ejemplo para la determinación de la mejor diferencia de fase. Para $\theta_R \neq 0$ se presentó la complicación de que no existe argumento de simetría que pueda garantizar que las esferas naden en la dirección z. Por ello fué necesario introducir el ángulo γ entre la dirección de nado y la dirección z como un parámetro adicional con respecto al cual se maximiza la eficiencia de nado. Se encontró que dentro de la precisión de los cálculos numéricos la dirección de nado óptimo coincide con la dirección z.

En contraste con el nado de una sola esfera, que puede nadar sólo si sus deformaciones se caracterizan por dos o mas multipolos, se encuentra que dos cuerpos con desplazamientos superficiales descritos solamente por un armónico esférico, adquieren una velocidad translacional a segundo orden en perturbaciones.

Considerando las deformaciones descritas por la suma de dos multipolos consecutivos, se encuentra que tanto para el caso en que se tienen monopolar y bipolar o bipolar y cuadrupolar, la eficiencia óptima es alcanzada cuando las esferas nadan una detrás de la otra. Las diferencias de fase correspondientes son cercanas a los valores $5\pi/3$ o $2\pi/3$, respectivamente. Para multipolos más altos es más eficiente

cuando las esferas nadan una al lado de la otra, con una diferencia de fase de π.

Si se consideran más multipolos también se encuentra que las esferas nadan mejor una al lado de la otra con una diferencia de fase de π.

Como el campo de velocidades dispersado por cada cuerpo decae con la distancia, y los campos con multipolos de orden alto decrecen mas rápidamente, las interacciones hidrodinámicas influyen cada vez menos en la eficiencia a grandes distancias de separación entre los cuerpos, y a distancias finitas para multipolos de orden más alto. Si se toma el límite de distancia de separación muy grande y de multipolos muy altos, se reproducen los resultados obtenidos por Felderhof y Jones para el nado de un solo cuerpo.

Se debe mencionar que el incremento en la eficiencia encontrado para dos cuerpos que nadan juntos, es importante sólo si sus deformaciones son caracterizadas por multipolos de orden moderado. Lo que significa que los organismos que nadan con multipolos bajos, y con baja eficiencia para un solo cuerpo, pueden incrementar considerablemente sus eficiencia nadando junto con otro, pero organismos que pueden alcanzar alta eficiencia de nado cuando nadan solos, con deformaciones descritas por multipolos de orden muy alto, pueden muy difícilmente incrementarla.

Con el fin de encontrar a que tipos de organismos pueden ser aplicables los resultados encontrados, se deben relacionar los multipolos cuyos órdenes son mas tangibles a criaturas físicas. Como el orden de los mutipolos es igual al número de nodos que las deformaciones tienen entre los polos de la esfera, órdenes altos significa que las deformaciones involucran una escala de longitud tangencial que es pequeña comparada con su radio. Por lo que si imaginamos microorganismos primitivos incapaces de generar campos multipolares de alto orden, se espera que tales organismos puedan nadar con una eficencia considerablemente alta cuando lo hacen en par.

Por otro lado, existen organismos que producen multipolos de orden alto realizando deformaciones de pequeña escala en sus superficies. Como de la investigación para el nado de un solo cuerpo realizada por Felderhof y Jones se sabe que la deformaciones correspondientes a multipolos de orden muy alto llevan a formas semejantes a aletas, algunos animales, tales como algún tipo de peces, pueden ser considerados en este grupo, aún cuando sus movimientos no son muy pequeños. Tales organismos alcanzan una eficiencia de nado muy alta cuando nadan solos, pero si el movimiento puede describirse con las aproximaciones del trabajo presente, podrían, aunque muy difícilmente, mejorar la eficiencia al nadar en par.

Apéndice: Versión en Inglés

Apéndice A

Introduction

It is fascinating to observe the motion of fish swimming, or that of birds flying, but it is even more interesting to try to understand how they do it. Several scientists have been working on the problem of finding the explanation for the mechanism of swimming.

What does a body do to propel itself through a fluid? For some cases, this question seems to be answered. But there is another very interesting observation, some swimmers achieve a velocity which does not correspond to their muscle power. Why, what do they do to move with so much efficiency? We can observe, too, the swimming or flying in groups, for example a flock of ducks, we can see that they fly in a peculiar formation. We may imagine that the purpose of such a formation is to fly more efficiently.

There are observations, too, of very small organisms (spermatozoa, for instance). These organisms swim very slowly, and the dynamics of swimming is quite different from that for a fish. For this kind of living bodies one observes that when they swim in a group, and two or more of them swim one closely beside the other, then the undulating motion of their tails, which they use for propulsion, begins to be in phase. Again we ask ourselves, why do they do it? Different models for this kind of motion were developed by Taylor [1], who considered also interaction, and later by other authors, but for single bodies only.

When a solid body moves in a viscous and incompressible fluid with a steady velocity, the fluid adheres to its surface, which is expressed by non slip boundary conditions to be satisfied on the surface. The fluid motion can be divided in two regimes which are characterized by the thickness of the boundary layer. The boundary layer is a thin layer adjacent to the solid body within which the vorticity varies

rapidly as a combined effect of viscous diffusion and convection [2]. In this layer the effects of viscosity are very important, and outside it the viscous effects are zero or vary only slowly. To characterize the boundary layer, the Reynolds number is defined, a dimensionless number which gives the ratio of body size to thickness of the viscous boundary layer $R = L\rho U/\eta$. Here L is a characteristic dimension and U the velocity of the body, while ρ is the mass density and η the shear viscosity of the fluid. In cases in which the body is vibrating the corresponding number is the Stokes number, which is given by $S = \omega L^2 \rho/\eta$, where ω is the vibration frequency.

In the Stokes regime, where $S << 1$, the inertia may be neglected completely, and the fluid is described by the creeping flow equations [3]. In the absence of inertia the trajectory of a swimmer is determined completely by the geometry of the sequence of shapes that the swimmer assumes and it is independent of the quickness of the motion [4, 5].

It was first shown by Taylor [1] that in the limit of zero Stokes number an infinite sheet can swim by performing wavy modulations. He extended his work to explore the reactions between tails of two neighbouring small organisms with propulsive tails. He found that if the waves of two tails are in phase much less energy is dissipated between them than if the waves are in antiphase. He introduced this model in order to explain the observations by J. Gray et. al., that very small living bodies (for example spermatozoa) swim by sending waves of lateral displacement down a thin tail. Gray also mentioned that many authors have observed that when two heads of spermatozoa are in intimate contact, their tails tend to beat synchronously [1].

The work of Taylor for the case of one sheet, was extended by A.J. Reynolds [6], who included fluid inertia and considered straining of the waving surface, and a nearby surface to the body. E.O. Tuck [7] corrected Reynolds's work, including convection effects, which Reynolds had neglected in the Navier-Stokes equations. J.E. Drummond [8] extended Taylor's work to larger amplitudes of motion of a sheet.

In the same limits the motions of a sphere were studied by Lighthill, Blake and Shapere and Wilczek [9, 10, 4]. Blake added a correction to Lighthill's paper on squirming motions of a nearly spherical body. In his paper Blake attempted to model the dynamics of ciliary propulsion. He wrote the following: "In 1675, the Dutch microscopist Leeuwenhoek was perhaps the first person to view and record the movements of cilia. In a letter to the Royal Society, he described the incredibly thin feet or little legs by which a small animal can propel itself through water. Muller, in 1876, appears to have been the first person to use the name cilia" [10]. In order

to describe the motion of these animals. Blake used a mathematical model involving an envelope. He supposed an instantaneous surface covering the end of numerous undulating cilia. In his paper he wrote that an organism called Opalina, which had been studied in detail, a flat oval-shaped organism, generates waves travelling in the same direction as the effective beat. He approximated its shape by a sphere, because this is the simplest body of finite extent.

Shapere and Wilczek generalized Blake's work. They formulated the problem in terms of a gauge field in the space of forms, and applied their results to a sphere and cylinders of arbitrary cross section and defined a notion of efficiency to determine optimal swimming strokes.

Now, in the Euler regime, outside the boundary layer, the viscous forces can be neglected, and the fluid can be considered as an ideal fluid, that is, of zero viscosity, which corresponds to the limit of high Reynolds numbers. Saffman [11] showed that a body can swim in an ideal fluid.

The mechanism of swimming at high Reynolds numbers with separation of the viscous boundary layer was described by Taylor and Lighthill. Taylor studied the swimming of animals like snakes, eels and marine worms, and idealized them by considering the equilibrium of a flexible cylinder immersed in water, with bending waves of constant amplitude travelling down it at constant velocity [12]. He assumed that the force on each element of the cylinder is the same as that which would act on a corresponding element of a long straight cylinder moving at the same velocity and inclination to the direction of motion.

Lighthill [13] tried to explain why the velocity achieved by fish or swimming mammals is very high in relation to their available muscle power. In order to understand it, it is necessary to calculate the flow outside the boundary layer. He did that considering what he called a "slender fish". This is a fish or swimming mammal, whose dimensions and movements perpendicular to its direction of motion are small compared to its length, while its cross section varies along it gradually. In his work he considered a slender fish performing swimming movements only in a single direction perpendicular to its direction of motion. He determined movements producing thrust with a small vortex drag penalty and made some remarks on the boundary layer development which they might induce.

T. Yao Tsu Wu [14] studied the propulsion of a fish considering high Reynolds numbers with the imposition of the Kutta condition in a sharp trailing edge.

B.U. Felderhof and R.B. Jones [15], considered the mechanism of swimming for arbitrary Stokes number S, but small amplitude of deformations. They considered

a simply connected body of arbitrary shape immersed in a viscous incompressible fluid and included the possibility of a mean rotational motion. A nonvanishing swimming velocity is obtained at second order in perturbation theory. For harmonic time variation they gave a natural definition of the swimming efficiency which is essentially the quotient of the average velocity and the average rate of energy dissipation. They presented in detail two explicit examples in which at first order the flow velocity is irrotational. In a second paper [16] they applied the theory to a spherical body with a surface displacement varying harmonically in time. They expressed the translational velocity and the rate of energy dissipation, averaged over a period, as quadratic forms in the surface displacement. The swimming efficiency is thus given as the ratio of these quadratic forms. Its optimum can be calculated from the maximum eigenvalue of a generalized eigenvalue problem involving hermitian matrices.

In the present work we are going to use the results found by Felderhof and Jones to describe the swimming of two spherical bodies. The objective of the present work is the investigation of the joint swimming of two deformable spherical bodies in a viscous incompressible fluid. We are particularly interested in the conditions under which they swim more efficiently than they would on their own, and we shall try to find the optimum swimming mode for translational swimming.

Since joint swimming in a stationary situation implies that the relative position of the bodies does not change, we have to find swimming modes leading to equal velocities of both spheres, with the hydrodynamic interaction taken into account. We are going to show that a simple possibility to satisfy this requirement is to assume the same kind of deformations for both spheres, but with a delay or phase difference. We are going to solve the problem for arbitrary Stokes number, but small amplitude of deformations, and we suppose that the first order velocity field may be described as potential flow. Since the hydrodynamic two-sphere problem is not solved in closed form, we are going to use an approximate method to determine the swimming velocity.

In the first chapter, we give a brief introduction to hydrodynamics with the aim of providing the basic ideas and equations necessary for the understanding of the present work.

In the second chapter, we summarize the analysis of the related one-body problem by Felderhof and Jones so that we can use the expressions found by them for the average swimming velocity of each sphere and the energy dissipation. Also we want to adapt their methods for the determination of the maximum efficiency to the two-

body case, and last but not least we need their results for comparison of joint and separate swimming.

In the third chapter, we solve the two-body problem in analytic form. We calculate the first order flow velocity and pressure, and hence the swimming velocity of each sphere, averaged over a period, and the rate of energy dissipation of the system. We extend the definition of the swimming efficiency to the two-body problem.

In the fourth chapter, we state the numerical methods used to determine the maximum swimming efficiency and the corresponding swimming modes, and we present the results.

Finally, we draw the conclusions and point out the perspectives of the work.

Apéndice B

Brief Introducion to Hydrodynamics

For a better understanding of the present work, we want to give a brief introduction to hydrodynamics. We are not going to go into the details, because these can be found in many textbooks, but we think we should mention some basic aspects and known results concerning the present problem.

B.1 Navier-Stokes Equation

From the point of view of fluid dynamics, a fluid is considered as a continuous medium. This means that if we consider any volume of fluid, even a small one, it is assumed to be always large enough to contain a very great number of molecules. Taking this into account, in fluid dynamics the terms particle of fluid or point of fluid mean small volumes of fluid, which are mathematically treated as infinitesimal, but which in reality are nevertheless large in comparison with the distance between the molecules [17].

The mathematical description of the state of a moving fluid is effected by means of functions which give the distribution of the fluid velocity $\boldsymbol{v}(\boldsymbol{r}, t)$ and any two thermodynamic quantities, for example the density of the fluid $\rho(\boldsymbol{r}, t)$ and its pressure $p(\boldsymbol{r}, t)$. All the thermodynamic quantities can be determined if we know any two of them and the equation of state [17]. Then, if we give the three components of the velocity, the pressure and the density, the state of the fluid motion is determined completely.

In the present work, we are interested in the description of solid bodies moving

in a viscous incompressible fluid. A fluid is considered to be incompressible if the mass density in each volume element is constant throughout its motion.

There exist two different specifications to describe the motion of a fluid. These are called the Eulerian and the Lagrangian specification.

The Eulerian specification is like that of an electromagnetic field in that the flow quantities are defined as functions of position $\boldsymbol{r}$ in space and of time t. The primary flow quantity is the velocity of the fluid $\boldsymbol{v}(\boldsymbol{r},t)$. This specification can be thought of as providing a picture of the flow quantities at each instant during the motion.

In the Lagrangian specification, we consider a selected element of fluid and describe its dynamic history. The flow quantities are described as functions of time and of the choice of the fluid element. The primary flow quantity, according to the Lagrangian specification is the velocity $\boldsymbol{v}(\boldsymbol{a},t)$, where $\boldsymbol{a}$ is the position of the center of mass of the specified fluid element at some initial time t_0. Here it is understood that the initial linear dimensions of the element are so small as to guarantee smallness at all relevant subsequent instants in spite of distortion and extension of the element [2].

The equations which describe the motion of a viscous fluid in the Euler picture are the Navier-Stokes and continuity equations, which for an incompressible fluid take the form

$$\rho\left[\frac{\partial \boldsymbol{v}}{\partial t}+(\boldsymbol{v}\cdot\nabla)\boldsymbol{v}\right]=\eta\nabla^2\boldsymbol{v}-\nabla p, \qquad \nabla\cdot\boldsymbol{v}=0. \tag{B.1}$$

The field quantities describing the motion of the fluid are its velocity $\boldsymbol{v}$ and pressure p, they depend on position and time. The dynamic viscosity η and, in the incompressible case, the mass density ρ are parameters characterising the fluid. The above equations can be derived considering some volume V_0, and applying to it the principles of conservation of momentum and mass to get the Navier-Stokes and the continuity equation, respectively.

The flux of momentum is represented by the stress tensor, which for a viscous fluid is given by

$$\sigma_{ij}=-p\delta_{ij}+\eta\left(\frac{\partial v_i}{\partial x_j}+\frac{\partial v_j}{\partial x_i}\right). \tag{B.2}$$

If we consider a solid body moving in a viscous fluid, we must give the boundary conditions to be satisfied together with the equations of motion. In the case of interactions between a viscous fluid and a solid body there always appear forces of molecular atraction between the fluid and the surface of the solid body, and as a consequence of these forces, the fluid layer immediately adjacent to the surface of

the body adheres to it. Thus the velocity of a viscous fluid vanishes at the boundary with a solid body which is at rest:

$$v|_s = 0. \tag{B.3}$$

This is called the stick boundary condition. In the general case of a moving surface the fluid velocity must be equal to the velocity of the surface [17].

B.2 Energy Dissipation

In a viscous fluid the presence of viscosity results in dissipation of energy, which finally is transformed into heat. In order to calculate the energy dissipation in an incompressible fluid, we look at its total kinetic energy, which is given by

$$E_{kin} = \frac{\rho}{2} \int v^2 d\boldsymbol{r}. \tag{B.4}$$

Due to viscosity of the fluid, its kinetic energy decreases. The loss rate is called dissipation and denoted by

$$D(t) = -\dot{E}_{kin}, \tag{B.5}$$

where the dot denotes the time derivative $\frac{\partial}{\partial t}$. In order to determine the dissipation we write $\partial \rho v^2/2\partial t = \rho v_i \partial v_i/\partial t$ in the time derivative of the kinetic energy, and substitute for $\partial v_i/\partial t$ from the Navier-Stokes equation (for details see [17]). This expression is then used in the integral, which is evaluated over the whole volume occupied by the fluid. Hence it is found that the dissipation is given by

$$D(t) = \frac{\eta}{2} \int \left(\frac{\partial v_i}{\partial x_k} + \frac{\partial v_k}{\partial x_i} \right)^2 d\boldsymbol{r} = 2\eta \int (\nabla \boldsymbol{v}(\boldsymbol{r},t))^s : (\nabla \boldsymbol{v}(\boldsymbol{r},t))^s d\boldsymbol{r}, \tag{B.6}$$

where in the first expression we employ the sum convention, thus the square implies the double sum over the subscripts, and in the second the superscript indicates the symmetrization of the tensor. Since dissipation leads to a decrease in kinetic energy, the viscosity η is positive.

The above integrand may alternatively be expressed as

$$\frac{\eta}{2} \left(\frac{\partial v_i}{\partial x_k} + \frac{\partial v_k}{\partial x_i} \right)^2 = \frac{\partial}{\partial x_i} (\sigma_{ik} v_k) - \left(\frac{\partial}{\partial x_i} \sigma_{ik} \right) v_k = \nabla \cdot (\boldsymbol{\sigma} \cdot \boldsymbol{v}) - (\nabla \cdot \boldsymbol{\sigma}) \cdot \boldsymbol{v}. \tag{B.7}$$

Thus if we consider now a stationary situation, where there are no external forces or torques, the divergence of the stress tensor vanishes, $\nabla \cdot \boldsymbol{\sigma} = 0$, and the above volume integral may be converted into a surface integral:

$$D = \int_S \boldsymbol{v} \cdot \boldsymbol{\sigma} \cdot \hat{\boldsymbol{n}}\, dS. \tag{B.8}$$

with $\hat{\boldsymbol{n}}$ the outwardly directed normal to S. An analogous relation holds for the average rate of dissipation for the case of fields periodic in time.

In the case of an infinitely extended fluid in contact with solid bodies, which may be in a state of constant motion, its surface is made up of the bodies' surfaces. The interpretation of the surface integral may thus be that the energy dissipated in the fluid must be compensated by the energy passed to the fluid by the bodies in order to maintain their motion.

B.3 Navier-Stokes Equation in a Rotating System of Reference

For problems where the external boundary of a fluid is in motion, it is convenient to choose a coordinate system where the boundary is at rest. This implies a transformation of the Navier-Stokes equation to the new system. In the following we are going to transform the equation of motion to a system which is rotating about a fixed point O in the inertial laboratory frame with constant angular velocity $\boldsymbol{\Omega}$. To this end, we must find the relation between the acceleration $\boldsymbol{a}_O$ with respect to the inertial system to that with respect to the rotating frame.

We denote the position of a fluid element with respect to the inertial frame by $\boldsymbol{r}_O$. It is the same in both frames and may be expressed in terms of the unit vectors $\hat{\boldsymbol{e}}_i$ ($i = 1, 2, 3$), fixed in the rotating system, as

$$\boldsymbol{r}_O = \boldsymbol{r} = x_i \hat{\boldsymbol{e}}_i. \tag{B.9}$$

The velocity $\boldsymbol{v}_O$ and acceleration $\boldsymbol{a}_O$ with respect to the inertial frame are defined as the first and second time-derivative of the position. In the rotating frame, we must take into account the change of the unit vectors due to the rotation of the system, which is given by

$$\frac{d\hat{\boldsymbol{e}}_i}{dt} = \boldsymbol{\Omega} \times \hat{\boldsymbol{e}}_i. \tag{B.10}$$

We find (using Leibniz's formula for the second derivative):

$$\boldsymbol{v}_O = \frac{d\boldsymbol{r}_O}{dt} = v_i\hat{\boldsymbol{e}}_i + x_i\boldsymbol{\Omega}\times\hat{\boldsymbol{e}}_i, \tag{B.11}$$

$$\boldsymbol{a}_O = \frac{d^2\boldsymbol{r}_O}{dt^2} = a_i\hat{\boldsymbol{e}}_i + 2v_i\boldsymbol{\Omega}\times\hat{\boldsymbol{e}}_i + x_i\boldsymbol{\Omega}\times(\boldsymbol{\Omega}\times\hat{\boldsymbol{e}}_i), \tag{B.12}$$

where

$$v_i = \frac{dx_i}{dt}, \tag{B.13}$$

$$a_i = \frac{d^2x_i}{dt^2} \tag{B.14}$$

are the components of the velocity $\boldsymbol{v}$ and acceleration $\boldsymbol{a}$ with respect to the rotating frame. Thus, the desired relations are

$$\boldsymbol{v}_O = \boldsymbol{v} + \boldsymbol{\Omega}\times\boldsymbol{r}, \tag{B.15}$$

$$\boldsymbol{a}_O = \boldsymbol{a} + 2\boldsymbol{\Omega}\times\boldsymbol{v} + \boldsymbol{\Omega}\times(\boldsymbol{\Omega}\times\boldsymbol{r}), \tag{B.16}$$

In terms of the velocity $\boldsymbol{v}(\boldsymbol{r},t)$ relative to the rotating system, in the Eulerian specification, we have

$$\boldsymbol{a} = \frac{\partial\boldsymbol{v}}{\partial t} + \boldsymbol{v}\cdot\nabla\boldsymbol{v}. \tag{B.17}$$

Thus the Navier-Stokes equation in the rotating system is identical in form to that in the inertial system if we include a ficticious force density

$$\boldsymbol{f} = -2\rho\boldsymbol{\Omega}\times\boldsymbol{v} - \rho\boldsymbol{\Omega}\times(\boldsymbol{\Omega}\times\boldsymbol{r}). \tag{B.18}$$

acting upon the fluid in addition to the real forces. The first term, $-2\rho\boldsymbol{\Omega}\times\boldsymbol{v}$ is the Coriolis force, which is perpendicular to both the velocity $\boldsymbol{v}$ and the angular velocity $\boldsymbol{\Omega}$, and the second term, $-\rho\boldsymbol{\Omega}\times(\boldsymbol{\Omega}\times\boldsymbol{r})$, is the centrifugal force. Since the angular velocity $\boldsymbol{\Omega}$ does not depend on position, the centrifugal force can be written as the gradient of a potential,

$$-\boldsymbol{\Omega}\times(\boldsymbol{\Omega}\times\boldsymbol{r}) = \frac{1}{2}\nabla(\boldsymbol{\Omega}\times\boldsymbol{r})^2, \tag{B.19}$$

and can be included in the pressure term.

Thus we finally arrive at the Navier-Stokes equation in the rotating system:

$$\rho\left[\frac{\partial\boldsymbol{v}}{\partial t} + (\boldsymbol{v}\cdot\nabla)\boldsymbol{v} + 2\boldsymbol{\Omega}\times\boldsymbol{v}\right] = \eta\nabla^2\boldsymbol{v} - \nabla p', \qquad \nabla\cdot\boldsymbol{v} = 0, \tag{B.20}$$

where

$$p' = p - \frac{\rho}{2}(\boldsymbol{\Omega}\times\boldsymbol{r})^2, \tag{B.21}$$

is the modified pressure which contains the centrifugal force.

Apéndice C

Solution of the One Body Problem

In this chapter we report the results obtained by B.U. Felderhof and R.B. Jones in the investigation of small-amplitude swimming of a single deformable sphere in an incompressible infinite fluid described by the Navier-Stokes equations.

The surface deformations are assumed to be harmonic in time. The theory is based on a perturbation expansion in powers of the amplitude of surface deformations. Felderhof and Jones found that at second order the body acquires a nonvanishing swimming velocity. They gave a natural definition of the swimming efficiency. We are interested in the calculation of this quantity.

C.1 Basic Equations

In this section we formulate the equations governing the problem of swimming. We consider a spherical body of radius a immersed in an incompressible fluid of infinite extent, with shear viscosity η and mass density ρ. The body performs variations of shape harmonic in time. Due to the boundary conditions to be satisfied on the surface of the body, a flow pattern is produced. In return, this acts on the body which thus is displaced through the fluid.

The translational and rotational velocities of the sphere, time-averaged over a period T of deformation, are denoted by $\boldsymbol{U}$ and $\boldsymbol{\Omega}$, respectively. Since the sphere translates and rotates, while its surface is deforming, it is convenient to choose a reference system which moves with rigid motion, in which on average the body is at rest. We call this system K_0, and we choose the origin of it in the center of the undeformed sphere. With this treatment, the mechanical equation of motion must include centrifugal and Coriolis terms. As was explained in the previous chapter,

the centrifugal force can be included in the pressure, and the Coriolis term must be added to the equation .

The field velocity $\boldsymbol{v}(\boldsymbol{r},t)$ and the pressure $p(\boldsymbol{r},t)$ of the fluid are assumed to satisfy the Navier-Stokes equation, which, as valid in the reference system K_0, is given by (B.20)

$$\rho\left(\frac{\partial \boldsymbol{v}}{\partial t}+(\boldsymbol{v}\cdot\nabla)\boldsymbol{v}+2\boldsymbol{\Omega}\times\boldsymbol{v}\right)=\eta\nabla^2\boldsymbol{v}-\nabla p. \qquad \nabla\cdot\boldsymbol{v}=0. \tag{C.1}$$

Here, p is the modified pressure containing the centrifugal potential. In eqn. (B.21) this was indicated by a prime, which we shall drop here.

The position of a chosen point on the surface of the sphere, labelled by the polar and azimuthal angles with respect to the undeformed body θ and φ, respectively, is given as

$$\boldsymbol{r}_S(\theta,\varphi,t)=a\hat{\boldsymbol{r}}+\boldsymbol{\xi}(\theta,\varphi,t), \tag{C.2}$$

where $\hat{\boldsymbol{r}}$ is the radial unit vector, and $\boldsymbol{\xi}$ is the displacement vector.

At the surface of the sphere, the fluid satisfies stick boundary conditions. This requires that the fluid velocity must be equal to the velocity of the surface of the body:

$$\boldsymbol{v}(\boldsymbol{r}_S,t)=\frac{\partial \boldsymbol{r}_S}{\partial t}. \tag{C.3}$$

and we find

$$\boldsymbol{v}(\boldsymbol{r}_S,t)=\frac{\partial \boldsymbol{\xi}}{\partial t}. \tag{C.4}$$

To solve the problem we must as well consider the condition to be satisfied at infinity. The flow velocity tends to

$$\boldsymbol{v}(\boldsymbol{r},t)\approx -\boldsymbol{U}-\boldsymbol{\Omega}\times\boldsymbol{r} \qquad \text{as} \quad r\to\infty, \tag{C.5}$$

and from the equations (C.1) and (C.5), we get the asymptotic behavior of the pressure

$$p(\boldsymbol{r},t)\approx p_0+\rho(\boldsymbol{\Omega}\times\boldsymbol{U})\cdot\boldsymbol{r}-\frac{\rho}{2}(\boldsymbol{\Omega}\times\boldsymbol{r})^2 \qquad \text{as} \qquad r\to\infty, \tag{C.6}$$

where p_0 is the pressure in absence of any motion.

C.2 Small Amplitude Swimming

Solving the nonlinear equation exactly is beyond hope. There are several methods which help to find an approximate solution, we are going to use in this case regular perturbation theory. Felderhof and Jones used the ratio ξ/a as the perturbation parameter. They constructed an approximate solution to equation (C.1) with boundary conditions (C.4) by formal expansion of the velocity field and pressure in powers of $\xi = |\boldsymbol{\xi}|$, writing

$$\boldsymbol{v} = \boldsymbol{v}_1 + \boldsymbol{v}_2 + \cdots, \qquad p = p_0 + p_1 + p_2 + \cdots. \tag{C.7}$$

where the subscript refers to the power of ξ. Correspondingly, the translational and rotational velocities are expanded as

$$\boldsymbol{U} = \boldsymbol{U}_1 + \boldsymbol{U}_2 + \cdots, \qquad \boldsymbol{\Omega} = \boldsymbol{\Omega}_1 + \boldsymbol{\Omega}_2 + \cdots. \tag{C.8}$$

Now, the velocity field at the surface of the sphere can be formally expanded as

$$\boldsymbol{v}(a\hat{\boldsymbol{r}} + \boldsymbol{\xi}) = \boldsymbol{v}(a\hat{\boldsymbol{r}}, t) + (\boldsymbol{\xi} \cdot \nabla)\, \boldsymbol{v}(\boldsymbol{r}, t)\Big|_{r=a} + \cdots. \tag{C.9}$$

With the help of this expansion, the boundary condition can be applied to the undeformed surface.

To first order the equation of motion reduces to the linearized Navier-Stokes equation

$$\rho \frac{\partial \boldsymbol{v}_1(\boldsymbol{r}, t)}{\partial t} = \eta \nabla^2 \boldsymbol{v}_1(\boldsymbol{r}, t) - \nabla p_1(\boldsymbol{r}, t), \qquad \nabla \cdot \boldsymbol{v}_1(\boldsymbol{r}, t) = 0. \tag{C.10}$$

with the first order boundary condition

$$\boldsymbol{v}_1(a\hat{\boldsymbol{r}}, t) = \frac{\partial \boldsymbol{\xi}(a\hat{\boldsymbol{r}}, t)}{\partial t}. \tag{C.11}$$

In order to find the translational velocity averaged over a period T and the mean rotational velocity, we perform a time average of the first order equations and boundary conditions. We obtain the field equations

$$\eta \nabla^2 \langle \boldsymbol{v}_1 \rangle(\boldsymbol{r}) - \nabla \langle p_1 \rangle(\boldsymbol{r}) = 0, \qquad \nabla \cdot \langle \boldsymbol{v}_1 \rangle(\boldsymbol{r}) = 0, \tag{C.12}$$

and the boundary condition

$$\langle \boldsymbol{v}_1 \rangle(a\hat{\boldsymbol{r}}) = 0. \tag{C.13}$$

These equations constitute a Stokes problem. By the assumption that there are no external forces acting on the body, the equations have the trivial solution

$$\langle \boldsymbol{v}_1 \rangle(\boldsymbol{r}) = 0, \qquad \langle p_1 \rangle(\boldsymbol{r}) = 0. \tag{C.14}$$

The first order velocities $\boldsymbol{U}_1$ and $\boldsymbol{\Omega}_1$ vanish: the sphere does not swim to first order. The field velocity $\boldsymbol{v}_1(\boldsymbol{r},t)$ and the pressure $p_1(\boldsymbol{r},t)$ tend to zero at infinity.

To second order the equation of motion is given by

$$\rho\left(\frac{\partial \boldsymbol{v}_2(\boldsymbol{r},t)}{\partial t}+\boldsymbol{v}_1(\boldsymbol{r},t)\cdot\nabla\boldsymbol{v}_1(\boldsymbol{r},t)\right)=\eta\nabla^2\boldsymbol{v}_2(\boldsymbol{r},t)-\nabla p_2(\boldsymbol{r},t).$$
$$\nabla\cdot\boldsymbol{v}_2(\boldsymbol{r},t)=0. \tag{C.15}$$

The boundary condition at second order is written as

$$\boldsymbol{v}_2(a\hat{\boldsymbol{r}},t)=-(\boldsymbol{\xi}(\hat{\boldsymbol{r}},t)\cdot\nabla)\boldsymbol{v}_1(\boldsymbol{r},t)\Big|_{r=a}. \tag{C.16}$$

We want to find the second order translational and rotational swimming velocities $\boldsymbol{U}_2$ and $\boldsymbol{\Omega}_2$. To that purpose it is not necessary to solve the complete second order problem, we only need to solve the average equations. The average equation of motion is given by

$$\eta\nabla^2\langle\boldsymbol{v}_2\rangle(\boldsymbol{r})-\nabla\langle p_2\rangle(\boldsymbol{r})=\rho\langle\boldsymbol{v}_1\cdot\nabla\boldsymbol{v}_1\rangle(\boldsymbol{r}),\qquad\nabla\cdot\langle\boldsymbol{v}_2\rangle(\boldsymbol{r})=0. \tag{C.17}$$

The time-averaged second order boundary condition is

$$\langle\boldsymbol{v}_2\rangle(a\hat{\boldsymbol{r}})=\langle-(\boldsymbol{\xi}\cdot\nabla)\boldsymbol{v}_1\rangle(a\hat{\boldsymbol{r}}). \tag{C.18}$$

The second order pressure p_2 tends to zero at infinity. The averaged field velocity tends to

$$\langle\boldsymbol{v}_2(\boldsymbol{r})\rangle\approx-\boldsymbol{U}_2-\boldsymbol{\Omega}_2\times\boldsymbol{r}\qquad\text{as}\quad r\to\infty. \tag{C.19}$$

As we see, the right hand side of the equations (C.17) and (C.18) can be found from the first order equations. The second order velocities can be found from the behavior at infinity (C.19). For the complete determination of the average second order flow $\langle\boldsymbol{v}_2\rangle,\langle p_2\rangle$ it is necessary to use the condition that on average there is no net flow of momentum or angular momentum towards infinity.

C.3 Body and Surface Contributions

Before we continue with the solution of the averaged equations of motion, we shall explain the distinction between body and surface contributions. There are two kinds of forces which act on a body. To the first group belong the long-range forces, these forces decrease slowly with the distance, they penetrate a fluid and are capable of acting on all its elements. An example of such a force is the gravitation. Others are

the fictitious centrifugal and Coriolis forces introduced in the equation of motion in a rotating reference system. The long-range forces which act on an element of fluid are proportional to the volume of the element, thus they are called body forces. The second group are the short-range forces, they have mocular origin and decrease very quickly with the distance between interacting elements. If an element of fluid is acted on by such forces which are produced by the interaction between the fluid and an external body (a solid) outside this element, these forces can act only on a very thin layer adjacent to the boundary of the element of fluid. In order to calculate the short-range forces acting on an element it is necessary to consider the surface of the element, the volume is irrelevant. This kind of forces is called surface forces [2].

Now we return to the problem of swimming. Felderhof and Jones found that the second order problem can be divided conveniently into two parts, one corresponding to the surface contribution, and the other to the body contribution. They defined the following surface velocity

$$\boldsymbol{u}_S(\hat{\boldsymbol{r}},t) = -\boldsymbol{\xi}(\hat{\boldsymbol{r}},t)\cdot\nabla\boldsymbol{v}_1(\boldsymbol{r},t)\Big|_{r=a}. \tag{C.20}$$

The second order time-averaged solution is written as the sum

$$\langle\boldsymbol{v}_2\rangle = \langle\boldsymbol{v}_{2B}\rangle + \langle\boldsymbol{v}_{2S}\rangle, \qquad \langle p_2\rangle = \langle p_{2B}\rangle + \langle p_{2S}\rangle. \tag{C.21}$$

The subscripts $2S$ and $2B$ correspond to the surface and volumetric contributions, respectively. The swimming velocities $\boldsymbol{U}_2$ and $\boldsymbol{\Omega}_2$ are decomposed as

$$\boldsymbol{U}_2 = \boldsymbol{U}_{2B} + \boldsymbol{U}_{2S}, \qquad \boldsymbol{\Omega}_2 = \boldsymbol{\Omega}_{2B} + \boldsymbol{\Omega}_{2S}, \tag{C.22}$$

respectively. From the second order equation of motion and the second order boundary conditions we obtain separate equations for the body contribution and for the surface contribution with the respective boundary conditions.

The surface contributions satisfy the equations

$$\eta\nabla^2\langle\boldsymbol{v}_{2S}\rangle - \nabla\langle p_{2S}\rangle = 0, \qquad \nabla\cdot\langle\boldsymbol{v}_{2S}\rangle = 0. \tag{C.23}$$

with boundary condition

$$\langle\boldsymbol{v}_{2S}\rangle(a\hat{\boldsymbol{r}}) = \langle\boldsymbol{u}_S\rangle(\hat{\boldsymbol{r}}). \tag{C.24}$$

The bulk contributions satisfy

$$\eta\nabla^2\langle\boldsymbol{v}_{2B}\rangle - \nabla\langle p_{2B}\rangle = \rho\langle(\boldsymbol{v}_1\cdot\nabla)\boldsymbol{v}_1\rangle, \qquad \nabla\cdot\langle\boldsymbol{v}_2\rangle = 0. \tag{C.25}$$

with boundary condition

$$\langle\boldsymbol{v}_{2B}\rangle(a\hat{\boldsymbol{r}}) = 0. \tag{C.26}$$

C.4 Irrotational Flow

In the following we are going to specialize to irrotational first order flow. The dynamic properties of the flow for a simply connected body were given by Felderhof and Jones, the details of the analysis of the equations presented in the last section, were given by them in [15]. In the present work we report their equations because the knowledge of these is essential in order to understand the problem of two swimming bodies. The details of the analysis of the dynamics can be studied in the mentioned paper. Here we are going to report the more important results that can be applied to the two-body problem.

For the two-body problem we shall restrict ourselves to potential flow at first order. Thus we must find the case of a surface deformation $\boldsymbol{\xi}(\hat{\boldsymbol{r}}.t)$ for which the first order flow velocity $\boldsymbol{v}_1(\boldsymbol{r},t)$ is irrotational, $\nabla \times \boldsymbol{v}_1(\boldsymbol{r},t) = 0$. This implies that the velocity $\boldsymbol{v}_1(\boldsymbol{r},t)$ can be written as the gradient of a potential:

$$\boldsymbol{v}_1(\boldsymbol{r},t) = \nabla\phi_1(\boldsymbol{r},t), \tag{C.27}$$

(which leads to the name of potential flow). From the continuity equation we then find that the potential satisfies Laplace's equation:

$$\nabla^2\phi_1(\boldsymbol{r},t) = 0. \tag{C.28}$$

The potential is assumed to vanish at infinity. The first order pressure can be derived by inserting equation (C.27) into the first order equation of motion (C.10), we obtain

$$p_1(\boldsymbol{r},t) = -\rho\frac{\partial\phi_1(\boldsymbol{r},t)}{\partial t}. \tag{C.29}$$

It is found that for potential flow at first order, the body contributions to the velocities vanish. This can be derived from equations (C.25) and (C.26). We get

$$\langle \boldsymbol{v}_{2B}\rangle(\boldsymbol{r}) = 0, \qquad \langle p_{2B}\rangle(\boldsymbol{r}) = -\frac{\rho}{2}\langle \boldsymbol{v}_1^2\rangle, \tag{C.30}$$

which implies a mere change of pressure. Now we find immediately

$$\boldsymbol{U}_{2B} = 0, \qquad \boldsymbol{\Omega}_{2B} = 0. \tag{C.31}$$

In the following we shall consider only surface contributions.

C.5 Harmonic Variation

Let us consider in particular displacement functions which vary harmonically in time with frequency $\omega = 2\pi/T$. It is convenient to introduce complex notation. The surface displacement is written as

$$\boldsymbol{\xi}(\theta,\varphi,t) = \mathrm{Re}\left\{\boldsymbol{\xi}_\omega(\theta,\varphi)e^{-i\omega t}\right\}, \tag{C.32}$$

with complex amplitude $\boldsymbol{\xi}_\omega(\theta,\varphi)$. The corresponding first order flow velocity and pressure are given by

$$\boldsymbol{v}_1(\boldsymbol{r},t) = \mathrm{Re}\left\{\boldsymbol{v}_\omega(\boldsymbol{r})e^{-i\omega t}\right\}, \qquad p_1(\boldsymbol{r},t) = \mathrm{Re}\left\{p_\omega(\boldsymbol{r})e^{-i\omega t}\right\}. \tag{C.33}$$

From equation (C.20), we find that the time-averaged surface velocity becomes

$$\langle \boldsymbol{u}_S(\hat{\boldsymbol{r}})\rangle = -\frac{1}{2}\mathrm{Re}\left\{\boldsymbol{\xi}_\omega^* \cdot \nabla \boldsymbol{v}_\omega\right\}\Big|_{r=a}. \tag{C.34}$$

C.6 Velocity and Dissipation

The equation of motion (C.23) for the surface contribution of the average second-order field is the linearized Navier-Stokes equation for steady, incompressible flow. A complete set of solutions of this equation appropriate to spherical symmetry was given by H. Lamb [18], [3, p. 62]. Here we use (except for normalization factors) the solutions $\{\boldsymbol{v}^{\pm}_{lm\sigma}, p^{\pm}_{lm\sigma}\}$ as formulated by B. Cichocki, B.U. Felderhof and R. Schmitz [19]:

$$\begin{aligned}
\boldsymbol{v}^{+}_{lm0}(\boldsymbol{r}) &= r^{l-1}\boldsymbol{A}_{lm}(\hat{\boldsymbol{r}}), \quad p^{+}_{lm0}(\boldsymbol{r}) = 0,\\
\boldsymbol{v}^{+}_{lm1}(\boldsymbol{r}) &= ir^{l}\boldsymbol{C}_{lm}(\hat{\boldsymbol{r}}), \quad p^{+}_{lm1}(\boldsymbol{r}) = 0,\\
\boldsymbol{v}^{+}_{lm2}(\boldsymbol{r}) &= r^{l+1}\left[\frac{(l+1)(2l+3)}{2l}\boldsymbol{A}_{lm}(\hat{\boldsymbol{r}}) + \boldsymbol{B}_{lm}(\hat{\boldsymbol{r}})\right],\\
p^{+}_{lm2}(\boldsymbol{r}) &= \eta\frac{(l+1)(2l+1)(2l+3)}{l}r^{l}Y_{lm}(\hat{\boldsymbol{r}}).
\end{aligned} \tag{C.35}$$

$$\begin{aligned}
\boldsymbol{v}^{-}_{lm0}(\boldsymbol{r}) &= \frac{1}{(2l+1)^2}r^{-l}\left[\frac{l+1}{l(2l-1)}\boldsymbol{A}_{lm}(\hat{\boldsymbol{r}}) - \frac{1}{2}\boldsymbol{B}_{lm}(\hat{\boldsymbol{r}})\right],\\
p^{-}_{lm0}(\boldsymbol{r}) &= \eta\frac{1}{2l+1}r^{-l-1}Y_{lm}(\hat{\boldsymbol{r}}),\\
\boldsymbol{v}^{-}_{lm1}(\boldsymbol{r}) &= \frac{i}{l(l+1)(2l+1)}r^{-l-1}\boldsymbol{C}_{lm}(\hat{\boldsymbol{r}}), \quad p^{-}_{lm1}(\boldsymbol{r}) = 0,\\
\boldsymbol{v}^{-}_{lm2}(\boldsymbol{r}) &= \frac{l}{(l+1)(2l+1)^2(2l+3)}r^{-l-2}\boldsymbol{B}_{lm}(\hat{\boldsymbol{r}}), \quad p^{-}_{lm2}(\boldsymbol{r}) = 0.
\end{aligned} \tag{C.36}$$

The Y_{lm} ($l = 0, 1, 2, \ldots$; $m = -l, -l+1, \ldots, l-1, l$) are scalar spherical harmonics as defined by Edmonds [20]. The vector spherical harmonics $\boldsymbol{A}_{lm}$, $\boldsymbol{B}_{lm}$ and $\boldsymbol{C}_{lm}$ form a complete set of vector fields defined on a spherical surface. They are given explicitly in terms of the Y_{lm} as [21]

$$\boldsymbol{A}_{lm} = lY_{lm}\hat{\boldsymbol{r}} + \frac{\partial Y_{lm}}{\partial\theta}\hat{\boldsymbol{e}}_\theta + \frac{1}{\sin\theta}\frac{\partial Y_{lm}}{\partial\varphi}\hat{\boldsymbol{e}}_\varphi, \tag{C.37}$$

$$\boldsymbol{B}_{lm} = -(l+1)Y_{lm}\hat{\boldsymbol{r}} + \frac{\partial Y_{lm}}{\partial\theta}\hat{\boldsymbol{e}}_\theta + \frac{1}{\sin\theta}\frac{\partial Y_{lm}}{\partial\varphi}\hat{\boldsymbol{e}}_\varphi, \tag{C.38}$$

$$\boldsymbol{C}_{lm} = \frac{1}{\sin\theta}\frac{\partial Y_{lm}}{\partial\varphi}\hat{\boldsymbol{e}}_\theta - \frac{\partial Y_{lm}}{\partial\theta}\hat{\boldsymbol{e}}_\varphi, \tag{C.39}$$

with the unit vectors in spherical coordinates $\hat{\boldsymbol{r}}$, $\hat{\boldsymbol{e}}_\theta$, and $\hat{\boldsymbol{e}}_\varphi$. These vector spherical harmonics satisfy the orthogonality relations

$$\int d\Omega \boldsymbol{A}^*_{l'm'} \cdot \boldsymbol{A}_{lm} = l(2l+1)\delta_{l'l}\delta_{m'm}, \tag{C.40}$$

$$\int d\Omega \boldsymbol{B}^*_{l'm'} \cdot \boldsymbol{B}_{lm} = (l+1)(2l+1)\delta_{l'l}\delta_{m'm}, \tag{C.41}$$

$$\int d\Omega \boldsymbol{C}^*_{l'm'} \cdot \boldsymbol{C}_{lm} = l(l+1)\delta_{l'l}\delta_{m'm}, \tag{C.42}$$

$$\int d\Omega \boldsymbol{A}^*_{l'm'} \cdot \boldsymbol{B}_{lm} = \int d\Omega \boldsymbol{B}^*_{l'm'} \cdot \boldsymbol{C}_{lm} = \int d\Omega \boldsymbol{C}^*_{l'm'} \cdot \boldsymbol{A}_{lm} = 0. \tag{C.43}$$

The solutions (C.35) with a superscript "+" are regular everywhere, whereas a superscript "−" (C.36) denotes outgoing solutions which have a singularity at the origin and tend to zero for $r \to \infty$.

Every solution of (C.23) can be expanded in the above set, but in order to obtain a unique solution, we must specify its behaviour for $r \to \infty$ in addition to the boundary condition (C.24) at $r = a$.

First, we look at the solution $(\tilde{\boldsymbol{v}}_{2S}, \tilde{p}_{2S})$ which tends to zero at infinity. It is expressed as a series containing only the outgoing solutions (C.36):

$$\tilde{\boldsymbol{v}}_{2S} = \sum_{lm\sigma} \tilde{c}_{lm\sigma}\boldsymbol{v}^-_{lm\sigma}, \quad \tilde{p}_{2S} = \sum_{lm} \tilde{c}_{lm0}p^-_{lm0}. \tag{C.44}$$

The expansion coefficients $\{\tilde{c}_{lm\sigma}\}$ must be determined from the boundary condition (C.24) at $r = a$. This can be done using a set of adjoint functions orthonormal to the functions of the set $\boldsymbol{v}^-_{lm\sigma}$ [19], but since we are interested only in the few coefficients which allow us to calculate the translational and rotational swimming velocities, we do not introduce the adjoint set here.

Now, the conditions that the solution actually must satisfy are, that on average there are no net fluxes of momentum or angular momentum to infinity. The

flux of momentum is represented by the stress tensor, which is written in cartesian components as

$$\sigma_{\alpha\beta} = \eta\left(\frac{\partial v_\alpha}{\partial x_\beta} + \frac{\partial v_\beta}{\partial x_\alpha}\right) - p\delta_{\alpha\beta}. \tag{C.45}$$

To second order and considering only the surface contributions, the two conditions can be represented as

$$\boldsymbol{\mathcal{F}}_{2S} = \int_{S_\infty} \langle\boldsymbol{\sigma}_{2S}\rangle \cdot \hat{\boldsymbol{n}}\, S = 0. \qquad \boldsymbol{\mathcal{T}}_{2S} = \int_{S_\infty} \boldsymbol{r} \times (\langle\boldsymbol{\sigma}_{2S}\rangle \cdot \hat{\boldsymbol{n}})\, dS = 0, \tag{C.46}$$

where S_∞ represents a surface of very large radius and $\hat{\boldsymbol{n}} = \hat{\boldsymbol{r}}$ the unit vector normal to the surface.

We may now calculate the stress corresponding to each term in the series (C.44) and analyse its asymptotic behaviour for $r \to \infty$ in order to test the conditions (C.46) of vanishing fluxes of momentum and angular momentum. This analysis shows, that the fields $\boldsymbol{v}^-_{1m0}$, p^-_{1m0} lead to a force

$$\tilde{\boldsymbol{\mathcal{F}}} = -\frac{4\pi\eta}{3}\sum_{m=-1}^{1} \tilde{c}_{1m0}\boldsymbol{A}_{1m}, \tag{C.47}$$

and the fields $\boldsymbol{v}^-_{1m1}$ to a torque

$$\tilde{\boldsymbol{\mathcal{T}}} = -i\frac{4\pi\eta}{3}\sum_{m=-1}^{1} \tilde{c}_{1m1}\boldsymbol{A}_{1m}. \tag{C.48}$$

Using the relations

$$\boldsymbol{B}_{1m} = (1 - 3\hat{\boldsymbol{r}}\hat{\boldsymbol{r}}) \cdot \boldsymbol{A}_{1m}, \quad Y_{1m} = \hat{\boldsymbol{r}} \cdot \boldsymbol{A}_{1m}, \quad \boldsymbol{C}_{1m} = \boldsymbol{A}_{1m} \times \hat{\boldsymbol{r}}, \tag{C.49}$$

the corresponding parts of the velocity and pressure fields may be expressed in terms of this force and torque as:

$$\begin{aligned}
\tilde{\boldsymbol{v}}_{\mathcal{F}} &= \sum_{m=-1}^{1} \tilde{c}_{1m0}\boldsymbol{v}^-_{1m0} = -\frac{\mathbf{1} + \hat{\boldsymbol{r}}\hat{\boldsymbol{r}}}{8\pi\eta r} \cdot \tilde{\boldsymbol{\mathcal{F}}}, \\
\tilde{p}_{\mathcal{F}} &= \sum_{m=-1}^{1} \tilde{c}_{1m0}p^-_{1m0} = -\frac{\hat{\boldsymbol{r}} \cdot \tilde{\boldsymbol{\mathcal{F}}}}{4\pi r^2},
\end{aligned} \tag{C.50}$$

$$\tilde{\boldsymbol{v}}_{\mathcal{T}} = \sum_{m=-1}^{1} \tilde{c}_{1m1}\boldsymbol{v}^-_{1m1} = \frac{\hat{\boldsymbol{r}} \times \tilde{\boldsymbol{\mathcal{T}}}}{8\pi\eta r^2}, \quad \tilde{p}_{\mathcal{T}} = 0. \tag{C.51}$$

Looking at the angular dependence of the solutions (C.36), we notice that the above terms may be isolated from the series (C.44) by taking the angular integrals (at a fixed radius r)

$$\begin{aligned}\int d\Omega\, \tilde{\boldsymbol{v}}_{2S}(\boldsymbol{r}) &= \sum_{m=-1}^{1} \tilde{c}_{1m0} \int d\Omega\, \boldsymbol{v}^{-}_{1m0}(\boldsymbol{r}) = -\frac{2}{3\eta r}\tilde{\boldsymbol{\mathcal{F}}},\\ \int d\Omega\, \hat{\boldsymbol{r}} \times \tilde{\boldsymbol{v}}_{2S}(\boldsymbol{r}) &= \sum_{m=-1}^{1} \tilde{c}_{1m1} \int d\Omega\, \hat{\boldsymbol{r}} \times \boldsymbol{v}^{-}_{1m1}(\boldsymbol{r}) = -\frac{1}{3\eta r^2}\tilde{\boldsymbol{\mathcal{T}}}.\end{aligned} \tag{C.52}$$

This will allow us to relate these terms to the portions of the surface velocity from which they arise due to the boundary condition (C.24).

In order to satisfy the conditions (C.46), we must add to the solution $(\tilde{\boldsymbol{v}}_{2S}, \tilde{p}_{2S})$ a solution of the homogeneous Stokes problem (C.23)

$$\boldsymbol{v}^{St}_{2S} = \boldsymbol{v}^{St}_{\mathcal{F}} + \boldsymbol{v}^{St}_{\mathcal{T}} - \boldsymbol{U}_{2S} - \boldsymbol{\Omega}_{2S} \times \boldsymbol{r} + \boldsymbol{v}^{St-}, \quad p^{St}_{2S} = p^{St}_{\mathcal{F}} + p^{St-}. \tag{C.53}$$

with

$$\boldsymbol{v}^{St}_{\mathcal{F}} = -\tilde{\boldsymbol{v}}_{\mathcal{F}}, \quad p^{St}_{\mathcal{F}} = -\tilde{p}_{\mathcal{F}}, \quad \boldsymbol{v}^{St}_{\mathcal{T}} = -\tilde{\boldsymbol{v}}_{\mathcal{T}}, \tag{C.54}$$

chosen such that the total force and torque vanish:

$$\tilde{\boldsymbol{\mathcal{F}}} + \boldsymbol{\mathcal{F}}^{St} = \tilde{\boldsymbol{\mathcal{T}}} + \boldsymbol{\mathcal{T}}^{St} = 0. \tag{C.55}$$

The boundary condition for the Stokes solution on the surface of the sphere is

$$\boldsymbol{v}^{St}_{2S}(a\hat{\boldsymbol{r}}) = 0, \tag{C.56}$$

so that the boundary condition (C.24) is still satisfied. Therefore, the Stokes solution involves regular solutions $\boldsymbol{v}^{+}_{1m0}$ and $\boldsymbol{v}^{+}_{1m1}$, which may be combined to the fields $-\boldsymbol{U}_{2S} - \boldsymbol{\Omega}_{2S} \times \boldsymbol{r}$ leading to the expected asymptotic behaviour for $r \to \infty$. The additional contributions $(\boldsymbol{v}^{St-}, p^{St-})$ are outgoing solutions which do not lead to a force or torque. They may be required in order to satisfy the boundary condition (C.56).

The latter allows to determine the translational and rotational velocities $\boldsymbol{U}_{2S}$ and $\boldsymbol{\Omega}_{2S}$. To this end we write the term $\boldsymbol{v}^{St}_{\mathcal{F}}$ at $r = a$ in the form

$$\boldsymbol{v}^{St}_{\mathcal{F}}(a\hat{\boldsymbol{r}}) = \frac{\tilde{\boldsymbol{\mathcal{F}}}}{6\pi\eta a} - \frac{\mathbf{1} - 3\hat{\boldsymbol{r}}\hat{\boldsymbol{r}}}{24\pi\eta a} \cdot \tilde{\boldsymbol{\mathcal{F}}}. \tag{C.57}$$

We notice, that the first part may be cancelled by the homogeneous field $-\boldsymbol{U}_{2S}$ with

$$\boldsymbol{U}_{2S} = \frac{\tilde{\boldsymbol{\mathcal{F}}}}{6\pi\eta a}. \tag{C.58}$$

In order to compensate the second as well, we look for a solution with the same angular dependence which vanishes at infinity. This solution is found to be a superposition of the $\boldsymbol{v}^{-}_{1m2}$, with radial dependence r^{-3}. The velocity field $\boldsymbol{v}^{St}_{T}$ cancels against $-\boldsymbol{\Omega}\times\boldsymbol{r}$ at $r=a$ if

$$\boldsymbol{\Omega}=\frac{\boldsymbol{T}}{8\pi\eta a^3}. \tag{C.59}$$

(The coefficients relating the translational and rotational velocities to the force and torque are just the corresponding elements of the mobility matrix for a hard sphere with stick boundary conditions.)

The Stokes solution is thus given by

$$\begin{aligned} \boldsymbol{v}^{St}_{2S}(\boldsymbol{r}) &= -\boldsymbol{U}_{2S}\cdot\left[1-\frac{3a}{4r}(1+\hat{\boldsymbol{r}}\hat{\boldsymbol{r}})-\frac{a^3}{4r^3}(1-3\hat{\boldsymbol{r}}\hat{\boldsymbol{r}})\right]-\boldsymbol{\Omega}\times\boldsymbol{r}\left[1-\frac{a^3}{r^3}\right], \\ p^{St}_{2S} &= \boldsymbol{U}_{2S}\cdot\frac{3\eta a\hat{\boldsymbol{r}}}{2r^2}. \end{aligned} \tag{C.60}$$

Specifying $r=a$ in the angular integrals (C.52) over $\tilde{\boldsymbol{v}}_{2S}$, and substituting the boundary condition (C.24), we find that the force and torque and thus the translational and rotational velocities are related to the corresponding integrals over the surface velocity:

$$\boldsymbol{U}_{2S} = -\frac{1}{4\pi}\int d\Omega\,\langle\boldsymbol{u}_S\rangle(\hat{\boldsymbol{r}}), \tag{C.61}$$

$$\boldsymbol{\Omega}_{2S} = -\frac{3}{8\pi a}\int d\Omega\,\hat{\boldsymbol{r}}\times\langle\boldsymbol{u}_S\rangle(\hat{\boldsymbol{r}}). \tag{C.62}$$

We notice that the second order surface contributions to the translational and rotational velocities are given by angular integrals over the surface velocity $\langle\boldsymbol{u}_S\rangle$, and thus are completely determined by the solution of the first order equations (C.10).

As we said before we are considering potential flow to first order in the surface deformations, and in this case the body contributions vanish. There is another case for which the body contributions can be neglected. The situation corresponds to very slow flow motion. In this case the body contributions are bilinear in the first order velocity and they may be neglected in the creeping flow limit in comparison with the surface contributions.

Due to the presence of viscosity there is dissipation of energy, which is transformed into heat. For an incompressible flow the rate at which energy is dissipated is given by eqn. (B.8), which for the time-averaged dissipation reads:

$$\langle D\rangle=\int_S\langle\boldsymbol{v}\cdot\boldsymbol{\sigma}\rangle(\boldsymbol{r})\cdot\hat{\boldsymbol{n}}\,dS, \tag{C.63}$$

Up to second order in the surface deformations, this is given by the expression

$$\langle D \rangle = \int_{S_0} (\boldsymbol{v}_1 \cdot \boldsymbol{\sigma}_1)(\boldsymbol{r}) \cdot \hat{\boldsymbol{n}}\, dS, \tag{C.64}$$

which is entirely determined by the first order solution. Here S_0 denotes the undisplaced (spherical) surface.

Now, using the complex notation introduced in the preceding section, we may express the time-averaged second order rate of energy dissipation as

$$\langle D \rangle = -\frac{1}{2}\mathrm{Re} \int_{S_0} \boldsymbol{v}_\omega^* \cdot \boldsymbol{\sigma}_\omega \cdot \hat{\boldsymbol{r}}\, dS, \tag{C.65}$$

where the frequency component of the stress tensor is given by

$$\sigma_{\omega,ij} = \eta \left(\frac{\partial v_{\omega i}}{\partial x_j} + \frac{\partial v_{\omega j}}{\partial x_i} \right) - p_\omega \delta_{ij}. \tag{C.66}$$

By comparing the swimming velocity of a particular swimming stroke with its energy dissipation we obtain a measure for the efficiency. It is defined as [15]

$$\eta_t = 4\pi\eta\omega a^2 U_2^s / \langle D_2 \rangle. \tag{C.67}$$

By symmetry we have restricted the attention to modes which produce a swimming motion in the z direction.

C.7 Linear Mode Analysis

In the preceding sections we showed that the velocity and the rate of dissipation of the sphere to second order in the surface deformations depend only on the first order flow fields. If we know the latter, we can calculate both quantities, and from them we can determine the swimming efficiency. Its explicit form will be given in the next chapter, where we use it for the two-body problem. In the present section we are going to find the flow field at first order. From the first order Navier-Stokes equation (C.10), using complex notation and removing the exponential time dependence factor, we obtain

$$\eta[\nabla^2 \boldsymbol{v}_\omega - \alpha'^2 \boldsymbol{v}_\omega] - \nabla p_\omega = 0, \qquad \nabla \cdot \boldsymbol{v}_\omega = 0, \tag{C.68}$$

with the parameter

$$\alpha' = (-i\omega\rho/\eta)^{1/2}. \tag{C.69}$$

This kind of equation was solved by Felderhof and Jones [22] in spherical coordinates. They found that (as in the case of stationary flow we considered earlier for the second-order fields) the solution can be written as the sum of two terms, one of which may be interpreted as an incident flow, and the other as outgoing scattered waves which tend to zero at infinity. Since there is no incident field in the case considered here, we only need the outgoing modes. They are denoted as $\boldsymbol{v}_{lm}^{\sigma-}$, $p_{lm}^{\sigma-}$, where $l = 0, 1, 2, \ldots$ and $m = -l, \ldots, l$ are integers and σ can take the three values N, M or P. Since we consider irrotational flow and the P-modes are the only irrotational ones, we need not write the superscript σ. The modes for potential flow are given by

$$\boldsymbol{v}_{lm}^{-}(\boldsymbol{r}) = \frac{-1}{\alpha^2(2l+1)} r^{-l-1} \boldsymbol{B}_{lm}(\hat{\boldsymbol{r}}), \tag{C.70}$$

$$p_{lm}^{-}(\boldsymbol{r}) = \eta \frac{1}{2l+1} r^{-l-1} Y_{lm}(\hat{\boldsymbol{r}}), \tag{C.71}$$

with scalar and vector spherical harmonics Y_{lm} and $\boldsymbol{B}_{lm}$ introduced earlier in this chapter.

The first order flow can be expanded in terms of these modes in the form

$$\boldsymbol{v}_\omega = \sum_{lm} v_{lm} \boldsymbol{v}_{lm}^{-}, \tag{C.72}$$

with complex amplitudes v_{lm}.

The surface displacement $\boldsymbol{\xi}(\theta, \varphi)$ can in general be expanded in terms of vector spherical harmonics. As may be seen from the boundary condition, in order to have irrotational flow there may be only contributions of the $\boldsymbol{B}_{lm}$ type in this expansion, which for convenience may be expressed by the velocity modes:

$$\boldsymbol{\xi}_\omega = \sum_{lm} \xi_{lm} \boldsymbol{v}_{lm}^{-}(a\hat{\boldsymbol{r}}). \tag{C.73}$$

If we apply the boundary condition, we get

$$v_{lm} = -i\omega \xi_{lm}. \tag{C.74}$$

For the pressure we find that it can be written as

$$p_\omega(\boldsymbol{r}) = -i\omega \sum_{lm} \xi_{lm} p_{lm}^{-}. \tag{C.75}$$

The potential follows from equation (C.29). In the complex notation it is given as

$$\phi_\omega(\boldsymbol{r}) = -\frac{i}{\omega\rho} p_\omega(\boldsymbol{r}). \tag{C.76}$$

The above expansion of the fields allows to re-express the swimming velocity and the rate of energy dissipation, as given in equations (C.65) and (C.61). For the surface contribution to the velocity in the case of potential flow we find

$$\boldsymbol{U}_2 = \mathrm{Re}\left\{\frac{i\omega}{8\pi}\sum_{lm,l'm'}\xi^*_{lm}\boldsymbol{b}_{lm,l'm'}\xi_{l'm'}\right\} \tag{C.77}$$

with coefficients

$$\boldsymbol{b}_{lm,l'm'} = -\int_{S_0}(\boldsymbol{v}^{-*}_{lm}\cdot\nabla)\boldsymbol{v}_{l'm'}d\Omega. \tag{C.78}$$

It can be written as

$$\boldsymbol{U}_2 = \frac{\omega}{8\pi}\sum_{lm,l'm'}\xi^*_{lm}\underset{\approx}{B}_{lm,l'm'}\xi_{l'm'} \tag{C.79}$$

with the combination

$$\underset{\approx}{B}_{lm,l'm'} = \frac{i}{2}(b_{lm,l'm'} - b^*_{l'm',lm}). \tag{C.80}$$

For the average rate of dissipation one finds

$$\langle D_2\rangle = \frac{1}{2}\eta a^2\omega^2\sum_{lm,l'm'}\xi^*_{lm}\underset{\approx}{A}_{lm,l'm'}\xi_{l'm'} \tag{C.81}$$

with matrix elements

$$\underset{\approx}{A}_{lm,l'm'} = \frac{1}{2}(a_{l}m,l'm' + a^*_{l'm',lm}) \tag{C.82}$$

and coefficients

$$a_{lm,l'm'} = -\frac{1}{\eta}\int_{S_0}\boldsymbol{v}^{-*}_{lm}\cdot\boldsymbol{\sigma}_{l'm'}\cdot\hat{\boldsymbol{r}}d\Omega, \tag{C.83}$$

where $\boldsymbol{\sigma}_{lm}$ is the stress tensor (C.66) corresponding to the mode $\boldsymbol{v}^-_{lm}$ and p^-_{lm}. In the expressions (C.79) and (C.81), the swimming velocity and the rate of energy dissipation are written as quadratic forms in the infinite-dimensional vector space of surface displacements. The components of these vectors are the complex deformation amplitudes ξ_{lm}. Each form is related to a Hermitian matrix. Always the z-axis can be chosen as coincident with the direction of the motion ($\boldsymbol{U}_2$). In accordance with equation (C.67), we write the efficiency as

$$\eta_t = \frac{1}{\pi}\frac{|\langle\boldsymbol{\xi}|\underset{\approx}{B}^{z}|\boldsymbol{\xi}\rangle|}{\langle\boldsymbol{\xi}|\underset{\approx}{A}|\boldsymbol{\xi}\rangle}, \tag{C.84}$$

where

$$\langle \boldsymbol{\xi} | \underset{\approx}{B}^{z} | \boldsymbol{\xi} \rangle = \sum \xi_{lm}^{*} B_{lm,l'm'} \xi_{l'm'}. \tag{C.85}$$

and similarly for the dissipation.

In order to get the most efficient mode of swimming, it is necessary to maximize η_t over the space of surface displacements. This corresponds to finding the maximum eigenvalue λ_{max} of the generalized eigenvalue problem

$$\underset{\approx}{B}^{z} | \boldsymbol{\xi} \rangle = \lambda \underset{\approx}{A} | \boldsymbol{\xi} \rangle. \tag{C.86}$$

In this case, $\underset{\approx}{A}$ and $\underset{\approx}{B}^{z}$ are Hermitian matrices, and $\underset{\approx}{A}$ is positive definite. The greatest velocity for a given rate of energy dissipation is given by

$$\eta_t = \frac{|\lambda_{max}|}{\pi}. \tag{C.87}$$

The problem can be studied for every value of m, but for the chosen direction of the z-axis the greatest efficiency is achieved for $m = 0$. Then we restrict the further considerations to this case. The fields are independent of the azimuthal angle φ. For simplicity in the calculations we change to nondimensional coefficients ξ_l by using the relation

$$\xi_{l0} = -\frac{i\omega a^2 \rho}{\eta} \sqrt{4\pi(2l+1)}\, \xi_l a^{l+1} \tag{C.88}$$

The corresponding surface displacement is

$$\boldsymbol{\xi}_{\omega}(\hat{\boldsymbol{r}}) = -\sqrt{4\pi} a \sum_{l=0}^{\infty} \frac{1}{\sqrt{2l+1}} \xi_l \boldsymbol{B}_{l0}(\hat{\boldsymbol{r}}). \tag{C.89}$$

The complex scalar potential of the first order flow is given explicitly by

$$\phi_{\omega} = i\omega a^2 \sum_{l=0}^{\infty} \xi_l \left(\frac{a}{r}\right)^{l+1} P_{l+1}(\cos\theta), \tag{C.90}$$

with Legendre polynomials $P_l(\cos\theta)$.

Apéndice D

Swimming of Two Bodies

D.1 Solution of the Two-Body Problem

Our aim here will be to calculate the velocity field $\boldsymbol{v}_\omega(1,2)$ and the pressure $p_\omega(1,2)$ of the flow to first order in perturbations for the two-body problem, from which we can determine the average translational and rotational velocities of the two bodies.

We make the same assumptions about the bodies and the way they displace themselves as in the case of a single body, i.e. we consider two equal spherical bodies with radius a, the surfaces of which are undergoing small (as compared to the radius) deformations

$$\boldsymbol{\xi}^{(k)}(\hat{\boldsymbol{r}},t) = \mathrm{Re}\left\{\boldsymbol{\xi}_\omega^{(k)} e^{-i\omega t}\right\}, \quad (k=1,\,2), \tag{D.1}$$

which are harmonic in time.

We have in mind a situation where both spheres are swimming together, that means we look for a steady state in which the average velocities of both spheres coincide, such that the separation distance between their centers, $\boldsymbol{R}$, is the same after a period T of deformation. Moreover, we then take $\boldsymbol{R}$ to be constant.

The spheres do not overlap, so the distance between them must exceed their diameter: $R > 2a$. In writing down this condition, deformations of the bodies towards the separating space have been neglected. As the distance approaches the diameter, the present description loses its validity firstly because the deformations must tend to zero in order not to violate the non-overlap condition, and secondly because the expansions in spherical harmonics do not converge any more, so that lubrication theory should be applied.

The locations of the centers of the spheres are denoted by $\boldsymbol{R}_1$ and $\boldsymbol{R}_2$, respectively, thus $\boldsymbol{R} = \boldsymbol{R}_2 - \boldsymbol{R}_1$. We introduce a reference system (figure D.1) with the z-axis

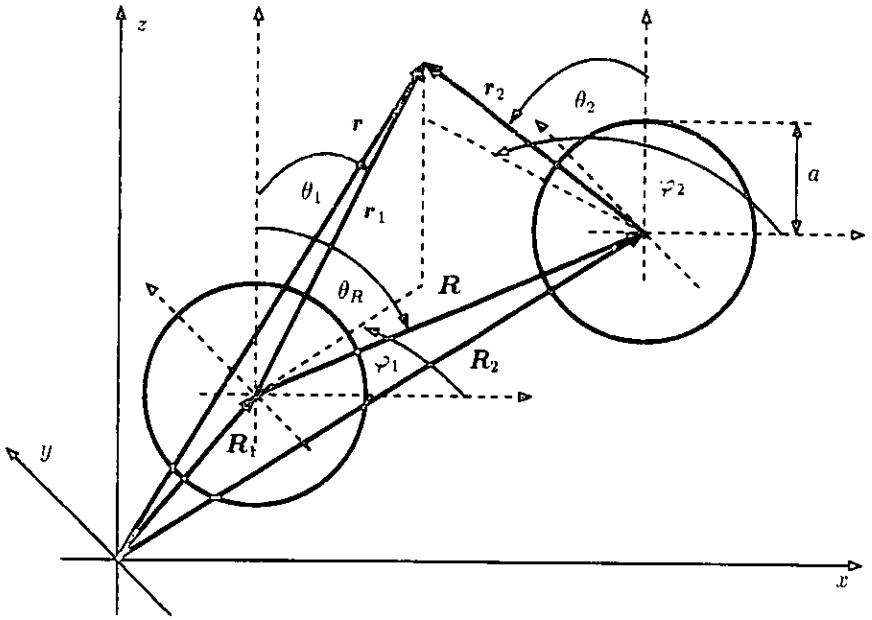

Figure D.1: Reference system for two spheres swimming at a distance $\boldsymbol{R}$, as described in the text

chosen in the direction of the translational velocity of each sphere in absence of the other, and with the y-axis perpendicular to the separation vector $\boldsymbol{R}$. The orientation of the x-axis is chosen such that $\boldsymbol{R}\cdot\hat{\boldsymbol{e}}_x > 0$ ($X_2 > X_1$, where X_k is the x-position of the center of sphere k). In the case that $\boldsymbol{R}\,||\,\hat{\boldsymbol{e}}_z$ the orientation of the x- and y-axis is undetermined by the above, but in this case it does not matter anyway.

As indicated in the figure, $\boldsymbol{r}_1 = \boldsymbol{r} - \boldsymbol{R}_1$ and $\boldsymbol{r}_2 = \boldsymbol{r} - \boldsymbol{R}_2$ are the coordinates of the field point with respect to the centers $\boldsymbol{R}_1$ and $\boldsymbol{R}_2$, respectively. The azimuthal and polar angles φ_k and θ_k for each sphere ($k = 1, 2$) are then defined as usual in a coordinate frame parallel to the one described above but with the origin shifted to the center of the respective sphere.

The polar angle corresponding to the separation vector $\boldsymbol{R}$, θ_R, vanishes if sphere 1 is swimming behind sphere 2, and $\theta_R = \pi/2$, if both spheres are swimming one aside the other.

We write the velocity field in presence of the bodies as

$$\boldsymbol{v}_\omega(1,2;\boldsymbol{r}) = \nabla\phi_\omega(1,2;\boldsymbol{r}), \tag{D.2}$$

where $\phi_\omega(1,2;\boldsymbol{r})$ is the hydrodynamic potential in the presence of both spheres. Now, in the region outside the spheres the potential must be harmonic and can be written as the sum of the potential due to the deformations of sphere 1 in absence of sphere 2 plus the potential due to the deformations of sphere 2 in absence of sphere 1 plus the potential due to the hydrodynamic interactions. This can be expressed by the twin expansion:

$$\begin{aligned}\phi_\omega(1,2;\boldsymbol{r}) = & \\ & i\omega a^2 \sum_{l=0}^{\infty} \xi_l^1 \left(\frac{a}{r_1}\right)^{l+1} P_l(\cos\theta_1) + i\omega a^2 \sum_{l=0}^{\infty} \xi_l^2 \left(\frac{a}{r_2}\right)^{l+1} P_l(\cos\theta_2) \\ & + \sum_{l=0}^{\infty} \sum_{m=-l}^{l} \left[A_{lm}^1 r_1^{-l-1} P_l^m(\cos\theta_1) e^{im\varphi_1} + A_{lm}^2 r_2^{-l-1} P_l^m(\cos\theta_2) e^{im\varphi_2} \right]. \qquad \text{(D.3)}\end{aligned}$$

where P_l^m is the associate Legendre function.

The two terms within the double sum can be understood in analogy to the electrostatic case of two spherical inclusions in a dielectric medium, as corresponding to 2^l poles induced in them by the outgoing fields from the respective other sphere. Thus, in order to solve the problem, we are going to apply a method given by B.U. Felderhof et al. [23] to solve the related electrostatic problem.

This is a generalization of the method used by Jeffrey [24] to solve the problem for the case where the inclusions are uniform spheres in an incident electric field.

In this method the coefficients A_{lm}^1 and A_{lm}^2 in the twin expansion are determined by the conditions just outside either body. The method will be described in the following.

For one body, centered at the origin, the hydrodynamic potential in the region outside it, but within a sphere which excludes the sources of the applied multipole field, may be analysed in terms of multipolar contributions:

$$\phi(\boldsymbol{r}) = \sum_{l=0}^{\infty} \sum_{m=-l}^{l} \phi_{lm}(r) P_l^m(\cos\theta) e^{im\varphi}, \qquad \text{(D.4)}$$

where θ and φ are the polar and azimuthal angles, respectively, of $\boldsymbol{r}$. The radial functions may be written as

$$\phi_{lm}(r) = i\omega a^2 \xi_l \left(\frac{a}{r}\right)^{l+1} \delta_{m0} + \phi_{0,lm}(r) + \phi_{ind,lm}(r). \qquad \text{(D.5)}$$

Here, the first term corresponds to the potential due to the deformations of the sphere when there is no incident field. By itself, it satisfies the condition that the flow follows the deformations of the sphere, which again are azimuthally symmetric.

Now, if there is an incident multipolar field, the two following terms appear. Due to the linearity of the equation of motion at first order in perturbations, they must satisfy the boundary conditions as imposed on the undeformed spherical surface. Their radial dependence must thus be of the form (see appendix G).

$$[\phi_{0,lm}(r) + \phi_{ind,lm}(r)] \propto (-r^l + \alpha_l r^{-l-1}), \tag{D.6}$$

where the first term is the potential of the applied 2^l pole field and the second term is due to the induced 2^l pole moment.

The fields incident on each body enter the considerations due to the fact that the fields outgoing from them propagate to the respective other one, where they act as applied fields. This is in contrast to the case of a single sphere, where there is no incident field.

The coefficient α_l is the 2^l pole polarizability of the body. The multipole polarizabilities are the generalization of the dipole polarizability, which corresponds to the case $l = 1$. They are determined by the properties of the body and the boundary conditions on its surface, in our case hard spheres with stick boundary conditions:

$$\left.\frac{d[\phi_{0,lm}(r) + \phi_{ind,lm}(r)]}{dr}\right|_{r=a} = 0. \tag{D.7}$$

We find

$$\alpha_l = -\frac{l}{l+1}a^{2l+1}. \tag{D.8}$$

In order to obtain the coefficients A^1_{lm} and A^2_{lm}, we require that just outside sphere 1, the potential must be written as a superposition of potentials of the form (D.4) with (D.5) and (D.6), where (r, θ, φ) must be replaced by $(r_1, \theta_1, \varphi_1)$, and similarly just outside the sphere 2. To accomplish this we must expand the multipole potentials centered at one sphere in terms of those centered at the other, which we do with the pair of formulas [25]

$$r_2^{-l-1} P_l^m(\cos\theta_2) e^{im\varphi_2} = \sum_{l'=0}^{\infty} \sum_{m'=-l'}^{l'} (-1)^{l+m'} \frac{(l+l'+m'-m)!}{(l-m)!(l'+m')!} \frac{r_1^{l'} P_{l+l'}^{m-m'}(\cos\theta_R)}{R^{l+l'+1}} P_{l'}^{m'}(\cos\theta_1) e^{im'\varphi_1} \tag{D.9}$$

which is valid for $r_1 < R$, and

$$r_1^{-l-1} P_l^m(\cos\theta_1) e^{im\varphi_1} = \sum_{l'=0}^{\infty} \sum_{m'=-l'}^{l'} (-1)^{l'+m'} \frac{(l+l'+m'-m)!}{(l'+m')!(l-m)!} \frac{r_2^{l'} P_{l+l'}^{m-m'}(\cos\theta_R)}{R^{l+l'+1}} P_{l'}^{m'}(\cos\theta_2) e^{im'\varphi_2} \tag{D.10}$$

which is valid for $r_2 < R$.

Using (D.10), the condition just outside the surface of the sphere centered at $\boldsymbol{R}_2$ yields

$$\frac{A^1_{lm}}{\alpha_l} = (-1)^{m+1} \sum_{l'=0}^{\infty} \sum_{m'=-l'}^{l'} (-1)^{l'} \frac{(l+l'+m'-m)!}{(l'+m')!(l-m)!} \frac{P^{m-m'}_{l+l'}(\cos\theta_R)}{R^{l+l'+1}} [A^2_{l'm'} + i\omega a^{l'+3} \xi^2_{l'} \delta_{m0}]. \quad \text{(D.11)}$$

and similarly from (D.9), the condition just outside the sphere centered at $\boldsymbol{R}_1$ yields

$$\frac{A^2_{lm}}{\alpha_l} = (-1)^{l+m+1} \sum_{l'=0}^{\infty} \sum_{m'=-l'}^{l'} \frac{(l+l'+m'-m)!}{(l'+m')!(l-m)!} \frac{P^{m-m'}_{l+l'}(\cos\theta_R)}{R^{l+l'+1}} [A^1_{l'm'} + i\omega a^{l'+3} \xi^1_{l'} \delta_{m0}]. \quad \text{(D.12)}$$

In order to solve this system of equations, we define the following coefficients

$$d^{(k)}_{lm} = i\omega a^3 \xi^{(k)}_l \delta_{m0} + a^{-l} A^{(k)}_{lm} \qquad \text{for} \quad k = 1, 2. \quad \text{(D.13)}$$

From the two preceeding equations and (D.8) we obtain for these coefficients

$$d^{(1)}_{lm} = \xi^{(1)}_l \delta_{m0} + (-1)^m \frac{l}{l+1} \sum_{l'=0}^{\infty} \sum_{m'=-l'}^{l'} \frac{(l+l'+m-m')!}{(l+m)!(l'-m')!} x^{l+l'+1} P^{m-m'}_{l+l'}(\cos\theta_R) d^{(2)}_{l'm'}, \quad \text{(D.14)}$$

$$d^{(2)}_{lm} = \xi^{(2)}_l \delta_{m0} + (-1)^{l+m} \frac{l}{l+1} \sum_{l'=0}^{\infty} \sum_{m'=-l'}^{l'} \frac{(l+l'+m-m')!}{(l+m)!(l'-m')!} x^{l+l'+1} P^{m-m'}_{l+l'}(\cos\theta_R) d^{(1)}_{l'm'}, \quad \text{(D.15)}$$

where $x = a/R$, $\xi^{(1)} = i\omega a^3 \xi^1$ and $\xi^{(2)} = i\omega a^3 \xi^2$. The form of the equations suggests to put

$$d_{lm} = d^{(1)}_{lm} + (-1)^l d^{(2)}_{lm}, \quad \text{(D.16)}$$

$$m_{lm} = d^{(1)}_{lm} - (-1)^l d^{(2)}_{lm}, \quad \text{(D.17)}$$

and we get

$$d_{lm} = [\xi^{(1)}_l + (-1)^l \xi^{(2)}_l] \delta_{m0} + (-1)^m \frac{l}{l+1} \sum_{l'=0}^{\infty} \sum_{m'=-l'}^{l'} \frac{(l+l'+m-m')!}{(l+m)!(l'-m')!} x^{l+l'+1} P^{m-m'}_{l+l'}(\cos\theta_R) d_{l'm'}, \quad \text{(D.18)}$$

$$m_{lm} = [\xi^{(1)}_l - (-1)^l \xi^{(2)}_l] \delta_{m0} - (-1)^m \frac{l}{l+1} \sum_{l'=0}^{\infty} \sum_{m'=-l'}^{l'} \frac{(l+l'+m-m')!}{(l+m)!(l'-m')!} x^{l+l'+1} P^{m-m'}_{l+l'}(\cos\theta_R) m_{l'm'}. \quad \text{(D.19)}$$

Expressing the system in matrix form, we find

$$\underset{\sim}{d} = \underset{\sim}{\xi}^{(1)} + \underset{\approx}{C}\underset{\sim}{\xi}^{(2)} + \underset{\approx}{F}\underset{\approx}{G}\underset{\sim}{d}, \tag{D.20}$$

$$\underset{\sim}{m} = \underset{\sim}{\xi}^{(1)} - \underset{\approx}{C}\underset{\sim}{\xi}^{(2)} - \underset{\approx}{F}\underset{\approx}{G}\underset{\sim}{m}, \tag{D.21}$$

where $\underset{\sim}{d}$ and $\underset{\sim}{m}$ are vectors with components d_{lm} and m_{lm}, respectively, while $\underset{\approx}{C}$, $\underset{\approx}{F}$ and $\underset{\approx}{G}$ are correspondingly defined matrices. The matrices $\underset{\approx}{F}$ and $\underset{\approx}{C}$ are diagonal with elements

$$F_{lm,l'm'} = (-1)^m \frac{l}{l+1}\delta_{ll'}\delta_{mm'}, \tag{D.22}$$

$$C_{lm,l'm'} = (-1)^l \delta_{ll'}\delta_{mm'}, \tag{D.23}$$

so that $\underset{\approx}{C}^{-1} = \underset{\approx}{C}$. Further, the matrix $\underset{\approx}{G}$ has elements

$$G_{lm,l'm'} = x^{l+l'+1}\frac{(l+l'+m-m')!}{(l+m)!(l'-m')!}P_{l+l'}^{m-m'}(\cos\theta_R). \tag{D.24}$$

The components of the vectors $\underset{\sim}{\xi}^{(k)}$ are given by

$$\xi_{lm}^{(k)} = \xi_l^{(k)}\delta_{m0}, \tag{D.25}$$

for $k = 1, 2$.

From equations (D.20) and (D.21) we find that the vectors $\underset{\sim}{d}$ and $\underset{\sim}{m}$ are given by the formulas

$$\underset{\sim}{d} = \underset{\approx}{C}_1(\underset{\sim}{\xi}^{(1)} + \underset{\approx}{C}\underset{\sim}{\xi}^{(2)}), \tag{D.26}$$

$$\underset{\sim}{m} = \underset{\approx}{C}_2(\underset{\sim}{\xi}^{(1)} - \underset{\approx}{C}\underset{\sim}{\xi}^{(2)}), \tag{D.27}$$

with

$$\underset{\approx}{C}_1 = (\underset{\approx}{I} - \underset{\approx}{F}\underset{\approx}{G})^{-1}, \tag{D.28}$$

$$\underset{\approx}{C}_2 = (\underset{\approx}{I} + \underset{\approx}{F}\underset{\approx}{G})^{-1}. \tag{D.29}$$

In this form we have solved the problem to find the potential flow generated by the two spheres to first order in perturbations, we only have to transform back to our original coefficients. From (D.16) and (D.17) we get

$$\underset{\sim}{d}^{(1)} = \frac{1}{2}(\underset{\sim}{d} + \underset{\sim}{m}), \tag{D.30}$$

$$\underset{\sim}{d}^{(2)} = \frac{1}{2}\underset{\approx}{C}(\underset{\sim}{d} - \underset{\sim}{m}). \tag{D.31}$$

We define the following matrices

$$\underset{\approx}{D}^1_1 = \underset{\approx}{C}_1 + \underset{\approx}{C}_2. \tag{D.32}$$

$$\underset{\approx}{D}^1_2 = (\underset{\approx}{C}_1 - \underset{\approx}{C}_2)\underset{\approx}{C}. \tag{D.33}$$

$$\underset{\approx}{D}^2_1 = \underset{\approx}{C}(\underset{\approx}{C}_1 - \underset{\approx}{C}_2). \tag{D.34}$$

$$\underset{\approx}{D}^2_2 = \underset{\approx}{C}(\underset{\approx}{C}_1 + \underset{\approx}{C}_2)\underset{\approx}{C}. \tag{D.35}$$

Finally, using (D.20) and (D.21) we find

$$\underset{\sim}{d}^{(1)} = i\omega a^3[\underset{\approx}{D}^1_1\underset{\sim}{\xi}^{(1)} + \underset{\approx}{D}^1_2\underset{\sim}{\xi}^{(2)}], \tag{D.36}$$

$$\underset{\sim}{d}^{(2)} = i\omega a^3[\underset{\approx}{D}^2_1\underset{\sim}{\xi}^{(1)} + \underset{\approx}{D}^2_2\underset{\sim}{\xi}^{(2)}], \tag{D.37}$$

From equation (D.13) we get the coeffients $A^{(1)}_{lm}$ and $A^{(2)}_{lm}$ and in this form we obtain the flow potential for the two sphere problem.

D.2 Velocity Field and Pressure

In this section we calculate the velocity field and the pressure for the two-body problem to first order in perturbations. As mentioned in chapter (C), the average velocities $\boldsymbol{U}_1$, $\boldsymbol{U}_2$ and the rates D_1, D_2 of energy dissipated from the surface of each body to second order in perturbations depend only on the first order flow fields. The velocity field at first order in perturbations is obtained from the equation

$$\boldsymbol{v}_\omega(1;2;\boldsymbol{r}) = \nabla\phi_\omega(\boldsymbol{r}). \tag{D.38}$$

In order to calculate the average velocities and energy dissipation for sphere 1 and sphere 2, we have to write the velocity field and pressure of the flow using coordinates with respect to a reference system centered in $\boldsymbol{R}_1$ and another centered in $\boldsymbol{R}_2$, respectively. Then we can use the equations obtained for a single sphere.

Using a coordinate system centered in $\boldsymbol{R}_1$ we get from equations (D.3), (D.9) and (D.13):

$$\phi_\omega(1,2;\boldsymbol{r}) = \sum_{l=0}^{\infty}\sum_{m=-l}^{l}\left[\frac{a^l}{r_1^{l+1}}d^{(1)}_{lm} + (-1)^m\frac{r_1^l}{a^{l+1}}e^{(2)}_{lm}\right]P_l^m(\cos\theta_1)e^{im\varphi_1}. \tag{D.39}$$

In similar form, for the coordinate system centered in $\boldsymbol{R}_2$, equations (D.3), (D.10), and (D.13) yield:

$$\phi_\omega(1,2;\boldsymbol{r}) = \sum_{l=0}^{\infty}\sum_{m=-l}^{l}\left[\frac{a^l}{r_2^{l+1}}d^{(2)}_{lm} + (-1)^{l+m}\frac{r_2^l}{a^{l+1}}e^{(1)}_{lm}\right]P_l^m(\cos\theta_2)e^{im\varphi_2}. \tag{D.40}$$

Here, we have used the abbreviations

$$e_{lm}^{(1)} = \sum_{l'=0}^{\infty} \sum_{m'=-l'}^{l'} \frac{(l+l'+m-m')!}{(l+m)!(l'-m')!} x^{l+l'+1} P_{l+l'}^{m-m'}(\cos\theta_R) d_{l'm'}^{(1)}, \tag{D.41}$$

$$e_{lm}^{(2)} = \sum_{l'=0}^{\infty} \sum_{m'=-l'}^{l'} (-1)^{l'} \frac{(l+l'+m-m')!}{(l+m)!(l'-m')!} x^{l+l'+1} P_{l+l'}^{m-m'}(\cos\theta_R) d_{l'm'}^{(2)}. \tag{D.42}$$

We shall write the equations with respect to both coordinate systems in terms of the scalar spherical harmonics [20] as

$$\phi_\omega(1,2;\boldsymbol{r}) = \sum_{l=0}^{\infty} \sum_{m=-l}^{l} (-1)^m \sqrt{\frac{4\pi(l+m)!}{(2l+1)(l-m)!}} \left[\frac{a^l}{r_1^{l+1}} d_{lm}^{(1)} + (-1)^{l+m} \frac{r_1^l}{a^{l+1}} e_{lm}^{(2)} \right] Y_{lm}(\theta_1, \varphi_1), \tag{D.43}$$

$$\phi_\omega(1,2;\boldsymbol{r}) = \sum_{l=0}^{\infty} \sum_{m=-l}^{l} (-1)^m \sqrt{\frac{4\pi(l+m)!}{(2l+1)(l-m)!}} \left[\frac{a^l}{r_2^{l+1}} d_{lm}^{(2)} + (-1)^{l+m} \frac{r_2^l}{a^{l+1}} e_{lm}^{(1)} \right] Y_{lm}(\theta_2, \varphi_2). \tag{D.44}$$

Using the equation (D.38) we get for the coordinate system centered in $\boldsymbol{R}_1$

$$\boldsymbol{v}_\omega(\boldsymbol{r}) = \sum_{l=0}^{\infty} \sum_{m=-l}^{l} (-1)^m \sqrt{\frac{4\pi(l+m)!}{(2l+1)(l-m)!}} \left[\frac{a^l}{r_1^{l+2}} d_{lm}^{(1)} \boldsymbol{B}_{lm}(\hat{\boldsymbol{r}}_1) + (-1)^{l+m} \frac{r_1^{l-1}}{a^{l+1}} e_{lm}^{(2)} \boldsymbol{A}_{lm}(\hat{\boldsymbol{r}}_1) \right], \tag{D.45}$$

and for the coordinate system centered in $\boldsymbol{R}_2$

$$\boldsymbol{v}_\omega(\boldsymbol{r}) = \sum_{l=0}^{\infty} \sum_{m=-l}^{l} (-1)^m \sqrt{\frac{4\pi(l+m)!}{(2l+1)(l-m)!}} \left[\frac{a^l}{r_2^{l+2}} d_{lm}^{(2)} \boldsymbol{B}_{lm}(\hat{\boldsymbol{r}}_2) + (-1)^{l+m} \frac{r_2^{l-1}}{a^{l+1}} e_{lm}^{(1)} \boldsymbol{A}_{lm}(\hat{\boldsymbol{r}}_2) \right]. \tag{D.46}$$

The unnormalized vector spherical harmonics $\boldsymbol{A}_{lm}$, $\boldsymbol{B}_{lm}$ and $\boldsymbol{C}_{lm}$ were introduced in chapter C.

They are related to the orthonormalized vector spherical harmonics given by Edmonds [20] according to

$$\boldsymbol{A}_{lm} = \sqrt{l(2l+1)}\boldsymbol{Y}_{ll-1\,m}. \tag{D.47}$$

$$\boldsymbol{B}_{lm} = \sqrt{(l+1)(2l+1)}\boldsymbol{Y}_{ll+1\,m}. \tag{D.48}$$

$$\boldsymbol{C}_{lm} = -i\sqrt{l(l+1)}\boldsymbol{Y}_{ll\,m}. \tag{D.49}$$

Finally, we express the flow velocity in the coordinate systems centered in $\boldsymbol{R}_1$ and $\boldsymbol{R}_2$, respectively, by the normalized spherical harmonics:

$$\boldsymbol{v}_\omega(\boldsymbol{r}) = \sum_{l=0}^{\infty}\sum_{m=-l}^{l}(-1)^m \sqrt{\frac{4\pi(l+m)!}{(l-m)!}}\left[\sqrt{l+1}\frac{a^l}{r_1^{l+2}}d_{lm}^{(1)}\boldsymbol{Y}_{ll+1\,m}(\hat{\boldsymbol{r}}_1) + (-1)^m\sqrt{l}\frac{r_1^{l-1}}{a^{l+1}}e_{lm}^{(2)}\boldsymbol{Y}_{ll-1\,m}(\hat{\boldsymbol{r}}_1)\right], \tag{D.50}$$

$$\boldsymbol{v}_\omega(\boldsymbol{r}) = \sum_{l=0}^{\infty}\sum_{m=-l}^{l}(-1)^m \sqrt{\frac{4\pi(l+m)!}{(l-m)!}}\left[\sqrt{l+1}\frac{a^l}{r_2^{l+2}}d_{lm}^{(2)}\boldsymbol{Y}_{ll+1\,m}(\hat{\boldsymbol{r}}_2) + (-1)^m\sqrt{l}\frac{r_2^{l-1}}{a^{l+1}}e_{lm}^{(1)}\boldsymbol{Y}_{ll-1\,m}(\hat{\boldsymbol{r}}_2)\right]. \tag{D.51}$$

For simplicity in the calculation of the velocity and rate of energy dissipation of both spheres, we may write the results in a short form. The flow velocity, in terms of a coordinate system centered in the sphere k, where $k = 1, 2$, is then given by

$$\boldsymbol{v}_\omega^{(k)} = \sum_{l=0}^{\infty}\sum_{m=-l}^{l}(-1)^m[a_{lm}^{(k)}r_k^{-l-2}\boldsymbol{Y}_{ll+1\,m} + b_{lm}^{(k)}r_k^{l-1}\boldsymbol{Y}_{ll-1\,m}], \tag{D.52}$$

with coefficients

$$a_{lm}^{(k)} = (-1)^m a^l\sqrt{\frac{4\pi(l+m)!}{(l-m)!}}\sqrt{l+1}d_{lm}^{(k)} \qquad \text{for} \quad k = 1, 2, \tag{D.53}$$

$$b_{lm}^{(1)} = \frac{1}{a^{l+1}}\sqrt{\frac{4\pi l(l+m)!}{(l-m)!}}e_{lm}^{(2)}, \tag{D.54}$$

$$b_{lm}^{(2)} = \frac{(-1)^l}{a^{l+1}}\sqrt{\frac{4\pi l(l+m)!}{(l-m)!}}e_{lm}^{(1)}. \tag{D.55}$$

The pressure field is found from equation (C.76). For the coordinate system centered in $\boldsymbol{R}_1$ we have the relation

$$p_\omega(\boldsymbol{r}) = i\omega\rho \sum_{l=0}^{\infty} \sum_{m=-l}^{l} (-1)^m \sqrt{\frac{4\pi(l+m)!}{(2l+1)(l-m)!}} \left[\frac{a^l}{r_1^{-l-1}} d_{lm}^{(1)} + (-1)^{l+m} \frac{r_1^l}{a^{l+1}} e_{lm}^{(2)} \right] Y_{lm}(\theta_1, \varphi_1). \tag{D.56}$$

and for the coordinate system centered in $\boldsymbol{R}_2$ we find

$$p_\omega(\boldsymbol{r}) = i\omega\rho \sum_{l=0}^{\infty} \sum_{m=-l}^{l} (-1)^m \sqrt{\frac{4\pi(l+m)!}{(2l+1)(l-m)!}} \left[\frac{a^l}{r_2^{-l-1}} d_{lm}^{(2)} + (-1)^{l+m} \frac{r_2^l}{a^{l+1}} e_{lm}^{(1)} \right] Y_{lm}(\theta_2, \varphi_2). \tag{D.57}$$

In similar form as for the flow velocity we define the coefficients for the flow pressure

$$a_{p,lm}^{(k)} = i\omega\rho(-1)^m a^l \sqrt{\frac{4\pi(l+m)!}{(2l+1)(l-m)!}} d_{lm}^{(k)} \qquad \text{for} \quad k = 1, 2, \tag{D.58}$$

$$b_{p,lm}^{(1)} = i\omega\rho \frac{1}{a^{l+1}} \sqrt{\frac{4\pi(l+m)!}{(2l+1)(l-m)!}} e_{lm}^2, \tag{D.59}$$

$$b_{p,lm}^{(2)} = i\omega\rho \frac{(-1)^l}{a^{l+1}} \sqrt{\frac{4\pi(l+m)!}{(2l+1)(l-m)!}} e_{lm}^1. \tag{D.60}$$

Using these coefficients, the pressure in terms of a coordinate system centered in $\boldsymbol{R}_k$, can be written as

$$p_{\omega k}(1,2;\boldsymbol{r}_k) = \sum_{l=0}^{\infty} \sum_{m=-l}^{l} \left[a_{p,lm}^{(k)} r_k^{-l-1} + b_{p,lm}^{(k)} r_k^l \right] Y_{lm}(\theta_k, \varphi_k). \tag{D.61}$$

We have found the time-averaged velocity field and pressure for the two body problem in terms of the coordinate system centered in $\boldsymbol{R}_k$. Thus, we can now calculate the average velocities and rates of energy dissipated by the spheres, and hence find their swimming efficiency.

We are interested in calculating the best swimming stroke for the two-body system. In order to be able to compare with the swimming of a single body, we define the swimming efficiency such that it coincides with that for one body if the spheres are infinitely far apart. Thus, the appropriate definition of the swimming efficiency of the two-body system is

$$\eta_T = 4\pi\eta\omega a^2 \frac{2|\boldsymbol{U}_{cm}|}{\langle D \rangle}, \tag{D.62}$$

where $\boldsymbol{U}_{cm}$ is the average center-of-mass velocity and $\langle D \rangle$ is the total average rate of dissipation. The former is given by

$$\boldsymbol{U}_{cm} = \frac{m_1 \boldsymbol{U}_1 + m_2 \boldsymbol{U}_2}{m_1 + m_2} = \frac{\boldsymbol{U}_1 + \boldsymbol{U}_2}{2}. \tag{D.63}$$

since m_1 and m_2, the respective masses of sphere 1 and 2, are equal for identical spheres.

For the case in which both spheres swim one behind the other, the swimming velocity is in the $\hat{\boldsymbol{z}}$ direction. In the following we are going to derive expressions in terms of the deformation amplitudes for the swimming velocities of each sphere and the rate of energy dissipation, and thus for the swimming efficiency.

D.3 Velocity of the Spheres

In the present section we calculate the velocity of the spheres, then we define the velocity of the system, and we calculate it for the case in which both spheres swim with the same velocity.

In order to calculate the velocity of the sphere k, with $k = 1, 2$, we use equation (C.61), yielding:

$$\boldsymbol{U}_k = -\frac{1}{4\pi} \int \langle \boldsymbol{u}_S^{(k)} \rangle (\hat{\boldsymbol{r}}_k) d\Omega_k. \tag{D.64}$$

where the time-averaged surface velocity $\boldsymbol{u}_S^{(k)}$ corresponding to sphere k, is given by (see equation C.34)

$$\langle \boldsymbol{u}_S^{(k)}(\hat{\boldsymbol{r}}, t) \rangle = -\frac{1}{2} \mathrm{Re} \left(\boldsymbol{\xi}_\omega^{(k*)}(\hat{\boldsymbol{r}}, t) \cdot \nabla \right) \boldsymbol{v}_\omega^{(k)}(\boldsymbol{r}, t) \Big|_{r_k = a}, \tag{D.65}$$

and we get

$$\boldsymbol{U}_k = \frac{1}{8\pi} \mathrm{Re} \int \left(\boldsymbol{\xi}_\omega^{(k)*} \cdot \nabla \right) \boldsymbol{v}_\omega^{(k)} \Big|_{r_k = a} d\Omega_k. \tag{D.66}$$

Next we use the equation (D.52) and find

$$\begin{aligned} \boldsymbol{U}_k = -\frac{a\sqrt{4\pi}}{8\pi} \mathrm{Re} \sum_{\mu=0}^{\infty} \sqrt{\mu + 1} \boldsymbol{\xi}_\mu^{k*} \sum_{l=0}^{\infty} \sum_{m=-l}^{l} \\ \left[a_{lm}^{(k)} \int_{S_k} \left(\boldsymbol{Y}^*_{\mu\, \mu+1\, 0} \cdot \nabla \right) r_k^{-l-2} \boldsymbol{Y}_{l\, l+1\, m} d\Omega_k \right. \\ \left. + b_{lm}^{(k)} \int_{S_k} \left(\boldsymbol{Y}^*_{\mu\, \mu+1\, 0} \cdot \nabla \right) r_k^{l-1} \boldsymbol{Y}_{l\, l-1\, m} d\Omega_k \right]. \end{aligned} \tag{D.67}$$

Solutions of this kind of integrals were given by B.U. Felderhof and R.B. Jones in their work on swimming of a spherical body [16]. Due to the symmetry of the problem, the component $U_{k,y}$ vanishes. The spheres swim in the x-z-plane. The second integral vanishes for all components of the velocity, and the first integral gives

$$\int_{S_k}(\boldsymbol{Y}^*_{\mu\,l+1\,0}\cdot\nabla)\frac{\boldsymbol{Y}_{l\,l+1\,m}}{r_k^{l+2}}=\frac{\sqrt{(l+2)(2l+3)}}{a^{l+3}}\delta_{\mu l+1}(l+1\,0\,1\,q|l+1\,1\,l\,m)\hat{\boldsymbol{e}}_q \qquad \text{(D.68)}$$

where $(lm'1q|l1jm)$ is a Clebsch-Gordan coefficient and $\hat{\boldsymbol{e}}_q$ are spherical unit vectors [16]. If we replace the values of $a_{lm}^{(k)}$ and $b_{lm}^{(k)}$ given by the equations (D.53), (D.54) and (D.55) together with the solution of the first integral, we find that the velocity of sphere k is given by

$$\boldsymbol{U}_k=U_{k,x}\hat{\boldsymbol{e}}_x+U_{k,z}\hat{\boldsymbol{e}}_z, \qquad \text{(D.69)}$$

with $U_{k,z}$ and $U_{k,x}$ given by

$$U_{k,z}=\frac{1}{4a^2}\langle\underline{\xi}^{(k)}|\underline{\underline{S}}|\underline{d}^{(k)}\rangle+\langle\underline{d}^{(k)}|\underline{\underline{\tilde{S}}}|\underline{\xi}^1\rangle, \qquad \text{(D.70)}$$

and

$$U_{k,x}=\frac{1}{8a^2}\langle\underline{\xi}^{(k)}|\underline{\underline{S}}_1|\underline{d}^{(k)}\rangle+\langle\underline{d}^{(k)}|\underline{\underline{\widetilde{S}}}_1|\underline{\xi}^{(k)}\rangle-\langle\underline{\xi}^{(k)}|\underline{\underline{S}}_2|\underline{d}^{(k)}\rangle-\langle\underline{d}^{(k)}|\underline{\underline{\widetilde{S}}}_2|\underline{\xi}^{(k)}\rangle, \qquad \text{(D.71)}$$

respectively, where $\underline{\underline{\widetilde{M}}}$ denotes the transposed of a matrix $\underline{\underline{M}}$. We wrote the results in matrix notation for simplicity. The matrices $\underline{\underline{S}}$, $\underline{\underline{S}}_1$ and $\underline{\underline{S}}_2$ have components

$$S_{lm,l'm'} = l(l+1)\delta_{l,l+1}\delta_{m,m'}\delta_{m',0}, \qquad \text{(D.72)}$$

$$S_{1lm,l'm'} = (l-1)l(l+1)\delta_{l,l+1}\delta_{m,0}\delta_{m',1}, \qquad \text{(D.73)}$$

$$S_{2lm,l'm'} = (l+1)\delta_{l,l+1}\delta_{m,0}\delta_{m',-1}. \qquad \text{(D.74)}$$

Now we want to write the velocity of each sphere in terms of the amplitudes of deformations. To do that we use the equation (D.36) for $k=1$:

$$\frac{U_{1,z}}{\omega a} = \frac{i}{8}\Big[\langle\underline{\xi}^{1*}|[\underline{\underline{S}}\,\underline{\underline{D}}^1_1-(\underline{\underline{\widetilde{S}}}\,\underline{\underline{\widetilde{D}}}^1_1)]|\underline{\xi}^1\rangle + \langle\underline{\xi}^{1*}|\underline{\underline{S}}\,\underline{\underline{D}}^1_2|\underline{\xi}^2\rangle-\langle\underline{\xi}^{2*}|(\underline{\underline{\widetilde{S}}}\,\underline{\underline{\widetilde{D}}}^1_2)|\underline{\xi}^1\rangle\Big], \qquad \text{(D.75)}$$

$$\frac{U_{1,x}}{\omega a} = \frac{i}{16}\Big[\langle\underline{\xi}^{1*}|\{(\underline{\underline{S}}_1-\underline{\underline{S}}_2)\underline{\underline{D}}^1_1-[(\underline{\underline{S}}_1-\underline{\underline{\widetilde{S}}}_2)\underline{\underline{D}}^1_1]\}|\underline{\xi}^1\rangle + \langle\underline{\xi}^{1*}|(\underline{\underline{S}}_1-\underline{\underline{S}}_2)\underline{\underline{D}}^1_2|\underline{\xi}^2\rangle-\langle\underline{\xi}^{2*}|[(\underline{\underline{S}}_1-\underline{\underline{\widetilde{S}}}_2)\underline{\underline{D}}^1_2]|\underline{\xi}^1\rangle\Big]. \qquad \text{(D.76)}$$

The translational velocity for the second sphere is found for $k = 2$ from equation (D.37)

$$\frac{U_{2,z}}{\omega a} = \frac{i}{8}\Big[\langle\xi^2|[\underset{\approx}{S}\underset{\approx}{D}{}^2_2 - (\widetilde{\underset{\approx}{S}\underset{\approx}{D}{}^2_2})]|\xi^2\rangle + \langle\xi^2|\underset{\approx}{S}\underset{\approx}{D}{}^2_1|\xi^1\rangle - \langle\xi^1|(\widetilde{\underset{\approx}{S}\underset{\approx}{D}{}^2_1})|\xi^2\rangle\Big]. \tag{D.77}$$

$$\frac{U_{2,x}}{\omega a} = \frac{i}{8}\Big[\langle\xi^2|\{(\underset{\approx}{S}_1 - \underset{\approx}{S}_2)\underset{\approx}{D}{}^2_2 - [(\underset{\approx}{S}_1 - \widetilde{\underset{\approx}{S}_2})\underset{\approx}{D}{}^2_2]\}|\xi^2\rangle + \langle\xi^2|(\underset{\approx}{S}_1 - \underset{\approx}{S}_2)\underset{\approx}{D}{}^2_1|\xi^1\rangle - \langle\xi^1|[(\underset{\approx}{S}_1 - \widetilde{\underset{\approx}{S}_2})\underset{\approx}{D}{}^2_1]|\xi^2\rangle\Big]. \tag{D.78}$$

We have found expressions for the translational velocity of spheres 1 and 2. Hence we can calculate the center-of-mass velocity and the swimming efficiency.

We define the dimensionless velocity $\boldsymbol{U}$ as

$$\boldsymbol{U} = \frac{2\boldsymbol{U}_{cm}}{\omega a} = \frac{\boldsymbol{U}_1 + \boldsymbol{U}_2}{\omega a}. \tag{D.79}$$

We get

$$\begin{aligned}\boldsymbol{U} = {} & \frac{i}{8}\Big[\langle\xi^1|(\underset{\approx}{F}{}^1_1 - \widetilde{\underset{\approx}{F}{}^1_1})|\xi^1\rangle + \langle\xi^1|(\underset{\approx}{F}{}^1_2 - \widetilde{\underset{\approx}{F}{}^2_1})|\xi^2\rangle \\ & + \langle\xi^2|(\underset{\approx}{F}{}^2_1 - \widetilde{\underset{\approx}{F}{}^1_2})|\xi^1\rangle + \langle\xi^2|(\underset{\approx}{F}{}^2_2 - \widetilde{\underset{\approx}{F}{}^2_2})|\xi^2\rangle\Big]\hat{\boldsymbol{e}}_z \\ & + \frac{1}{8}\Big[\langle\xi^1|(\underset{\approx}{G}{}^1_1 - \widetilde{\underset{\approx}{G}{}^1_1})|\xi^1\rangle + \langle\xi^1|(\underset{\approx}{G}{}^1_2 - \widetilde{\underset{\approx}{G}{}^2_1})|\xi^2\rangle \\ & + \langle\xi^2|\underset{\approx}{G}{}^2_1 - \widetilde{\underset{\approx}{G}{}^1_2}|\xi^1\rangle + \langle\xi^2|\underset{\approx}{G}{}^2_2 - \widetilde{\underset{\approx}{G}{}^2_2}|\xi^2\rangle\Big]\hat{\boldsymbol{e}}_x.\end{aligned} \tag{D.80}$$

where the matrices $\underset{\approx}{F}{}^j_i$ and $\underset{\approx}{G}{}^j_i$ are defined by the following relations

$$\underset{\approx}{F}{}^j_i = \underset{\approx}{S}\underset{\approx}{D}{}^j_i, \tag{D.81}$$

$$\underset{\approx}{G}{}^j_i = (\underset{\approx}{S}_1 - \underset{\approx}{S}_2)\underset{\approx}{D}{}^j_i, \tag{D.82}$$

where both i and j can take the values 1 or 2.

In order to investigate the properties of these matrices and to simplify our calculations we define the even and odd submatrices, $\underset{\approx}{M}_e$ and $\underset{\approx}{M}_o$, respectively, of a Matrix $\underset{\approx}{M}$:

$$M_{e\,lm,l'm'} = \begin{Bmatrix} M_{lm,l'm'} \\ 0 \end{Bmatrix} \text{ if } l + l' \text{ is } \begin{Bmatrix} \text{even} \\ \text{odd} \end{Bmatrix}, \tag{D.83}$$

$$M_{o\,lm,l'm'} = \begin{Bmatrix} 0 \\ M_{lm,l'm'} \end{Bmatrix} \text{ if } l + l' \text{ is } \begin{Bmatrix} \text{even} \\ \text{odd} \end{Bmatrix}, \tag{D.84}$$

such that

$$\underset{\approx}{M} = \underset{\approx}{M}_e + \underset{\approx}{M}_o. \tag{D.85}$$

With these definitions, the $\underset{\approx}{F}$-matrices satisfy the following relations

$$\underset{\approx}{F}^2_{o1} = \underset{\approx}{F}^1_{o2}, \tag{D.86}$$
$$\underset{\approx}{F}^2_{o2} = \underset{\approx}{F}^1_{o1}, \tag{D.87}$$
$$\underset{\approx}{F}^2_{e1} = -\underset{\approx}{F}^1_{e2}, \tag{D.88}$$
$$\underset{\approx}{F}^2_{e2} = -\underset{\approx}{F}^1_{e1}. \tag{D.89}$$
$$\tag{D.90}$$

The same symmetry relations hold for the $\underset{\approx}{G}$-matrices.

We are interested in finding the maximum swimming efficiency, which will lead to a generalized eigenvalue equation. As mentioned in the beginning of the chapter, we want to find it under the condition that both bodies swim with the same velocity.

$$\boldsymbol{U}_1 - \boldsymbol{U}_2 = 0. \tag{D.91}$$

We find that this condition may be satisfied if the complex amplitudes of the surface displacements of the second sphere are related to that of the first one by

$$\underset{\sim}{\xi}^{(2)} = e^{i\varphi}\underset{\sim}{\xi}^{(1)}, \tag{D.92}$$

that is, they only differ in a phase factor corresponding to a delay between the time-dependent deformations, and if, in addition, the amplitudes $\underset{\sim}{\xi}^{(1)}$ are of the form

$$\xi^{(1)}_l = i^l c_l, \tag{D.93}$$

where the c_l are real numbers.

With the help of this we write the velocity as

$$\boldsymbol{U} = \langle \underset{\sim}{\xi}^{(1)} | \underset{\approx}{B}^z | \underset{\sim}{\xi}^{(1)} \rangle \hat{\boldsymbol{e}}_z + \langle \underset{\sim}{\xi}^{(1)} | \underset{\approx}{B}^x | \underset{\sim}{\xi}^{(1)} \rangle \hat{\boldsymbol{e}}_x, \tag{D.94}$$

where the matrices $\underset{\approx}{B}^z$ and $\underset{\approx}{B}^x$ may be decomposed into their even and odd parts:

$$\underset{\approx}{B}^k = \underset{\approx}{B}^k_e + \underset{\approx}{B}^k_o. \tag{D.95}$$

with $k = x, z$. These components are given by

$$\underset{\approx}{B}^z_e = -\frac{1}{4}\sin\varphi(\underset{\approx}{F}^1_{e2} + \widetilde{\underset{\approx}{F}^1_{e2}}), \tag{D.96}$$

$$\underset{\approx}{B}^z_o = \frac{i}{4}\left[\underset{\approx}{F}^1_{o1} - \widetilde{\underset{\approx}{F}^1_{o1}} - 2\cos\varphi(\underset{\approx}{F}^1_{o2} - \widetilde{\underset{\approx}{F}^1_{o2}})\right]. \tag{D.97}$$

$$\underset{\approx}{B}^x_e = -\frac{1}{8}\sin\varphi(\underset{\approx}{G}^1_{e2} + \widetilde{\underset{\approx}{G}^1_{e2}}), \tag{D.98}$$

$$\underset{\approx}{B}^x_o = \frac{i}{8}\left[\underset{\approx}{G}^1_{o1} - \widetilde{\underset{\approx}{G}^1_{o1}} - 2\cos\varphi(\underset{\approx}{G}^1_{o2} - \widetilde{\underset{\approx}{G}^1_{o2}})\right]. \tag{D.99}$$

The matrices $\underset{\approx}{B}^k$ are Hermitian with the properties that their odd part is purely real and their even part is purely imaginary. These properties are important because they simplify the computation of numerical results.

In correspondance with the decomposition of the matrices $\underset{\approx}{B}^k$, the dimensionless velocity may be split into two parts:

$$\boldsymbol{U} = \boldsymbol{U}_e + \boldsymbol{U}_o, \tag{D.100}$$

where the subscripts e and o refer to the contributions from the even and odd parts of the matrices $\underset{\approx}{B}^k$, respectively:

$$\boldsymbol{U}_e = \langle\xi^1|\underset{\approx}{B}^z_e|\xi^1\rangle\hat{\boldsymbol{e}}_z + \langle\xi^1|\underset{\approx}{B}^x_e|\xi^1\rangle\hat{\boldsymbol{e}}_x, \tag{D.101}$$

$$\boldsymbol{U}_o = \langle\xi^1|\underset{\approx}{B}^z_o|\xi^1\rangle\hat{\boldsymbol{e}}_z + \langle\xi^1|\underset{\approx}{B}^x_o|\xi^1\rangle\hat{\boldsymbol{e}}_x. \tag{D.102}$$

In the determination of the greatest efficiency the problem arises that we do not know precisely the direction of the velocity $\boldsymbol{U}$. Therefore, we introduce an additional degree of freedom and consider the component U_γ of the velocity corresponding to a given direction, forming an angle γ with the z-axis:

$$U_\gamma = U_x\sin\gamma + U_z\cos\gamma = \langle\xi^1|(\underset{\approx}{B}^z\cos\gamma + \underset{\approx}{B}^x\sin\gamma)|\xi^1\rangle, \tag{D.103}$$

which is again a quadratic form in the surface displacements. We may obtain the modulus of the velocity by (numerically) maximizing this component with respect to γ:

$$U = \max_\gamma U_\gamma = U_{\gamma_0}. \tag{D.104}$$

This also yields the deviation γ_0 of the velocity vector from the z-axis.

We shall first maximize the component U_γ with respect to the deformation amplitudes ξ^1 for different angles γ using a numerical method which will be described in the next chapter. Afterwards we shall determine the value γ_0 for which the component achieves its maximum.

D.4 Average Rate of Energy Dissipation

In the present section we calculate the average rate of energy dissipation of the system as a quadratic form in the surface displacement. In an incompressible fluid in a stationary situation without external forces and torques, the energy dissipation may be expressed as an integral over the surface of the fluid. Since in the present work we consider an infinite fluid with two spherical bodies immersed in it, we can split the dissipation into two portions $\langle D_1 \rangle$ and $\langle D_2 \rangle$, each corresponding to the integral over the surface of the respective sphere. The total rate of energy dissipation, averaged over a period, is thus given by

$$\langle D \rangle = \langle D_1 \rangle + \langle D_2 \rangle. \tag{D.105}$$

The portions are given by the relation

$$\langle D_k \rangle = -\frac{1}{2}\mathrm{Re} \int\limits_{S_0(k)} \boldsymbol{v}_\omega^{k*} \cdot \boldsymbol{\sigma}_\omega^{(k)} \cdot \boldsymbol{dS}, \tag{D.106}$$

for $k = 1, 2$. The integral is evaluated at the undeformed surface of the sphere k. It may be expressed as

$$\langle D_k \rangle = -\frac{a^2}{2}\mathrm{Re} \int \left(\boldsymbol{v}_\omega^{k*} \cdot \boldsymbol{\sigma}_\omega^{(k)} \right)_{r_k=a} \cdot \hat{\boldsymbol{r}}_k d\Omega_k. \tag{D.107}$$

From equation (D.52) we get

$$\langle D_k \rangle = -\frac{1}{2}\mathrm{Re} \sum_{l=0}^{\infty} \sum_{m=-l}^{l} \left(a^{-l} a_{lm}^{k*} \int\limits_{S_k} \boldsymbol{Y}_{ll+1\,m}^* \cdot \boldsymbol{\sigma}_\omega \cdot \hat{\boldsymbol{r}}_k d\Omega_k + b_{lm}^{k*} a^{l+1} \int\limits_{S_k} \boldsymbol{Y}_{ll-1\,m} \cdot \boldsymbol{\sigma}_\omega \cdot \hat{\boldsymbol{r}}_k d\Omega_k \right). \tag{D.108}$$

These are integral of the generic form

$$\int\limits_{S_0} \boldsymbol{Y}_{ijm}^* \cdot \boldsymbol{\sigma}_\omega \cdot \hat{\boldsymbol{r}} d\Omega =$$

$$\int\limits_{S_0} (\boldsymbol{Y}_{ijm}^* \cdot \hat{\boldsymbol{r}}) \sigma_{rr} + \int\limits_{S_0} (\boldsymbol{Y}_{ijm}^* \cdot \hat{\boldsymbol{e}}_\theta) \sigma_{\theta r} + \int\limits_{S_0} (\boldsymbol{Y}_{ijm}^* \cdot \hat{\boldsymbol{e}}_\varphi) \sigma_{\varphi r}. \tag{D.109}$$

Here we have substitued the components of the stress tensor in spherical coordinates and we find that these three integrals do not cancel. Explicitly, these components of the stress tensor read:

$$\sigma_{rr} = -p + 2\eta \frac{\partial \boldsymbol{v}_\omega \cdot \hat{\boldsymbol{r}}}{\partial r}, \tag{D.110}$$

$$\sigma_{\theta r} = \eta \left(\frac{1}{r} \frac{\partial (\boldsymbol{v}_\omega \cdot \hat{\boldsymbol{r}})}{\partial \theta} + \frac{\partial (\boldsymbol{v}_\omega \cdot \hat{\boldsymbol{e}}_\theta)}{\partial r} - \frac{(\boldsymbol{v}_\omega \cdot \hat{\boldsymbol{e}}_\theta)}{r} \right), \tag{D.111}$$

$$\sigma_{\varphi r} = \eta \left(\frac{1}{r \sin\theta} \frac{\partial (\boldsymbol{v}_\omega \cdot \hat{\boldsymbol{r}})}{\partial \varphi} + \frac{\partial (\boldsymbol{v}_\omega \cdot \hat{\boldsymbol{e}}_\varphi)}{\partial r} - \frac{(\boldsymbol{v}_\omega \cdot \hat{\boldsymbol{e}}_\varphi)}{r} \right). \tag{D.112}$$

From these relations and equation (D.52) is found

$$\begin{aligned}\int_{S_0} \boldsymbol{Y}^*_{ijm}\cdot\boldsymbol{\sigma}_\omega\cdot\hat{\boldsymbol{r}}d\Omega &= -\int_{S_0}(\boldsymbol{Y}^*_{ijm}\cdot)p_{\omega k}d\Omega\\ &+\eta\sum_{l'm'}\Big\{a^k_{l'm'}\Big[\int_{S_0}[(\boldsymbol{Y}^*_{ijm}\cdot\nabla)\frac{\boldsymbol{Y}_{l'l'+1m'}}{r^{l'+2}}]\cdot\hat{\boldsymbol{r}}d\Omega\\ &+\int_{S_0}\boldsymbol{Y}^*_{ijm}\cdot(\hat{\boldsymbol{r}}\cdot\nabla)\frac{\boldsymbol{Y}_{l'l'+1m'}}{r^{l'+2}}d\Omega\Big]\\ &+b^k_{l'm'}\Big[\int_{S_0}[(\boldsymbol{Y}^*_{ijm}\cdot\nabla)r^{l'-1}\boldsymbol{Y}_{l'l'-1m'}]\cdot\hat{\boldsymbol{r}}d\Omega\\ &+\int_{S_0}\boldsymbol{Y}^*_{ijm}\cdot(\hat{\boldsymbol{r}}\cdot\nabla)r^{l'-1}\boldsymbol{Y}_{l'l'-1m'}d\Omega\Big]\Big\}. \qquad \text{(D.113)}\end{aligned}$$

We can see from equation (D.61) that the integral related to the pressure has the generic form

$$\int \boldsymbol{Y}^*_{jlm}\cdot Y_{l'm'}\hat{\boldsymbol{r}}d\Omega, \qquad \text{(D.114)}$$

so it reduces to normalization integrals for scalar harmonics. In evaluating the integrals multiplying the coefficients $a^k_{l'm'}$ and $b^k_{l'm'}$ we find integrals of the form [16]:

$$\begin{aligned}\int_{S_0}[(\boldsymbol{Y}^*_{jlm}\cdot\nabla)h(r)\boldsymbol{Y}_{j'l'm'}]\cdot\hat{\boldsymbol{r}}d\Omega &= h(a)\int_{S_0}[(\boldsymbol{Y}^*_{jlm}\cdot\nabla)\boldsymbol{Y}_{j'l'm'}]\cdot\hat{\boldsymbol{r}}d\Omega\\ &+h'(a)\int_{S_0}(\boldsymbol{Y}^*_{jlm}\cdot\hat{\boldsymbol{r}})(\boldsymbol{Y}_{j'l'm'}\cdot\hat{\boldsymbol{r}})d\Omega, \qquad \text{(D.115)}\end{aligned}$$

$$\int_{S_0}\boldsymbol{Y}^*_{jlm}\cdot[(\hat{\boldsymbol{r}}\cdot\nabla)(h(r)\boldsymbol{Y}_{j'l'm'})]d\Omega = h'(a)\int_{S_0}\boldsymbol{Y}^*_{jlm}\cdot\boldsymbol{Y}_{j'l'm'}\hat{\boldsymbol{r}}_k d\Omega, \qquad \text{(D.116)}$$

The second integral on the right hand side of the equation (D.115) reduces to normalization integrals for the scalar spherical harmonics, as can be seen from the relations (C.37) for the vector spherical harmonics. The first integral on the right hand side of the equation (D.115) can be evaluated by using the angular momentum coupling theory [20]. The integral (D.116) is the normalization for the vector spherical harmonics . A more detailed solution of the integrals is given in the appendix of the paper written by Felderhof and Jones, about swimming of one spherical body. [16]. By application of the mentioned results we find for the average rates of energy dissipation

$$\langle D_k \rangle = \frac{1}{2}\mathrm{Re}\sum_{l=0}^{\infty}\sum_{m=-l}^{l}\left\{\frac{a_{lm}^{(k)*}}{a^l}\left[\sqrt{\frac{l+1}{2l+1}}\left(\frac{a_{p,lm}^{(k)}}{a^{l+1}}+a^l b_{p,lm}^{(k)}\right)-2\eta\frac{l+2}{a^{l+3}}a_{lm}^{(k)}\right]\right.$$
$$\left.+a^{l+1}b_{lm}^{(k)*}\left[-\sqrt{\frac{l}{2l+1}}\left(\frac{a_{p,lm}^{(k)}}{a^{l+1}}+a^l b_{p,lm}^{(k)}\right)+2\eta(l+1)a^{l-1}b_{lm}^{(k)}\right]\right\}. \tag{D.117}$$

From this relation we get the rate of energy dissipation related to sphere k. The total rate of energy dissipation is given by (D.105). From the equations (D.58), (D.53), and the condition that both spheres swim with the same velocity, we get for the total rate of energy dissipation the following relation

$$\langle D \rangle = \langle \xi^{(1)} | \underset{\approx}{A} | \xi^{(1)} \rangle, \tag{D.118}$$

where the matrix $\underset{\approx}{A}$ may be decomposed as

$$\underset{\approx}{A} = \underset{\approx}{A}_o + \underset{\approx}{A}_e, \tag{D.119}$$

where the even and odd parts A_e and A_o are given by

$$\underset{\approx}{A}_e = \frac{1}{2}\{[(\widetilde{\underset{\approx}{D}^1_1}\underset{\approx}{R}_5\underset{\sim}{D}^1_1)_e+(\widetilde{\underset{\approx}{D}^1_2}\underset{\approx}{R}_5\underset{\sim}{D}^1_1)_e-(\widetilde{\underset{\approx}{H}^1_1}\underset{\approx}{R}_4\underset{\sim}{H}^1_1)_e-(\widetilde{\underset{\approx}{H}^1_2}\underset{\approx}{R}_4\underset{\sim}{H}^1_2)_e$$
$$+\cos\varphi[(\widetilde{\underset{\approx}{D}^1_1}\underset{\approx}{R}_5\underset{\sim}{D}^1_2)_e+(\widetilde{\underset{\approx}{D}^1_2}\underset{\approx}{R}_5\underset{\sim}{D}^1_1)_e-(\widetilde{\underset{\approx}{H}^1_1}\underset{\approx}{R}_4\underset{\sim}{H}^1_2)_e-(\widetilde{\underset{\approx}{H}^1_2}\underset{\approx}{R}_4\underset{\sim}{H}^1_1)_e]\}, \tag{D.120}$$

$$\underset{\approx}{A}_o = i\sin\varphi[(\widetilde{\underset{\approx}{D}^1_1}\underset{\approx}{R}_5\underset{\sim}{D}^1_2)_o-(\widetilde{\underset{\approx}{D}^1_1}\underset{\approx}{R}_5\underset{\sim}{D}^1_1)_o+(\widetilde{\underset{\approx}{H}^1_2}\underset{\approx}{R}_5\underset{\sim}{H}^1_1)_o-(\widetilde{\underset{\approx}{H}^1_1}\underset{\approx}{R}_5\underset{\sim}{D}^1_2)_o], \tag{D.121}$$

respectively. The matrices $\underset{\approx}{H}^1_1$, $\underset{\approx}{H}^1_2$, $\underset{\approx}{H}^2_1$ and $\underset{\approx}{H}^2_2$ are found from the relations

$$\underset{\approx}{H}^1_\alpha = \underset{\approx}{C}\underset{\approx}{F}\underset{\approx}{D}^1_\alpha, \tag{D.122}$$
$$\underset{\approx}{H}^2_\alpha = \underset{\approx}{F}\underset{\approx}{C}\underset{\approx}{D}^1_\alpha. \tag{D.123}$$

where α can take the values 1 or 2.

We remember that the condition of both spheres swimming with the same velocity in the direction $\hat{\mathbf{z}}$ is satisfied if the relations (D.92) and (D.93) between the deformation amplitudes of both spheres holds. In the above calculations we have used these conditions.

D.5 Swimming Efficiency

In the preceding section we expressed the swimming velocity and rate of energy dissipation of the system as quadratic forms in the space of the nondimensional coefficients ξ_l^1 related to the amplitude of deformation of the spheres. For simplicity in the following we drop the superscript 1. From equations (D.62), (D.103) and (D.118) we finally find that the swimming efficiency is given by

$$\eta_T = \frac{1}{\pi} \frac{\langle \xi | (\underset{\approx}{B}^z \cos\gamma + \underset{\approx}{B}^x \sin\gamma) | \xi \rangle}{\langle \xi | \underset{\approx}{A} | \xi \rangle}, \tag{D.124}$$

where the matrices $\underset{\approx}{B}^z$, $\underset{\approx}{B}^x$ and $\underset{\approx}{A}$ are Hermitian, and $\underset{\approx}{A}$ is positive definite. From these expressions we can see that the determination of the maximum swimming efficiency for the two-body problem is reduced to the calculation of the maximum eigenvalue of the generalized eigenvalue problem

$$(\underset{\approx}{B}^z \cos\gamma + \underset{\approx}{B}^x \sin\gamma) | \xi \rangle = \lambda \underset{\approx}{A} | \xi \rangle. \tag{D.125}$$

For a given rate of energy dissipation the greatest velocity is given by

$$\eta_T = \frac{|\lambda_{max}|}{\pi}. \tag{D.126}$$

We have reduced the two-body problem to a generalized eigenvalue problem, in analogy to the one-body problem. The difference is that we now have to deal with more complicated matrices. In the next chapter we are going to describe the methods to solve the eigenvalue problem for different modes of swimming. We shall apply them to find the best swimming stroke for the two-body system.

Apéndice E

Numerical Calculations

In the present chapter we are going to explain the procedure used to get the maximum efficiency of swimming for the case of two spheres.

We are going to begin with the simplest case, which is one sphere swimming behind the other, $\theta_R = 0$. Next we generalize the results to find the solution to the more general problem of arbitrary angle θ_R between the directions of the bodies' velocity and their distance.

The flow is generated by the surface displacements on each sphere, and the hydrodynamic interactions between them. We assumed in chapter D that the spheres have the same kind of deformations, but with a phase difference between them.

The surface displacement for sphere 1 is given by

$$\xi^1_\omega(\theta) = -\sqrt{4\pi}a \sum_{l=0}^{\infty} \xi_l \left[(l+1)P_l(\cos\theta)\hat{\boldsymbol{r}} + P^1_l(\cos\theta)\hat{\boldsymbol{\theta}}\right], \tag{E.1}$$

and for sphere 2 by

$$\xi^2_\omega(\theta) = e^{i\varphi}\xi^1_\omega(\theta). \tag{E.2}$$

E.1 One Sphere behind the Other

E.1.1 One Multipole

First we consider the case in which only one harmonic contributes to the surface displacement. This means, that it is described by

$$\xi^1_\omega(\theta) = -\sqrt{4\pi}a\xi_l \left[(l+1)P_l(\cos\theta)\hat{\boldsymbol{r}} + P^1_l(\cos\theta)\hat{\boldsymbol{\theta}}\right], \tag{E.3}$$

where l can take the value 1, 2, 3,.... B.U. Felderhof and R.B. Jones showed that in this case a single sphere does not swim. We want to investigate if for two spheres there is a contribution to the translational velocity. The expression for this velocity, in this case, reduces to

$$U = |\xi_l|^2 B^z_{l0,l0}, \tag{E.4}$$

and for the dissipation to

$$\langle D \rangle = |\xi_l|^2 A_{l0,l0}. \tag{E.5}$$

Then, the swimming efficiency can be written as

$$\eta_T = \frac{|\lambda|}{\pi}, \tag{E.6}$$

with

$$\lambda = \frac{B^z_{l0,l0}}{A_{l0,l0}}. \tag{E.7}$$

The diagonal elements $B_{l0,l0}$ and $A_{l0,l0}$ depend implicitly on the distance R between the centers of both spheres and the phase difference φ between their surface deformations. Now, we want to find out first, if and under which circumstances the spheres obtain a nonvanishing swimming velocity U, and then, if this is the case, we want to determine the phase difference and the distance between the centers of the spheres for which swimming is most efficient. To this end we shall plot graphs of the numerically calculated swimming efficiency versus the phase difference (fig. E.1) and vs. $x = a/R$ (where a is the radius of each sphere; fig. E.2) in order to find the absolute maximum. We find that for $l = 0$ and $l = 1$ the spheres do not swim, and that for large l their velocity falls off with increasing distance very quickly.

In figure E.1 we have plotted λ vs. the phase difference φ. The swimming efficiency can be obtained from the equation (E.6). In this figure we chose $x = 0.45$, which means a rather close distance between the spheres.

For deformations with $l = 0$ or $l = 1$ the translational velocity of the spheres vanishes, while for $l \geq 2$ they acquire a nonvanishing swimming velocity. For even multipoles $l = 2, 4, \ldots$ the spheres swim in the negative z-direction for phase differences in the range $0 < \varphi < \pi$, and in the positive z-direction for $\pi < \varphi < 2\pi$. For odd multipoles $l = 3, 5, \ldots$ the z-component of the velocity is positive for $0 < \varphi < \pi$ and negative for $\pi < \varphi < 2\pi$. For phase differences $\varphi = 0$ or $\varphi = \pi$ the spheres do not swim for any multipole order l.

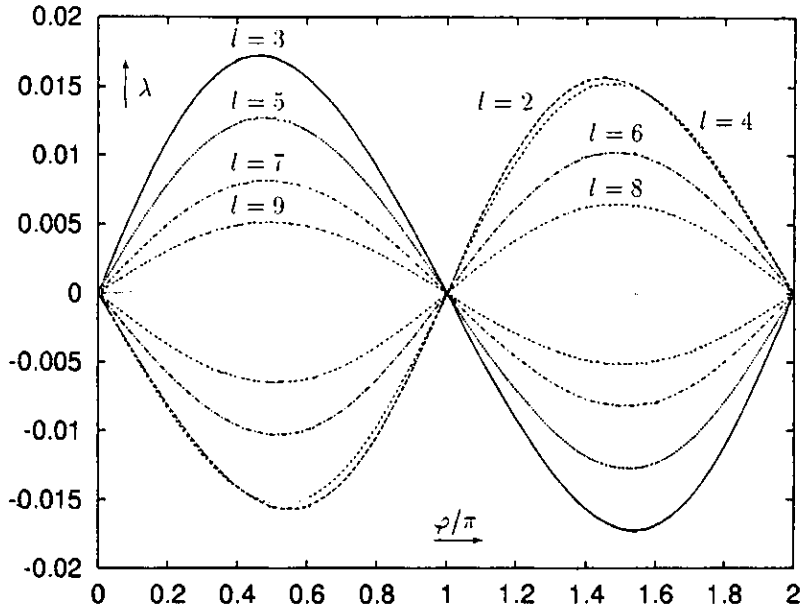

Figure E.1: λ for two spheres at a dimensionless inverse distance $x = 0.45$, with deformations as described by one multipole of order l, in dependence on the phase difference φ.

At the chosen distance, the maximum of the efficiency grows at going from $l = 2$ to $l = 3$, then decreases again at going to higher multipole orders, the maximum for $l = 4$ already being smaller than for $l = 2$. For very high multipole orders ($l \approx 30$) the efficiency tends to zero.

In figure E.2, we have plotted the swimming efficiency versus x. In this plot, we considered — for each l and x — only the maximum efficiency with respect to the phase difference φ. Thus every single point of one of the graphs here corresponds to the maximum of the graph for the same multipole order l in the preceding figure E.1 (for $x = 0.45$), or of a similar graph for the respective value of x. This plot allows to compare the dependence of the swimming efficiency on the distance between the spheres for different multipole orders l.

We notice again that for all distances the spheres do not swim if $l = 0$ or $l = 1$. For large separations of the spheres ($x \to 0$) the efficiency tends to zero. For increasing x it grows faster for higher multipole orders. Thus for $x < 0.43$ the efficiency is

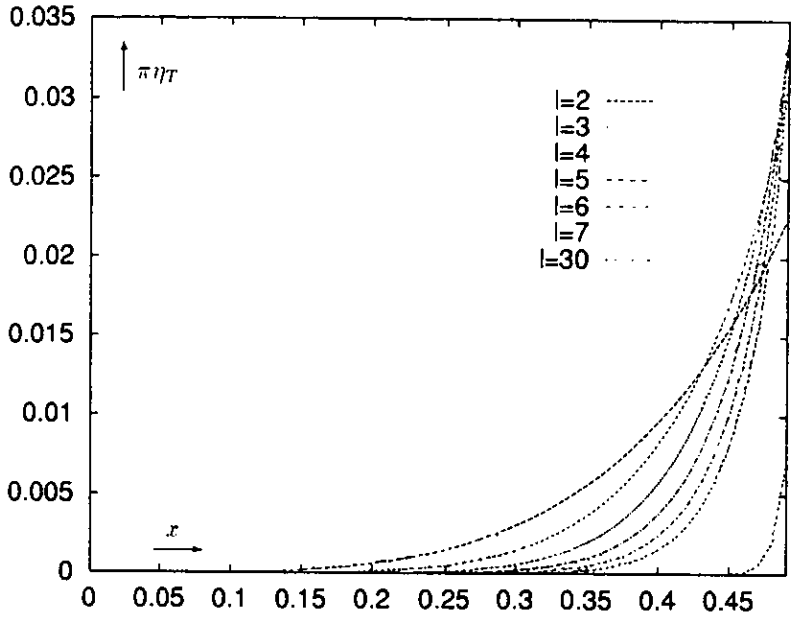

Figure E.2: Swimming efficiency η_T for two spheres, with deformations as described by one multipole of order l, in dependence on the dimensionless inverse distance x.

greatest for $l = 2$, then for $0.43 < x < 0.47$ the maximum is achieved for $l = 3$, then for $l = 4$ and so on, but for very high multipole orders the swimming efficiency remains small, as may be seen for example from the graph for $l = 30$ in this plot.

We conclude that as long as the surface deformations can be described by a single multipole contribution of order l, two spherical particles can, in contrast to a single one, acquire a finite swimming velocity for $l \geq 2$, that their swimming efficiency increases with decreasing distance between them, and that its maximum for distances at which the spheres are still well separated is achieved for the low multipole orders $l = 2, 3, 4, \ldots$, depending on the distance.

The following plots, figures E.3, E.4, visualize two different swimming modes, described by the single multipoles $l = 2$ and $l = 3$, respectively. We have chosen the distance between the spheres at which the maximum efficiency passes from the $l = 2$- to the $l = 3$-mode, $x = 0.43$ (cf. fig. E.2). The plot shows 24 pictures, each consisting of the shapes of both bodies, taken at equally spaced instants during a period. The sequence is to be read as the text of a book, from the left to the

right within the lines, and from the top to the bottom. The swimming direction is towards the top of the page, and sphere 1 is swimming behind sphere 2, thus it appears beneath the latter in each picture.

We may consider this as an example showing that the same swimming efficiency can be achieved by rather different swimming strokes.

E.1.2 Two Multipoles

In this case we consider contributions of two multipoles of subsequent order to the surface deformations. Thus, we have

$$\begin{aligned}\boldsymbol{\xi}^1_\omega(\theta) &= -\sqrt{4\pi}a\left\{\xi_l\left[(l+1)P_l(\cos\theta)\hat{\boldsymbol{r}} + P^1_l(\cos\theta)\hat{\boldsymbol{\theta}}\right]\right. \\ &\qquad \left. +\xi_{l+1}\left[(l+2)P_{l+1}(\cos\theta)\hat{\boldsymbol{r}} + P^1_{l+1}(\cos\theta)\hat{\boldsymbol{\theta}}\right]\right\}, \qquad \text{(E.8)}\\ \boldsymbol{\xi}^2_\omega(\theta) &= e^{i\varphi}\boldsymbol{\xi}^1_\omega(\theta). \qquad \text{(E.9)}\end{aligned}$$

The velocity of the spheres is given by

$$U = \langle\xi|\underset{\approx}{B}^z|\xi\rangle. \qquad \text{(E.10)}$$

and the dissipation by

$$\langle D\rangle = \langle\xi|\underset{\approx}{A}|\xi\rangle. \qquad \text{(E.11)}$$

Due to the symmetry of the problem there is no velocity component in the x-direction. The spheres can, however, swim in the positive or negative z-direction.

The swimming efficiency is found from

$$\eta_T = \frac{1}{\pi}\frac{|\langle\xi|\underset{\approx}{B}^z|\xi\rangle|}{\langle\xi|\underset{\approx}{A}|\xi\rangle}. \qquad \text{(E.12)}$$

We want to find its maximum with respect to the amplitudes of deformations. For simplicity, we may equivalently maximize the velocity U with the condition that the dissipation be constant, say $\langle D\rangle = 1$. Variation with respect to ξ leads to the generalized eigenvalue equation

$$\underset{\approx}{B}^z|\xi\rangle = \lambda\underset{\approx}{A}|\xi\rangle. \qquad \text{(E.13)}$$

As a necessary condition for the existence of nontrivial solutions $|\xi\rangle \neq 0$ the following determinant must vanish:

$$\det(\underset{\approx}{B}^z - \lambda\underset{\approx}{A}) = 0. \qquad \text{(E.14)}$$

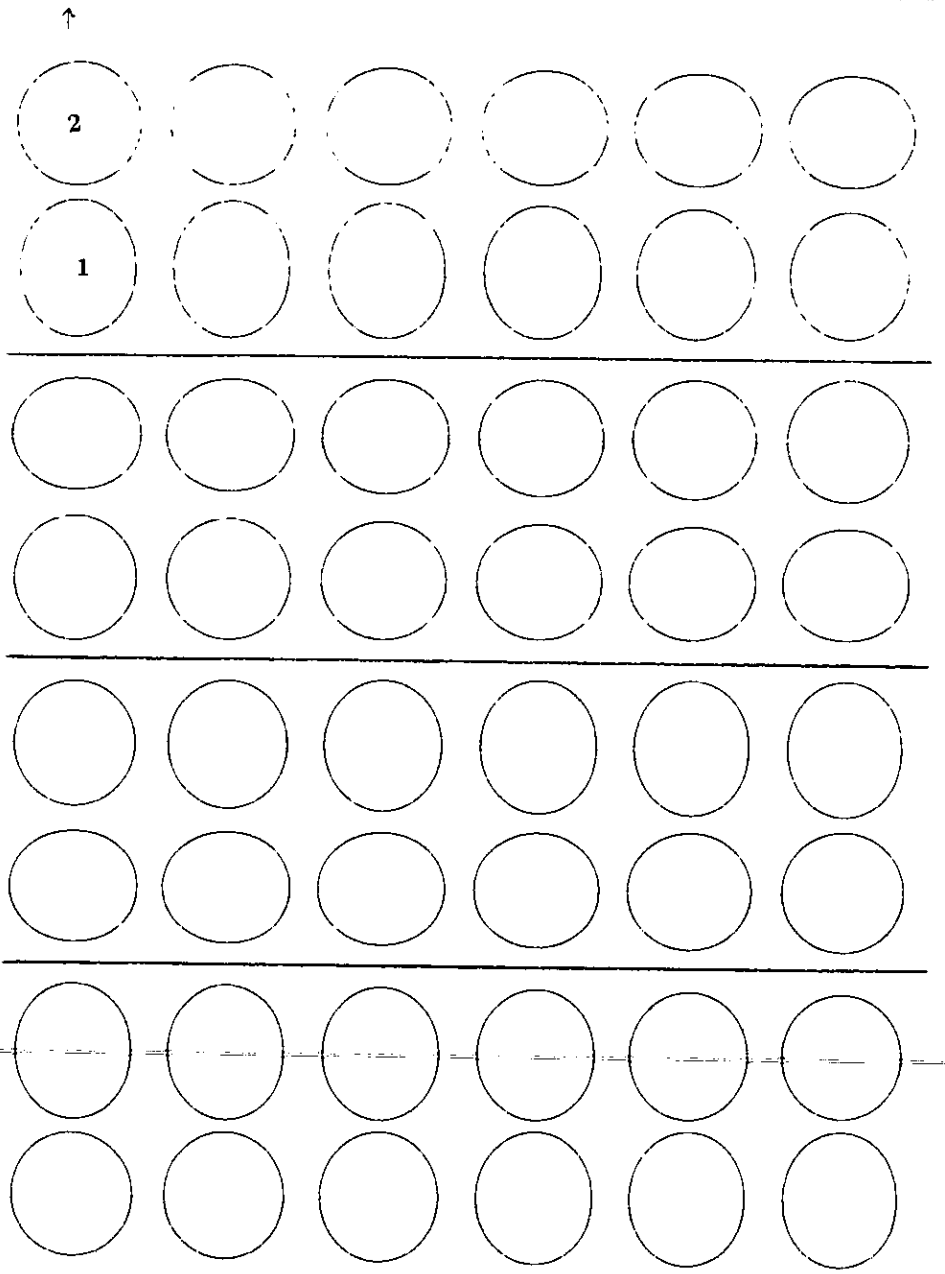

Figure E.3: Shapes of two spheres swimming one behind the other at a dimensionless inverse distance $x = 0.43$, with deformations as described by one multipole $l = 2$, at instants spaced 1/24 of a period.

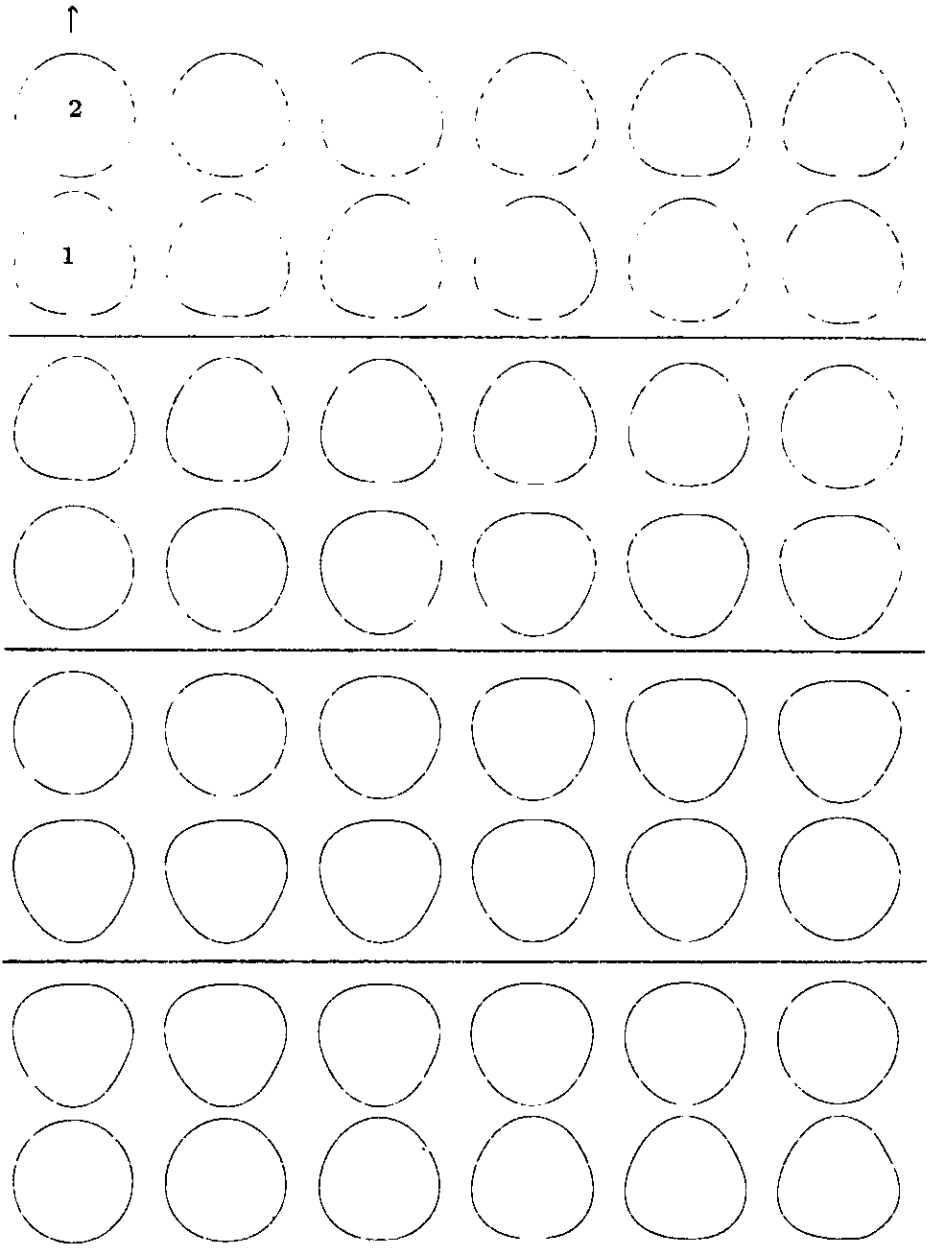

Figure E.4: Shapes of two spheres swimming one behind the other at a dimensionless inverse distance $x = 0.43$, with deformations as described by one multipole $l = 3$, at instants spaced $1/24$ of a period.

This condition yields a quadratic equation for the eigenvalues λ, of which we select the greatest, λ_0. We then solve the system of equations

$$\underset{\approx}{B}^{z}|\xi_0\rangle = \lambda_0 \underset{\approx}{A}|\xi_0\rangle \tag{E.15}$$

to obtain the deformations ξ_0 for which the efficiency achieves its maximum. We normalize ξ_0 such that

$$\langle\xi_0|\underset{\approx}{A}|\xi_0\rangle = 1. \tag{E.16}$$

Then

$$\langle\xi_0|\underset{\approx}{B}^{z}|\xi_0\rangle = \lambda_0. \tag{E.17}$$

The maximum swimming efficiency is then given by

$$\eta_{T\,max} = \frac{|\lambda_0|}{\pi}. \tag{E.18}$$

For the case of two multipole contributions we are going to use this method to determine the maximum efficiency of swimming. We have to remember that the matrices $\underset{\approx}{B}$ and $\underset{\approx}{A}$ depend implicitly on x and φ. Thus, we determine the swimming efficiency for various values of these parameters, and find the absolute maximum numerically.

In the figures E.5 and E.6 we have plotted the swimming efficiency η_T versus the phase difference φ between the deformations of both spheres. We have taken into account only motion in the positive z-direction.

For each graph in both figures we notice a maximum, where the efficiency is higher, and a minimum, where it is lower than that of a single sphere. We can see that in the first figure, where l is odd, the maximum efficiency is found for $0 < \varphi < \pi$ and the minimum for $-\pi < \varphi < 2\pi$. In the second figure, with l even, the maximum swimming efficiency is achieved for $\pi < \varphi < 2\pi$, and the minimum for $0 < \varphi < \pi$.

Predominantly, we are interested in the maxima, where the bodies gain efficiency by swimming together.

The dependence of the swimming efficiency on the phase difference φ is weaker for higher multipoles; in the limit of infinite multipole orders the efficiency tends to a constant and coincides with that for a single body. The gain in efficiency is thus only important for lower multipole orders.

In these graphs, the swimming direction was specified to be the positive z-direction. In order to consider spheres swimming in the opposite direction, we may simply reverse the time or, equivalently, replace the phase difference φ by

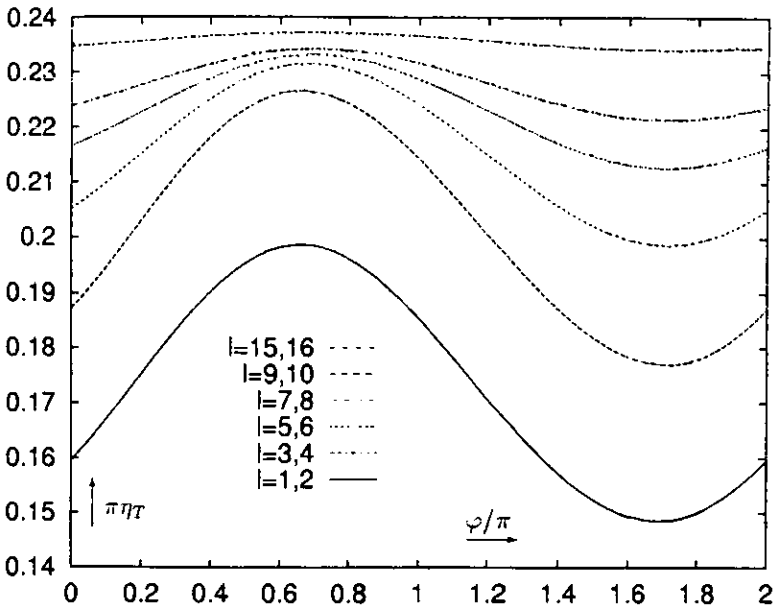

Figure E.5: Swimming efficiency η_T for two spheres at a dimensionless inverse distance $x = 0.45$, with deformations as described by two subsequent multipoles of order l (odd), $l + 1$, in dependence on the phase difference φ.

$2\pi - \varphi$. Thus, if we compare the swimming efficiencies in the positive and negative z-direction, but for fixed phase difference, we find, that for $0 < \varphi < \pi$ a higher efficiency is achieved for swimming in the positive z-direction, if the smaller of the multipole orders, l, is odd, and in the opposite direction, if l is even. For $\pi < \varphi < 2\pi$ swimming in the positive z-direction is more efficient for even l, and in the opposite direction for odd l.

The figure E.7 shows graphs of the efficiency, maximized with respect to the phase difference φ, versus the inverse distance x.

From this figure we can conclude that the spheres can swim more efficiently together than alone. We see that when the spheres approach one another, the swimming efficiency increases. For the lowest multipole orders, this increase starts at large distances between the spheres, but for higher orders the effect can be appreciable only for short distances. Then, two spheres with deformations corresponding to moderate multipole orders may achieve efficiencies for which a single sphere would

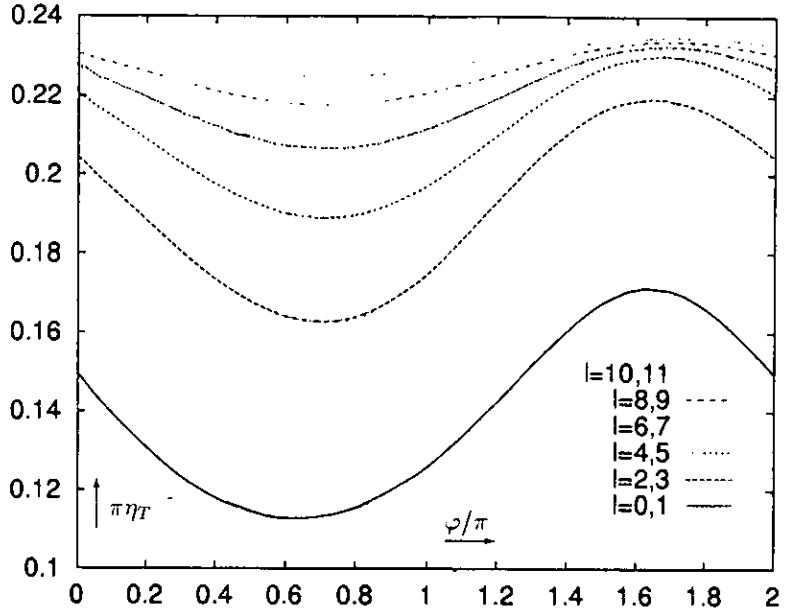

Figure E.6: Swimming efficiency η_T for two spheres at a dimensionless inverse distance $x = 0.45$, with deformations as described by two subsequent multipoles of order l (even), $l + 1$, in dependence on the phase difference φ.

need much higher multipoles. For high multipole orders the efficiency grows only at very short distances, where the validity of the present description becomes questionable.

We summarize, that for spherical bodies swimming by surface deformations as described by two multipoles of subsequent order, swimming one behind the other at a finite distance, with an appropriate phase difference between the deformations, is more efficient than swimming alone, as long as the multipole orders are not too high.

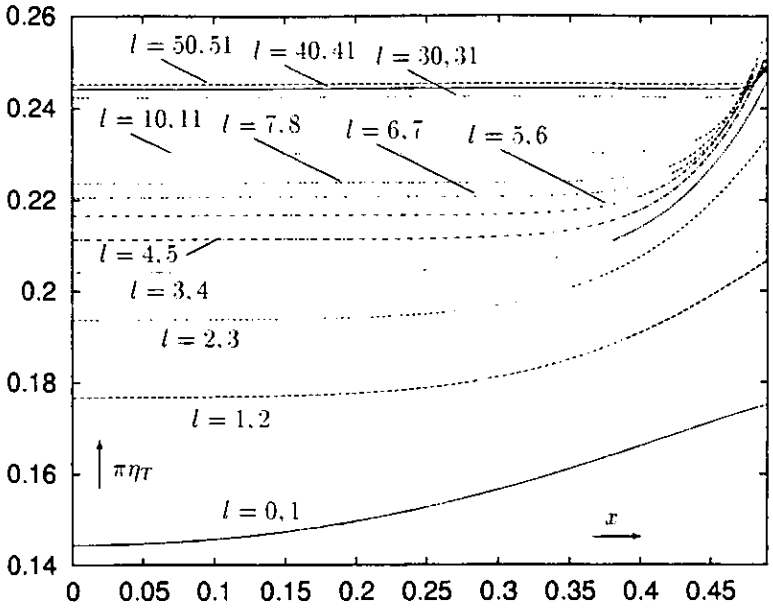

Figure E.7: Swimming efficiency η_T for two spheres with deformations as described by two subsequent multipoles of order l, $l+1$, in dependence on the dimensionless inverse distance x.

E.2 Arbitrary Number of Multipoles and Arbitrary Angle θ_R

In this section we give up the restriction to only two multipoles, as well as that to $\theta_R = 0$.

To find the most efficient way of swimming under these more general conditions, the method described in the preceding section is not very efficient, because the determination of all the eigenvalues requires the solution of a polynomial equation in λ, which can be done analytically for the case of two and three multipoles, when the equation is quadratic or cubic, respectively. The numerical solution of the higher order equations necessary for higher numbers of multipoles, however, would be rather time-consuming.

Felderhof and Jones [16] found a consistent method to determine the greatest eigenvalue, and this is just the one we are interested in, because it yields the maxi-

mum swimming efficiency. They used this method to find the maximum swimming efficiency for a single sphere.

For two spheres the problem is more complicated because the matrix $\underset{\approx}{A}$, related to the rate of energy dissipation, is nondiagonal, and the matrix $\underset{\approx}{B}$, related to the velocity, is not positive definite, but we can modify the method in order to adapt it to these complications. In the following we explain the modified procedure used for the two-sphere problem.

The matrix $\underset{\approx}{A}$ is a positive definite matrix, it can be regarded as defining the norm in the space of $|\xi\rangle$. Thus if we consider the solutions λ_i, $|\xi_i\rangle$ to the generalized eigenvalue equation

$$\underset{\approx}{B}|\xi_i\rangle = \lambda_i \underset{\approx}{A}|\xi_i\rangle, \tag{E.19}$$

then the eigenvectors corresponding to different eigenvalues are orthogonal in the sense

$$\langle\xi_i|\underset{\approx}{A}|\xi_j\rangle = 0, \qquad \text{if} \quad \lambda_i \neq \lambda_j, \tag{E.20}$$

and in the case of degenerate eigenvalues the corresponding eigenvectors may be chosen as orthogonal. The eigenvectors form a complete set in which an arbitrary vector $|\xi\rangle$ can be expanded:

$$|\xi\rangle = \sum_i c_i|\xi_i\rangle, \tag{E.21}$$

where the coefficients c_i can easily be found using the orthogonality of the eigenvectors:

$$c_i = \frac{\langle\xi_i|\underset{\approx}{A}|\xi\rangle}{\langle\xi_i|\underset{\approx}{A}|\xi_i\rangle}. \tag{E.22}$$

If a vector $|\xi_i\rangle$ is known to be an eigenvector, the corresponding eigenvalue can be found using

$$\lambda_i = \frac{\langle\xi_i|\underset{\approx}{B}|\xi_i\rangle}{\langle\xi_i|\underset{\approx}{A}|\xi_i\rangle}. \tag{E.23}$$

The form of the equations (E.23) and (E.22) shows that we may freely carry out unitary or scale transformation on $\underset{\approx}{A}$, $\underset{\approx}{B}$ and $|\xi\rangle$ in order to enhance stability of the numerical calculations. Felderhof and Jones found that for numerical study the following procedure is successful.

If we first construct the square root of $\underset{\approx}{A}$, we may then transform

$$\underset{\approx}{B} \to \hat{\underset{\approx}{B}} = \underset{\approx}{A}^{-1/2}\underset{\approx}{B}\underset{\approx}{A}^{-1/2}, \qquad \underset{\approx}{A} \to \hat{\underset{\approx}{A}} = I, \qquad |\xi\rangle \to |\hat{\xi}\rangle = \underset{\approx}{A}^{1/2}|\xi\rangle \tag{E.24}$$

to obtain the ordinary eigenvalue problem

$$\hat{\underset{\approx}{B}}|\hat{\xi}_i\rangle = \lambda_i|\hat{\xi}_i\rangle \tag{E.25}$$

with eigenvalues

$$\lambda_i = \frac{\langle\hat{\xi}_i|\hat{\underset{\approx}{B}}|\hat{\xi}_i\rangle}{\langle\hat{\xi}_i|\hat{\xi}_i\rangle}. \tag{E.26}$$

The first problem is thus the calculation of the inverse of the square root $\underset{\approx}{A}^{-1/2}$, because $\underset{\approx}{A}$ is a nondiagonal matrix. The usual way would be to diagonalize it, which requires the determination of all its eigenvalues ν and the corresponding eigenvectors. Any power of the diagonal matrix is then found by replacing its entries by that power, and in order to find the power of the original matrix the transformation leading to the diagonal form must be reversed.

We prefer, however, to use an approximate method to find $\underset{\approx}{A}^{-1/2}$ by expressing it as a power series. This leads to two problems: First, we obviously cannot expand about $\underset{\approx}{A} = 0$, and second, we have to make sure that the series converges.

We notice that the square root is well defined since $\underset{\approx}{A}$ is positive definite. Thus we can determine its maximum eigenvalue ν_{max} numerically and define a matrix $\underset{\approx}{A}'$ related to it by

$$\underset{\approx}{A}' = \frac{\underset{\approx}{A}}{\nu_{max}}, \tag{E.27}$$

the greatest eigenvalue of which is 1. We then may express this matrix in a form which allows to formulate a power expansion:

$$\underset{\approx}{A}' = \underset{\approx}{I} - (\underset{\approx}{I} - \underset{\approx}{A}'), \tag{E.28}$$

where the matrix $\underset{\approx}{I} - \underset{\approx}{A}'$ has eigenvalues $1 - \nu'$ in the range $0 \leq 1 - \nu' < 1$. This guarantees the convergence of the infinite series

$$\underset{\approx}{A}'^{-1/2} = \sum_{n=0}^{\infty}\binom{-1/2}{n}(\underset{\approx}{I} - \underset{\approx}{A}')^n, \tag{E.29}$$

which may be summed up to the required precision. The square root $\underset{\approx}{A}^{-1/2}$ is then found using the definition (E.27).

The transformation (E.24) now allows to consider an ordinary eigenvalue equation. The iterative method which we want to use for the calculation of the greatest eigenvalue is particularly simple for the case of a positive definite matrix, a property which the matrix $\hat{\underset{\approx}{B}}$ does not have, however. Neither does it possess pairs of positive and negative eigenvalues of equal modulus, in contrast to the corresponding matrix for the one-body case. Thus, we cannot apply the method used by Felderhof and Jones [16] to determine both eigenvalues of maximum modulus and the eigenvector corresponding to the positive one.

But since the efficiency depends only on the modulus U of the velocity, it is sufficient to determine the greatest eigenvalue λ^2_{max} of the square

$$\hat{\underset{\approx}{B}}^2 = \hat{\underset{\approx}{B}}\hat{\underset{\approx}{B}}. \tag{E.30}$$

Thus we may consider the eigenvalue equation

$$\hat{\underset{\approx}{B}}^2|\hat{\xi}\rangle = \lambda^2|\hat{\xi}\rangle. \tag{E.31}$$

from which we determine either the greatest or the most negative eigenvalue of $\hat{\underset{\approx}{B}}$:

$$\lambda_{max} = \pm\sqrt{\lambda^2_{max}}. \tag{E.32}$$

Next we are going to explain the numerical determination of the maximum (ordinary) eigenvalue μ_{max} and the corresponding eigenvector of a positive definite matrix $\underset{\approx}{M}$. We need it first to find the greatest eigenvalue of the matrix $\underset{\approx}{A}$, and then to determine the maximum eigenvalue and the corresponding eigenvectors of $\hat{\underset{\approx}{B}}^2$, which yield the maximum swimming efficiency for the two body problem.

The method makes use of the fact that application of a matrix to a vector enhances its component corresponding to the eigenvector with greatest eigenvalue relative to the others (unless the original vector is orthogonal to that eigenvector). Thus, if the matrix is applied repeatedly, the resulting vector becomes eventually a multiple of that eigenvector, except for arbitrarily small corrections. In order to keep the vectors finite, we start with a normalized vector $|\xi^0\rangle$ and normalize after each application of the matrix. This leads to the iteration

$$|\xi^{n+1}\rangle = \frac{\underset{\approx}{M}|\xi^n\rangle}{(\xi^n|\underset{\approx}{M}\underset{\approx}{M}|\xi^n)^{1/2}}. \tag{E.33}$$

Each of the vectors $|\hat{\xi}^n\rangle$ can be expanded in terms of the unknown eigenvectors $|\xi_i\rangle$:

$$|\xi^n\rangle = \sum_i c_i^n|\xi_i\rangle, \qquad \sum_i |c_i^n|^2 = 1. \tag{E.34}$$

From equations (E.31), (E.33) and (E.34) we obtain, after the iteration

$$\sum_i c_i^{n+1} |\hat{\xi}_i\rangle = \frac{\sum_i \mu_i c_i^n |\hat{\xi}_i\rangle}{(\sum_k |c_k^n|^2)^{1/2}}. \tag{E.35}$$

From the last equation we find the following ratio between any two components

$$\frac{c_i^{n+1}}{c_j^{n+1}} = \frac{\mu_i}{\mu_j} \frac{c_i^n}{c_j^n}. \tag{E.36}$$

When $n \to \infty$, the vector $|\hat{\xi}^n\rangle$ is dominated by the component corresponding to the greatest eigenvalue, μ_{max}, and thus it tends to the corresponding eigenvector.

$$|\hat{\xi}^n\rangle \to |\hat{\xi}_{max}\rangle. \tag{E.37}$$

Hence we find for the maximum eigenvalue:

$$\mu_{max} = \lim_{n \to \infty} \langle \hat{\xi}^n | \underset{\sim}{M} | \hat{\xi}^n \rangle. \tag{E.38}$$

In the last chapter we have explained that for a nonvanishing angle θ_R between the distance vector and the z-direction (which would be the swimming direction of the spheres if the hydrodynamic interactions were neglected) we first calculate the velocity component U_γ, and then determine its maximum, which yields the direction of the velocity of the spheres with optimum efficiency. We used the method described above to find the maximum swimming efficiency, and we found that it is achieved for very small angle γ_{max}. Due to the inaccuracy of the numerical calculations, we could not determine this angle precisely, but we always found $\gamma_{max} < 1/500$. Thus, the velocity component perpendicular to the z-axis is negligible and we can set $\gamma = 0$, thus considering spheres swimming in z-direction.

In the following graphs we show the results obtained for the case $\theta_R \neq 0$. For each point in these graphs we chose the maximum of efficiency with respect to the phase difference φ between the deformations of the spheres.

In the first figure E.8, we plotted the efficiency versus the angle θ_R, for fixed distance, $x = 0.4$. The contributions to the deformations are of all multipole orders less than an upper value L, $0 \leq l \leq L$.

We observe that for all angles θ_R the efficiency is the higher, the more and/or higher multipoles take part in the deformations.

As far as the dependence on θ_R is concerned, for the lowest multipole orders, $L = 1, 2$, the spheres swim more efficiently if one is behind the other, $\theta_R = 0$, and

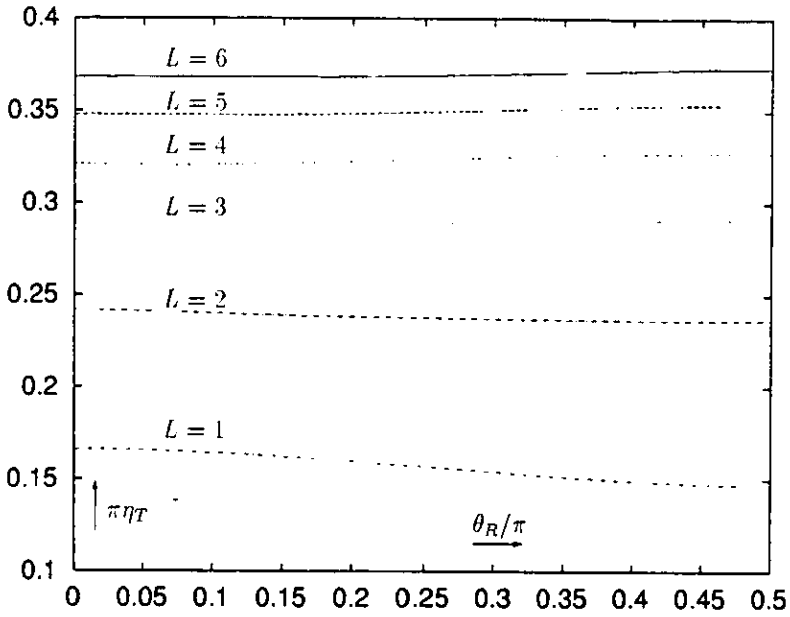

Figure E.8: Swimming efficiency η_T for two spheres at a dimensionless inverse distance $x = 0.40$, with deformations as described by multipoles of order $l = 0, \ldots, L$, in dependence on the angle θ_R.

the swimming efficiency decreases as they change towards the parallel swimming position, $\theta_R = \pi/2$. As soon as multipole orders higher than 2 are involved, the behaviour changes, and the efficiency grows as θ_R increases towards $\pi/2$. This may be explained with the help of the known features of optimum swimming of a single sphere. The angle $\theta_{R\,max}$ at which swimming together is most effective corresponds roughly to the direction into which spreads the main part of the velocity field generated by the spheres, since a sphere experiencing a stronger incoming flow can make more use of it for its own motion. This angle changes from $\theta = 0$ in the case of low multipole orders to $\theta = \pi/2$ for higher multipoles.

Figure E.9 shows graphs of the efficiency versus the inverse distance x between the spheres. Here the efficiency has been maximized with respect not only to the amplitudes of the different multipoles but also to the phase difference φ and the angle θ_R.

We can see that for all multipoles the efficiency increases as the spheres approach

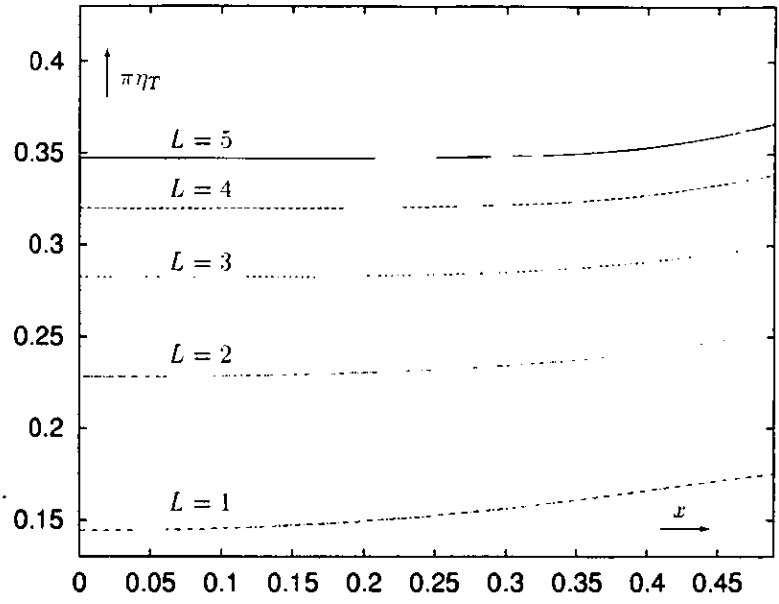

Figure E.9: Swimming efficiency η_T for two spheres with deformations as described by multipoles of order $l = 0, \ldots, L$, in dependence on the dimensionless inverse distance x.

one another, but the effect is weaker for higher multipole orders, similar to the cases studied in the previous section.

In order to show the dependence of the efficiency on both the distance R and the angle θ_R we have chosen a three-dimensional plot (fig. E.10) for the case of five multipoles, $l = 0, \ldots, 4$.

For large distances ($x < 0.1$) the interaction between the spheres is negligible, the efficiency coincides with that of a single sphere and does not depend on θ_R. For closer distances we notice an increase in efficiency, starting from $x \approx 0.2$ for parallel swimming ($\theta_R = \pi/2$), but only from $x \approx 0.35$ for one sphere swimming behind the other ($\theta_R = 0$). Considering the dependence on θ_R, the efficiency shows a minimum at $\theta_R \approx 0.07\pi$, which only may be noticed for $x \geq 0.4$, and the absolute maximum is achieved at $\theta_R = \pi/2$ for all x.

Plots for other ranges of multipole orders $l = 0, \ldots, L$ look very similar for $L \geq 3$, but with increasing L the dependence on θ_R and x gradually disappears.

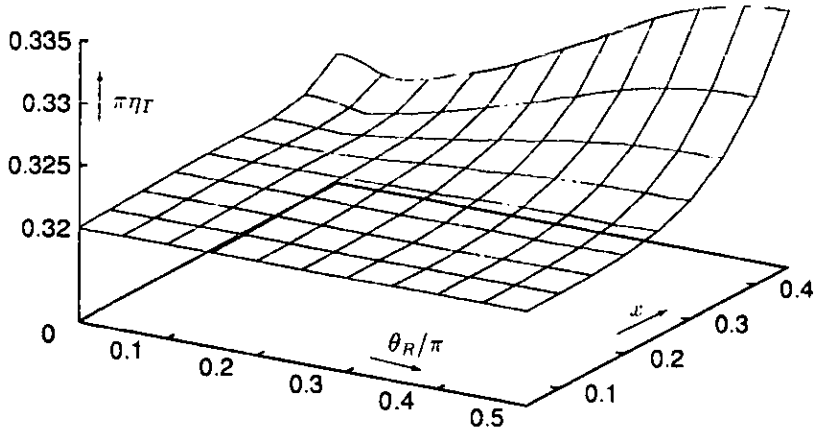

Figure E.10: Swimming efficiency η_T for two spheres with deformations as described by multipoles of order $l = 0, \ldots, 4$, in dependence on the angle θ_R and the dimensionless inverse distance x.

In order to obtain a better insight into the dependence of the efficiency on the phase difference φ and the angle θ_R we have plotted it into three-dimensional graphs, with fixed inverse distance $x = 0.4$, for different ranges of multipoles.

Here we did not distinguish between swimming in the positive or negative z-direction in the numerical determination of the multipole amplitudes leading to maximum efficiency. The latter coincides for phase differences φ and $2\pi - \varphi$, which is evident in the graphs, while only one half of them corresponds to a positive z-component of the velocity, and the other half to a negative one.

In the first of these graphs (fig. E.11) we consider the two lowest multipoles $l = 0, 1$.

We observe that the maximum efficiency is achieved for one sphere swimming behind the other, $\theta_R = 0$, and recall that the optimum phase difference φ for this case may be read off from fig. E.6. Since it lies in the interval $\pi < \varphi < 2\pi$ and was calculated for swimming in the positive z-direction, we conclude that the part to the rear of fig. E.11 corresponds to that direction. As the angle θ_R grows, the maximum of the efficiency with respect to the phase difference φ decreases, while

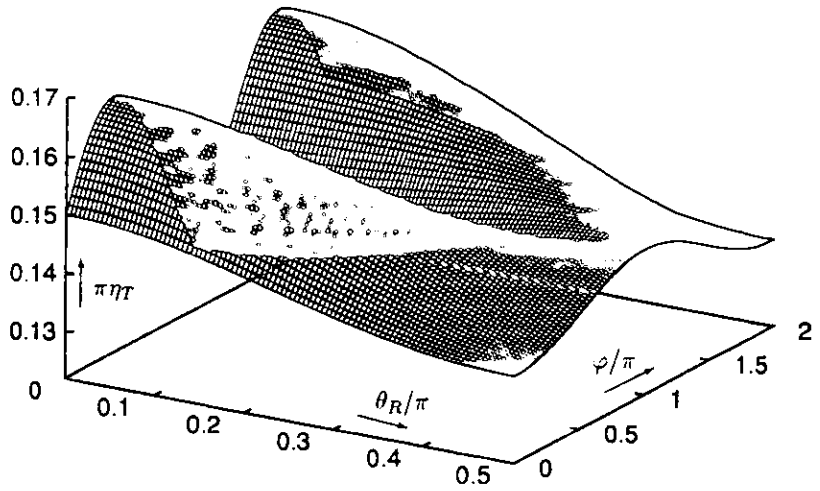

Figure E.11: Swimming efficiency η_T for two spheres at a dimensionless inverse distance $x = 0.40$, with deformations as described by multipoles of order $l = 0, 1$, in dependence on the angle θ_R and the phase difference φ.

the corresponding value of φ approaches π, reaching it for $\theta_R = \pi/2$: For parallel swimming the maximum efficiency is achieved when the deformations of the spheres are in antiphase.

In the following graph (fig. E.12) the deformations of the spheres are described by five multipoles $l = 0, \ldots, 4$.

In this graph we notice that the effects of hydrodynamic interaction between both spheres are more pronounced if the spheres swim parallel. The absolute maximum of efficiency is thus achieved for $\theta_R = \pi/2$ and $\varphi = \pi$.

Considering the angle θ_R as fixed, we may look at the dependence of the efficiency on the phase difference, which shows, for most angles θ_R, two maxima corresponding to optimum swimming in positive or negative z-direction. While the maximum values of the efficiency have already been plotted vs. θ_R (fig. E.8), we may now track the optimum phase difference for different angles θ_R. We observe an interesting behaviour: Starting at the absolute maximum, with decreasing θ_R the optimum phase difference is first shifted towards $\varphi = 0$ (or 2π, respectively), which is reached for $\theta_R \approx 0.3\pi$, then it changes again towards π, attaining this value for $\theta_R \approx 0.13\pi$,

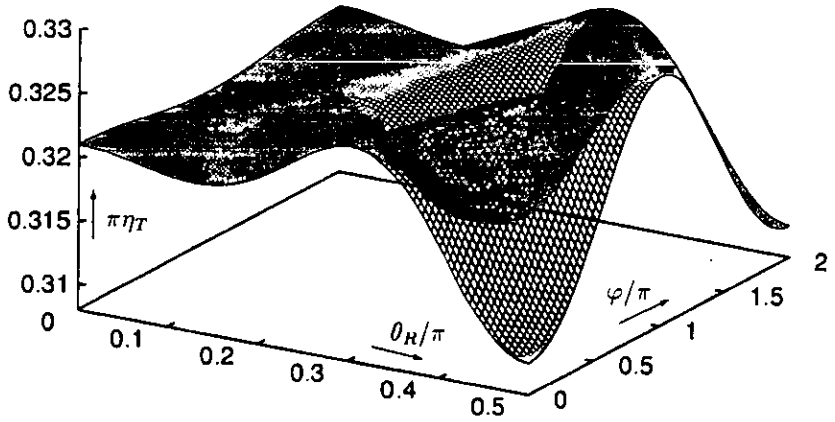

Figure E.12: Swimming efficiency η_T for two spheres at a dimensionless inverse distance $x = 0.40$, with deformations as described by multipoles of order $l = 0, \ldots, 4$, in dependence on the angle θ_R and the phase difference φ.

before it turns back for the last time, reaching $\varphi = 0, 2\pi$ for $\theta_R = 0$.

In figure E.13 there are contributions of the multipole orders $l = 0, \ldots, 10$ to the deformations of the spheres.

We observe that for angles $\theta_R < 0.27\pi$ the swimming efficiency is almost unaffected by the hydrodynamic interactions. As θ_R increases beyond this value the efficiency shows a similar dependence on this angle and on the phase difference as in the previous case ($l = 0, \ldots, 4$), and again the maximum is achieved for parallel swimming and a phase difference of π. As a difference from that case we notice that the variations of the efficiency, apart from becoming important for larger angles θ_R, are relatively smaller.

We conclude that, as higher multipoles are taken into account, the effects of the hydrodynamic interactions between the spheres concentrate on parallel swimming, but disappear for very high multipoles.

The greater importance of these effects for parallel swimming can be explained using the results of Felderhof and Jones concerning the swimming of a single sphere [16]. They found a first order potential solution in closed form, for which the swim-

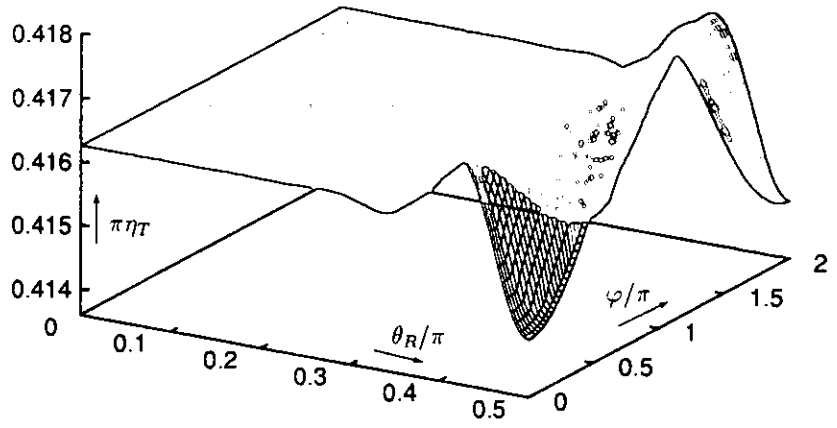

Figure E.13: Swimming efficiency η_T for two spheres at a dimensionless inverse distance $x = 0.40$, with deformations as described by multipoles of order $l = 0, \ldots, 10$, in dependence on the angle θ_R and the phase difference φ.

ming efficiency tends to the optimum when a certain limit is taken. For that solution the surface displacement is greatest near $\theta = \pi/2$, where θ measures the angle with respect to the swimming direction.

In our case, we know that as we take more multipoles, then the solution approaches the one-body solution, which means that for higher multipoles the surface deformations on each sphere begin to concentrate on its equator, if they swim in the z direction. Because of this kind of deformations we can expect that the hydrodynamic interaction are more important when the spheres swim parallel one beside the other.

Apéndice F

Discussion and Conclusions

We have studied small amplitude swimming of two spherical bodies in a viscous incompressible fluid, taking into account hydrodynamic interactions between them. Swimming here means that the bodies achieve a nonvanishing average translational and/or rotational velocity by periodic surface deformations.

The basic quantities to be determined are these velocities and the energy dissipated by the swimming bodies in a period. The latter allows to compare the efficiency of different swimming strokes, which is defined as the ratio of the velocity to the average rate of dissipation.

In order to express these velocities in terms of the deformations we were able to adopt the method developed by Felderhof and Jones [16] for the case of a single body. It is based on a perturbation expansion in the deformation amplitudes up to second order, and at this order the velocities as well as the rate of dissipation are completely determined by the time-dependent first-order solution of the hydrodynamic equations. For deformations harmonic in time the quantities are expressed as quadratic forms in the surface displacements, which are analysed in terms of multipoles.

In the case of two bodies we had to take into account the hydrodynamic interactions in the determination of the first-order velocity field. Thus the problem to be solved took the form of two coupled one-body problems. Again the velocities of each of the spheres and the rate of dissipation are expressed as quadratic forms, but now the corresponding matrices depend on the separation vector $\boldsymbol{R}$ between the centers, and there are far more extensive couplings between different mutipoles.

In order to simplify the analysis the first-order flow was assumed to be irrotational. We consider only translational motion.

We defined the swimming efficiciency for two spheres as twice the ratio of their center-of-mass velocity to the total rate of energy dissipated by both of them, so that it coincides with that for a single sphere if the hydrodynamic interactions vanish.

The optimization of the efficiency leads to a generalized eigenvalue problem for the surface displacements. The maximum eigenvalue and the corresponding eigenvector may be determined iteratively in a finite subspace of the vector space of deformation amplitudes.

We focused our attention on the case where the velocities of both spheres coincide, so that the distance between them does not change. In order to satisfy the condition of constant distance we chose surface displacements which had the same form for both bodies, but with a phase difference φ.

The deformations were chosen such that a single sphere (or two spheres at infinite distance) would swim in the z-direction. We considered the problem for arbitrary angle θ_R between this direction and that of the separation vector $\boldsymbol{R}$.

The iterative maximization of the efficiency was carried out for fixed values of the distance, the angle θ_R and the phase difference, and afterwards the dependence of the maxima on them could be investigated, for example for the determination of the best phase difference. For $\theta_R \neq 0$ the complication occurred that there is no symmetry argument which would guarantee that the swimming direction of the spheres at a finite distance is still the z-direction. Therefore, we introduced the angle γ between both directions as an additional parameter with respect to which we had to maximize the efficiency. We found that within the precision of the numerical method the direction of most efficient swimming coincides with the z-direction.

In contrast with a single sphere, which can swim only if its deformations are characterized by two or more multipoles of different order, we found that two bodies with surface displacements described by only one spherical harmonic may acquire a translational velocity at second order in perturbations.

Considering deformations described by a sum of two subsequent multipoles, we found that for monopolar and dipolar terms, as well as for dipolar and quadrupolar terms, the optimum swimming efficiency is achieved for the case in which one sphere swims behind the other. The corresponding phase difference is then close to $5\pi/3$ or $2\pi/3$, respectively. For higher multipoles it is more efficient when one sphere swims aside the other, with a phase difference of π.

Also if we consider more than two multipoles, we find that the spheres swim better if they do it one aside the other, again with a phase difference of π.

Since the first-order velocity fields going out from each body fall off with increas-

ing distance and the fields of higher multipole orders decrease more rapidly, the hydrodynamic interactions have less and less influence on the efficiency at larger separations of the bodies, and, at a finite distance, for multipole fields of higher order. If we take the limit of very large separation or high order multipoles we reproduce the results given by Felderhof and Jones for the one-body problem.

We must therefore remark that the predicted improvement of the efficiency for two bodies swimming together is important only if their deformations are characterized by moderate multipole orders. This means that organisms swimming by deformations of low order, and thus with a low one-body efficiency, can considerably improve their efficiency by swimming together with a second one, but organisms which are able to achieve a high one-body efficiency by deformations of high multipole order can hardly improve it.

In order to find out to which organisms our considerations might apply, we must relate the multipole orders by which the deformations are described to more tangible physical features. Since the multipole order is equal to the number of nodes which the deformations have between the poles of the sphere, high orders mean that the deformations involve a tangential length scale which is small compared to the radius. Thus, if we imagine rather primitive microorganisms unable to deform their shape on a small tangential scale compared to their size, they cannot generate multipole fields of high orders. We expect, that such organisms can swim with considerably higher efficiency together than on their own.

On the other hand, there are organisms which can produce higher order multipole fields by small-scale deformations of their surfaces. Since from the investigation of the one-body swimming problem by Felderhof and Jones it is known, that the deformations corresponding to high multipole orders lead to shapes similar to fins, animals like some kinds of fish could be counted among this second group, even if the amplitudes of their swimming movements are certainly not small. Such organisms achieve a high one-body swimming efficiency, but, as far as their motion may be described with the approximations of the present work, should hardly be able to improve this efficiency by swimming together with a second of the kind.

Apéndice G

Potential Flow about a Hard Sphere

In the present appendix we illustrate the method used to find the flow potential for a hard sphere of radius a in an incident flow. We consider a sphere immersed in an infinite incompressible fluid. We suppose that the flow velocity can be written as gradient of a potential, then the potential satisfies Laplace's equation

$$\nabla^2\phi = 0. \tag{G.1}$$

We require that the flow satisfies stick boundary conditions on the surface of the sphere, which means that

$$\phi'(r = a+) = 0. \tag{G.2}$$

Now we suppose, that the solution in absence of the sphere is given by $\phi_0(\boldsymbol{r})$, it can be considered as an incident flow, and ask for the perturbation caused by the presence of the sphere. The solution outside the sphere is written as

$$\phi(\boldsymbol{r}) = \phi_0(\boldsymbol{r}) + \phi_1(\boldsymbol{r}), \tag{G.3}$$

where $\phi(\boldsymbol{r})$ is required to satisfy the boundary condition at $r = a$, while $\phi_1(\boldsymbol{r})$ has to vanish for $r \to \infty$, since there the flow tends to the incident flow.

The potential $\phi_0(\boldsymbol{r})$ by itself satisfies the Laplace equation and can be written in terms of spherical harmonics

$$\phi_0(\boldsymbol{r}) = \sum_{l=0}^{\infty} \sum_{m=-l}^{l} c_{lm} r^l Y_{lm}(\theta, \varphi). \tag{G.4}$$

Since the problem is linear, it is sufficient to consider a particular term of the series only, which, choosing its coefficient to be unity, can be written as

$$\phi_0^{lm}(\boldsymbol{r}) = r^l Y_{lm}(\theta, \varphi). \tag{G.5}$$

Looking for the corresponding solution $\phi^{lm}(\boldsymbol{r})$, we try the ansatz

$$\phi^{lm}(\boldsymbol{r}) = f_{lm}(r)\phi_0^{lm}(\boldsymbol{r}). \tag{G.6}$$

Now we substitute this ansatz into Laplace's equation, to get

$$\frac{d^2 f_{lm}}{dr^2} + \frac{2(l+1)}{r}\frac{df_{lm}}{dr} = 0. \tag{G.7}$$

The solution of this equation with the desired behaviour at infinity is

$$f_{lm}(r) = 1 - \alpha_l r^{-(2l+1)}. \tag{G.8}$$

The coefficient α_l is found from the stick boundary condition (G.2) to be

$$\alpha_l = -\frac{l}{l+1}a^{2l+1}. \tag{G.9}$$

Bibliografía

[1] G.I. Taylor; *Analysis of the swimming of microscopic organism*, Proc. R. Soc. A **209** (1952) 447-461.

[2] G.K. Batchelor; Introduction to Fluid Dynamics, (Cambridge University Press; 1967).

[3] J. Happel and H. Brenner; Low-Reynolds Number Hydrodynamics (Noordhoff.Leiden.1973).

[4] A. Shapere and F. Wilczek; *Efficiencies of self propulsion at low Reynolds number*, J. Fluid Mech. **198** (1989) 587.

[5] A. Shapere and F. Wilczek; *A spherical envelope approach to ciliary propulsion*, J. Fluid Mech. **198** (1989) 557.

[6] A.J. Reynolds; *The swimming of minute organism*, J. Fluid Mech. **23** (1965) 241.

[7] E.O.Tuck; *A note on a swimming problem*, J. Fluid Mech. **31** (1968) 305.

[8] J.E. Drummond; *Propulsion by oscillating sheets and tubes in a viscous fluid*, J. Fluid Mech. **25** (1966) 787.

[9] M.J. Lighthill; *On the squirming motion of nearly spherical deformable bodies through liquids at very small Reynolds numbers*, Comm. Pure Appl. Math. **5** (1952) 109.

[10] J.R. Blake; *A spherical envelope approach to ciliary propulsion*, J. Fluid Mech. **46** (1971) 199.

[11] P.G. Saffman; *The self-propulsion of a deformable body in a perfect fluid*, J. Fluid Mech. **28** (1967) 385.

[12] G.I. Taylor: *Analysis of the swimming of long and narrow animals*, Proc. R. Soc. A **214** (1952) 158.

[13] M.J. Lighthill: *Note on the swimming of slender fish*, Comm. Pure Appl. Math. **9** (1960) 305.

[14] T.Y. Wu: *swimming of a waving plate*, J. Fluid Mech. **10** (1961) 321.

[15] B.U. Felderhof, R.B. Jones: *Inertial effects in small-amplitude swimming of a finite body*, Physica A **202** (1994) 94.

[16] B.U. Felderhof: *Small amplitude swimming of a sphere*, Physica A **202** (1994) 119.

[17] L.D. Landau, E.M. Lifshitz: Fluid Mechanics (Pergamon Press, second edition, 1989).

[18] H. Lamb: Hydrodynamics (Dover, New York, 1945), pp. 595, 632.

[19] B. Cichocki, B.U. Felderhof and R. Schmitz; *Hydrodynamic interactions between two spherical particles*, PCH **10**, 3 (1988) 383.

[20] A.R. Edmonds; Angular Momentum in Quantum Mechanics, (Princeton University Press, Princeton, New Jersey; 1957).

[21] B.U. Felderhof; *Force density induced on a sphere in linear hydrodynamics*, I. Fixed sphere, stick boundary conditions, Physica A **84** (1976) 557.

[22] B.U. Felderhof and R.B. Jones; *Hydrodynamic scattering theory of flow about a sphere*, Physica A **136** (1986) 77.

[23] B.U. Felderhof, G.W. Ford, and E.G.D. Cohen: *Two-Particle cluster integral in the expansion of the dielectric constant*, Journal of Statistical physics **28**, No. 4, 1982.

[24] D.J. Jeffrey; *Conduction through a random suspension of spheres*, Proc. R. Soc. A (1973) 335.

[25] B. U. Felderhof; *Wigner solids and diffusion controlled reactions in a regular array of Spheres*, Physica A **130** (1985) 34.